



UNIVERSIDADE FEDERAL DE PERNAMBUCO
Centro de Ciências da Saúde
Departamento de Ciências Farmacêuticas
Programa de Pós-Graduação em Ciências Farmacêuticas



TESE DE DOUTORADO

PONTOS QUÂNTICOS COMO SONDAS FLUORESCENTES NO ESTUDO DA CARCINOGENESE EM CÉLULAS GLIAIS

Maria Aparecida Barreto Lopes Seabra

Recife, 2014



UNIVERSIDADE FEDERAL DE PERNAMBUCO
Centro de Ciências da Saúde
Departamento de Ciências Farmacêuticas
Programa de Pós-Graduação em Ciências Farmacêuticas



PONTOS QUÂNTICOS COMO SONDAS FLUORESCENTES NO ESTUDO DA CARCINOGENESE EM CÉLULAS GLIAIS

Maria Aparecida Barreto Lopes Seabra

Tese apresentada ao Programa de Pós-Graduação em Ciências Farmacêuticas da UFPE como parte dos requisitos para a obtenção do Grau de Doutor em Ciências Farmacêuticas

Orientadora: Prof^a. Dr^a. Beate Saegesser Santos - UFPE

Co-orientadores: Prof^a. Dr^a. Belmira Andrade da Costa - UFPE

Prof. Dr. Vivaldo Moura Neto – UFRJ

Prof^a. Dr^a. Adriana Fontes - UFPE

Recife, 2014

Catálogo na fonte
Bibliotecária: Gláucia Cândida da Silva, CRB4-1662

S438p Seabra, Maria Aparecida Barreto Lopes.
Pontos quânticos como sondas fluorescentes no estudo da carcinogênese em Células Gliais / Maria Aparecida Barreto Lopes Seabra.
– Recife: O autor, 2014.
110 folhas: il. ; 30 cm.

Orientadora: Beate Saegesser Santos.
Tese (Doutorado) – Universidade Federal de Pernambuco, CCS.
Programa de Pós-Graduação em Ciências Farmacêuticas, 2014.
Inclui referências e apêndices.

1. Glioblastoma. 2. Pontos Quânticos. 3. Corantes Fluorescentes. I. Santos, Beate Saegesser . (Orientadora). II. Título.

615.3 CDD (23.ed.) UFPE (CCS 2016-002)

MARIA APARECIDA BARRETO LOPES SEABRA

**Pontos Quânticos como Sondas Fluorescentes no Estudo da Carcinogênese em
Células Gliais**

Tese apresentada ao Programa de Pós-Graduação em Ciências Farmacêuticas da Universidade Federal de Pernambuco, como requisito parcial para a obtenção do título de Doutora em Ciências Farmacêuticas.

Aprovada em: 24 / 03 / 2014

BANCA EXAMINADORA


Prof.^a Dr.^a Beate Saegesser Santos (Orientadora)
Universidade Federal de Pernambuco

Prof.^a Dr.^a Ana Cristina Lima Leite (Examinadora Interna)
Universidade Federal de Pernambuco

Prof.^a Dr.^a Ângela Amâncio dos Santos (Examinador Externo)
Universidade Federal de Pernambuco

Prof. Dr. Rubem Carlos Araújo Guedes (Examinador Externo)
Universidade Federal de Pernambuco


Prof.^a Dr.^a Maria Goreti Carvalho Pereira (Examinadora Externa)
Universidade Federal de Pernambuco



*Dedico este trabalho
primeiramente a Deus, pois
sem Ele nada disso seria
possível. E aos dois homens
da minha vida Gustavo e
Matheus Seabra.*

**“Nisto todos conhecerão que sois
Meus discípulos, se vos amardes
uns aos outros” disse Jesus.**

João 13:35.



AGRADECIMENTOS

A Deus pelo amor incondicional e por ser presente em todas as horas da minha vida. Por todas as minhas vitórias, como também pelos problemas que me trouxeram muito aprendizado, moldando meu caráter e minha personalidade.

A toda minha família, principalmente aos meus pais Geraldo e Terezinha que muitas vezes mesmo sem entender do que eu falava, acreditavam em mim. Principalmente minha mãe que estava do meu lado e me deu toda força e apoio para eu chegar até aqui. Ensinou-me a não desistir nunca. Eles não podem estar aqui hoje comigo fisicamente, mas estarão sempre em meu coração. Agradeço também ao meu irmão Antonio de Pádua que quando as coisas “apertavam” sempre me fez lembrar o que eu dizia quando adolescente e sonhadora; “ainda coloco o nome de um elemento químico na tabela periódica! Quero fazer a diferença!”.

Ao marido, amigo e companheiro Gustavo, que me ensinou e me ensina muito todos os dias. Pelo amor, carinho, atenção, e principalmente por acreditar em mim quando as dificuldades bateram na nossa porta. As nossas diferenças nos fazem crescer.

A uma pessoinha que me trouxe entusiasmo, força, coragem, me mostrou o que é o verdadeiro amor quando ele muitas vezes pagou o preço de não ter a mãe por perto. O abraço apertado nas horas certas, palavras de amor quando eu mais precisei. Hoje eu tenho certeza que meu coração vive fora do meu corpo e tem nome, Matheus.

A minha sogra Lenice, Ligia, Marco, Arthur, Júlia e Welker pelo apoio, carinho e amor.

Aos membros da banca, Professora Dra. Ana Cristina Leite, Professora Dra. Ângela Amâncio, Dra Goreti Pereira e ao professor Dr. Rubem Guedes por dedicarem tempo a este trabalho e pelo incentivo durante todos esses anos.

A minha orientadora Beate Santos, pelo incentivo desde a graduação em química, pela amizade, amor, pelo carinho, paciência, pelas noites perdidas e principalmente por acreditar no nosso trabalho.

Aos meus co-orientadores professor Dr. Vivaldo Moura Neto, professora Dra. Belmira Andrade e professora Dra. Adriana Fontes pelo apoio e incentivo na pesquisa e na minha carreira profissional. Quero agradecer especialmente a este professor que mesmo sem me conhecer acreditou nas minhas ideias no nosso primeiro encontro E também a professora Belmira que me deu a honra de conhecê-la e trabalhar com ela, ensinando-me muito mais que ciência, mas com humildade e humanidade como ser professora, pesquisadora, mulher e mãe. Muito obrigada.

Ao programa de Pós Graduação em Ciências Farmacêuticas (PPGCF), a todos os professores, alunos e secretárias que de alguma forma contribuíram para meu crescimento profissional como também aqueles que foram grandes amigos durante esta caminhada. Aos nossos representantes Danilo e Laércio Em especial ao meu querido professor Dr. Rodolfo de Farias. As secretárias do PPGCF que nos socorrem quando mais precisamos Nerilin, Júlia Hellen e Bárbara e que sempre estavam prontas para me ajudar. Aos meus estudantes Diogo Fragoso,

Jean, Gustavo Siqueira, Victor e a todos da turma que sempre me fazem uma pessoa melhor e mais feliz.

Aos meus grandes amigos e amigas do NanoBio pelo nosso convívio, brincadeiras, amizade, brigas, suporte e pelas discussões científicas que tivemos durante todo esse tempo. Pela paciência comigo durante esses anos, principalmente ao Tony, Clayton, Osnir, Anna Livia, Rafael e Denise que desde o início estavam presentes nas horas mais difíceis e durante todo este tempo. Aos meus queridos Thiago, Paulo Euzébio, Camila, Isabela, Aline, Natália, Dewson, Gustavo, Renan, Rafael (japa) e Lêda e todos aqueles que fazem parte do laboratório de Biofísica Química.

Um agradecimento especial ao Sr. Fredson, pois durante esses anos todos foi amigo e ajudou muito no laboratório. A Dona Deda e seu filho Sandro pelo carinho e suporte.

Ao professor e amigo Dr. Guenther Hochhaus pelo convite para passar um ano e meio desfrutando da sua presença e orientação, pelo incentivo em fazer um doutorado, pelo carinho dispensado a minha família e principalmente por acreditar em mim profissionalmente. Por me dar a liberdade de criar coisas novas no laboratório dele na Universidade da Flórida.

Aos “Hochhausians” que sempre foram para mim uma família desde o meu primeiro emprego em 2005 e por continuarem do meu lado mesmo tão distante fisicamente. Especialmente a Yufei Tang por me fazer crescer profissionalmente e como pessoa. Em especial quero agradecer a Saskia e Cláudia pela amizade, carinho, e apoio mesmo estando tão longe fisicamente.

A todos que fazem parte do “Pharmaceutics Department”- UF. Principalmente ao Prof. Dr. Sihong Song e os que fazem parte do seu laboratório. Aos amigos Ahmed Elshikha, Andrea Ritter, Mongjen Chen, Tina, Tianwei Guo, Dr. Lu Yuanqing, que me ajudaram com o cultivo das células, nos ensaios de toxicidade, doaram reagentes e me adotaram como parte deste laboratório.

As secretárias Sarah Foxx, Vivian Lantow, Kimberly Howell e Patricia Khan, pois sem elas as coisas não funcionariam tão bem como acontece e também pela amizade e carinho e também pelos momentos juntos fora do departamento. “Thank you”!

Ao Prof. Dr. Derendorf e seu laboratório pelo apoio e incentivo demonstrado na minha pesquisa. Principalmente a Ravi, Nívea, Alex, Andréa e todos os internos que tornaram minha passagem por lá muito mais agradável e alegre.

A Karen e Kim do Centro de Microscopia Eletrônica da Universidade da Flórida pela ajuda nas imagens para caracterização dos lipossomas.

Aos membros do laboratório do prof. Dr. Sócrates do Egito - UFRN pela amizade e carinho durante meu tempo na Universidade da Flórida. Principalmente quero agradecer ao Miguel e Henrique por ter sido minha “família brasileira” fora do Brasil, pelas discussões científicas, motivação, amizade e pelos momentos que dividimos durante um ano longe de casa.

Aos amigos queridos do laboratório da professora Belmira que foram os meus anjos desde que conheci. Obrigada Renata, Eraldo, Igor e Juliana. A Todos vocês que me adotaram como parte do laboratório como também amiga e companheira.

Ao Departamento de Física em especial ao professor Dr. Celso Melo e seu laboratório. Aos estudantes Etelino e Renata pela ajuda com as medidas do potencial zeta.

A professora Dra Regina Bressan, pelo apoio e doação dos animais para este estudo e ao pessoal do seu laboratório na Fundação Oswaldo Cruz – UFPE.

Ao professor Claudio do Departamento de Biofísica e seu laboratório, pelo carinho e acolhimento principalmente Sheila, Gysele, Djaná, Janilson, Darlene, Jéssica, Arthur e muitos outros. Em especial ao professor Oleg e sua esposa Liliya pelo carinho de sempre. Ao professor Reginaldo e professora Márcia do departamento de Biofísica e ao secretário Jorge.

Quero agradecer ao Departamento de Química Fundamental pela disponibilidade de sempre e apoio principalmente aos professores Gilberto F. de Sá, Daniela Navarro e Severino Júnior. Ao professor João Bosco e sua família por ter sido um grande suporte enquanto eu estava na Flórida, pelo carinho e amizade. A todos os alunos que sempre me fizeram sentir como se este departamento fosse minha casa.

Aos meus amigos e irmãos das igrejas “Servants of Christ” e Paróquia das Missões. Principalmente aqueles que por muitas vezes andaram de mãos dadas comigo como Victoria Harris, Kathy Benton, Beth Kirby, Alex Farmer, Ralph e Mary, Betânia Luna, Carminha e Clebson.

RESUMO

Glioblastoma (grau IV) é o tumor mais agressivo e infiltrante do sistema nervoso central (SNC), que mostra uma série de mutações, bem como alto grau de vascularidade, polimorfismo e atipia celular nuclear. Infelizmente, diagnóstico precoce de tumores cerebrais é difícil, uma vez que ferramentas de imagem não são eficientes para o diagnóstico correto desses tipos de tumores, levando a falhas no tratamento. Aqui nós descrevemos a síntese, caracterização e conjugação de pontos quânticos ou *quantum dots* (QDs) de telureto de cádmio (CdTe) recobertos com tiol e com o anticorpo contra a proteína ácida fibrilar glial (anti-GFAP), bem como, a preparação de lipossomas. O método de congelamento e descongelamento foi utilizado para encapsular os QDs em diferentes tipos de lipossomas e liberá-los em células tronco. Os lipossomas vazios e contendo CdTe QDs foram caracterizados por microscopia de fluorescência, microscopia eletrônica de transmissão, tamanho e potencial zeta. Os QDs CdTe-anti-GFAP foram utilizados para um novo direcionamento *in vivo* e método de imagem para detecção do tipo de tumor glioblastoma U87 xenotransplantado em cérebro de camundongos suíços machos. CdTe QDs não conjugados e CdTe QDs conjugados foram utilizados para marcar U87 linha de células de tumor *in vitro* e astrócitos saudáveis. A citotoxicidade dos CdTe QDs com fluorescência no verde (530 nm) e no vermelho (644 nm), foi avaliada utilizando MTT nas células U87. O crescimento do tumor foi visualizado no interior do cérebro pela marcação com hematoxilina e eosina e mostrou a entrega com sucesso nas células U87 no parênquima cerebral. CdTe QDs conjugados com anti - GFAP foram injectados na região do tumor e a sua marcação na linhagem celular U87 foi visualizada por microscopia de fluorescência, mostrando dupla marcação com especificidade para vimentina em glioblastomas imunorreactivos. Em comparação com as células tumorais U87, que facilmente foram marcadas com o CdTe QDs conjugados com anti- GFAP, observou-se que os astrócitos saudáveis mantidos em culturas primárias tiveram uma maior resistência à sua marcação e foram fracamente marcados. Os resultados descritos aqui direcionam para novas perspectivas na utilização de CdTe QDs na detecção de glioblastoma, sugerindo uma potencial aplicação em cirurgia guiada por imagem.

Palavras-chave: Glioblastoma. Pontos Quânticos. Sondas Fluorescentes. Modelo *in vivo*

ABSTRACT

Glioblastoma (grade IV) is the most aggressive and infiltrating tumor of the central nervous system (CNS), showing a variety of mutations as well as high degree of vascularity, cell polymorphism and nuclear atypia. Unfortunately, early diagnostic of brain tumors is hard, as imaging tools are not efficient for proper diagnosis of these types of tumors, leading to treatment failures. Here we describe the synthesis, characterization and conjugation of thiol-capped CdTe with anti-glial fibrillar acidic protein (anti-GFAP) and preparation of liposomes. The freeze and thaw method was used to encapsulate the QDs in different types of liposomes and deliver them into stem cells. The empty and containing CdTe QDs liposomes were characterized by fluorescence microscopy, transmission electron microscopy, size and zeta potential. A new *in vivo* targeting and imaging method for U87 glioblastoma tumor type xenotransplanted into male swiss mice brain using aqueous colloidal CdTe quantum dots conjugated to anti-GFAP (CdTe-anti-GFAP QDs) was developed. The red emitting CdTe QDs and the conjugated red-emitting CdTe QDs were used to label U87 tumor cell line *in vitro* and health astrocytes. Toxicity of isolated green (530 nm) and red (644 nm) emitting CdTe QDs, was evaluated using MTT assay applied to U87 cells. The tumor growth was visualized inside the brain by the hematoxylin and eosin staining and showed the successful delivery of the U87 cells into the brain parenchyma. CdTe-anti-GFAP QDs were injected into the tumor region and their uptake by the U87 cell line was visualized by fluorescence microscopy, showing specific double-labeling of vimentin-immunoreactive glioblastoma. Compared to U87 tumor cells, which easily take up anti-GFAP conjugated red-emitting CdTe QDs, healthy astrocytes kept in primary cultures offered more resistance to their incorporation and were weakly labeled. The results reported here provide new perspectives for using CdTe QDs in glioblastoma detection, suggesting their potential application in imaging-guided surgery.

Keywords: Glioblastoma. Quantum Dots. Fluorescent Probes. *in vitro* Model

LISTA DE FIGURAS

Figura 1. Classificação dos tumores cerebrais pela Organização Mundial de Saúde (OMS).....	19
Figura 2. Biópsia de um GBM humano classificado como Grau 4 [retirado de (ARNDT-JOVIN <i>et al.</i> , 2009)].....	20
Figura 3 Esquema de um nanocristal de semicondutor (QD) funcionalizado com uma proteína.	22
Figura 4. (A) O tecido mamário, onde os QDs (vermelhos) se ligam especificamente a receptores Her2. (B) Visualização dos tumores <i>in vivo</i>	22
Figura 5. Sequência de formação de lipossomas: (A) fosfolipídeos, (B) formação da bicamada, vesícula formada (D), onde há o rearranjo da bicamada em solução para não expor a região hidrofóbica (C).....	23
Figura 6 Morfologia dos lipossomas de acordo com o tamanho e com a quantidade de camadas. SUVs, LUVs e GUVs possuem uma única bicamada. Os OVV's possuem outras vesículas no seu interior e o MLVs possuem multicamadas.	24

LISTA DE ABREVIATURAS

PC	Fosfatidilcolina
DOTAP	1,2-Dioleoil-3-trimetilamônio-propano
DOPE	Dioleilfosfatidiletanolamina
Chol	Colesterol
QDs	Quantum Dots
CdTe	Telureto de Cádmio
AMS	Ácido Mercaptosuccínico
AMP	Ácido Mercaptopropiônico
AMA	Ácido Mercaptoacético
GBM	Glioblastoma Multiforme
BV	Banda de Valência
BC	Banda de Condução
E_{gap}	Energia do bandgap
SNC	Sistema Nervoso Central
NCI	National Cancer Institute (E.U.A.)
INCA	Instituto Nacional de Câncer (Brasil)
MET	Microscopia Eletrônica de Transmissão
PBS	Tampão Fosfato
GA	Glutaraldeído
PFA	<i>para</i> - Formaldeído
DMEM F-12	<i>Dulbecco's modified Eagle's medium suplementado F-12</i>
SFB	Soro Fetal Bovino
PEG	Polietilenoglicol
DLS	<i>Diffraction Light Scattering</i>
GFAP	proteína glial fibrilar ácida (do inglês Glial Fibrillary Acidic Protein)
EGF	Fator de crescimento epidermal
EGFR	Receptor do fator de crescimento epidermal
MTT	3-(4,5-dimetiltiazol-2yl)-2,5-difenilbrometo de tetrazolina)

SUMÁRIO

1	Introdução	13
2	Referencial Teórico.....	16
2.1	Células Neurais e Suas Patologias	16
2.2	Sondas para Histopatologia: aplicação dos Pontos Quânticos ou “Quantum Dots”	19
3	Objetivos Geral e Específicos.....	26
3.1	Objetivo Geral.....	26
3.2	Objetivos Específicos.....	26
4	Resultados	28
5	Conclusões e Perspectivas	30
5.1	Conclusões	30
5.2	Perspectivas.....	30
	Referências	32
	Apêndices	35
	Apêndice A: Quantum Dots in Biomedical Research.....	35
	Apêndice B: Non-Specific interactions of CdTe/CdS Quantum Dots with human blood mononuclear cells	58
	Apêndice C: Studies on intracellular delivery of carboxyl-coated CdTe quantum dots mediated by fusogenic liposomes	65
	Apêndice D: <i>IN VIVO</i> AND <i>IN VITRO</i> STUDIES OF THIOL - CAPPED CdTe QUANTUM DOTS AS A TOOL FOR BRAIN TUMOR DIAGNOSTICS..	75

1 INTRODUÇÃO

Tumor cerebral pode ser definido como o crescimento anormal das células do cérebro e pode ser classificado em tumor benigno e maligno. Segundo o *National Institute of Cancer* dos Estados Unidos, a estimativa em 2011 foi de 22.340 novos casos diagnosticados e 13.110 mortes por tumores cerebrais e do sistema nervoso (NATIONAL INSTITUTE OF CANCER, 2011), 69.720 novos casos de tumor cerebral primário maligno e não-maligno foram estimados em 2013 de acordo com o *Central Brain Tumor Registry of the United States* (CBTRUS) e a última atualização destes casos aconteceu em Novembro de 2012. Estas estimativas são baseadas especificamente em idade, sexo e grupos raciais. (AMERICAN BRAIN TUMOR ASSOCIATION, 2013)

Segundo a Organização Mundial de Saúde (OMS), as taxas de mortalidade e incidência dos tumores cerebrais e tumores do sistema nervoso central (SNC) têm caído um pouco desde a década passada, e os maiores valores diagnosticados são para pessoas brancas quando comparada a outras etnias e para homens quando comparados com as mulheres. Atualmente houve um aumento na incidência de tumores cerebrais sólidos em crianças, chegando a aproximadamente 21% dos tumores diagnosticados, embora a taxa de mortalidade neste grupo tenha caído nas três últimas décadas. Pode-se estimar que US\$ 3.7 bilhões têm sido utilizados para tratamentos desta patologia. (WORLD HEALTH ORGANIZATION, 2011)

De acordo com o Instituto Nacional de Câncer (INCA), as estimativas apontam para 2014 a ocorrência de 4.960 novos casos de câncer do sistema nervoso central (SNC) em homens e 4.130 em mulheres. (INSTITUTO NACIONAL DE CÂNCER, 2014) Durante as últimas décadas, a incidência e a mortalidade dos tumores de SNC aumentaram na maioria dos países desenvolvidos, principalmente nas faixas etárias mais avançadas. Este aumento para a incidência desses tumores é devido à melhoria na pesquisa e introdução de novas tecnologias diagnósticas menos invasivas.

A maioria dos tumores do SNC origina-se do cérebro, dos nervos cranianos e das meninges. Os gliomas são o tipo histológico mais frequente e representam cerca de 40 a 60 % de todos os tumores do SNC e aparecem mais frequentemente em adultos acima dos 45 anos.

Embora não sendo classificados entre os principais tumores que levam à mortalidade por número de pessoas, existe uma grande necessidade de um diagnóstico precoce de tumores cerebrais antes mesmo de ocorrer o desenvolvimento do tumor. Seu desenvolvimento é indicado por um aumento na vascularização, formação de pequenos coágulos ou regiões com crescimento desordenado de células e o estabelecimento do diagnóstico de tumor cerebral nem sempre é um processo simples (INSTITUTO NACIONAL DE CÂNCER, 2010).

Muitas doenças neurológicas não neoplásicas podem mimetizar tumores do SNC nos exames de neuroimagem ou mesmo na avaliação histológica, incluindo esclerose múltipla, acidente vascular cerebral (AVC), abscesso piogênico, cisticercose, infecções fúngicas e outras (OMURO et al., 2006). Os exames radiológicos são de extrema importância para diagnóstico, sendo primeiramente realizada a tomografia computadorizada (TC) de crânio, na qual podem ser observadas as calcificações e a parte cística do tumor. A ressonância magnética nuclear (RMN) também deve ser realizada, por colaborar com informações sobre a extensão, a anatomia do tumor e o planejamento da terapêutica cirúrgica (OMURO et al., 2006).

Estes diagnósticos requerem equipamentos de alto custo e nem todos os pacientes tem acesso a este tipo de “busca” pelo tumor que, ainda assim, são muitas vezes inconclusivos no diagnóstico do tipo do tumor. A única saída é a cirurgia e retirada total do tumor, o que geralmente afeta outras áreas do cérebro, uma vez que nem a região tumoral nem a periferia do mesmo são bem definidas, mesmo utilizando-se cirurgia. Observa-se então uma necessidade de um método de diagnóstico adjuvante que facilite, juntamente com os métodos de imagens, uma rápida e eficiente decisão, evitando a reincidência e assim a invasividade das células tumorais. Nas últimas décadas a nanotecnologia vem trazendo alternativas diagnósticas e terapêuticas nas ciências da vida. Uma delas é a nova classe de marcadores fluorescentes semicondutores denominados pontos quânticos ou *quantum dots* (QDs) os quais apresentam vantagens muito interessantes para uso como sondas *in vitro* e *in vivo* (FONTES et al., 2012).

Neste trabalho será descrita a síntese aquosa de pontos quânticos de CdTe funcionalizados com alquil-tióis e posteriormente conjugados ao anticorpo anti-GFAP (Glial Fibrillar Acidic Protein) para uso na imunomarcacão de células do Sistema Nervoso Central, bem como detecção *in vivo*, pois a maioria das células gliais expressam GFAP. A cultura primária de astrócitos de camundongos suíços machos e da linhagem tumoral humana U87 foi realizada como também um modelo xenográfico em ratos foi desenvolvido. Estes pontos quânticos foram também incorporados em lipossomas com intuito de uma liberaçao mais efetiva destes em células conhecidas (células tronco e hemácias).

Em seguida, os pontos quânticos conjugados e não conjugados foram utilizados para marcação destas células e dos tumores. Estes sistemas foram caracterizados através da microscopia de fluorescência e os tecidos tumorais através da coloração de hematoxilina e eosina, como também através da colocalização com o anticorpo anti-vimentina. Esta Tese está dividida em quatro seções: (1) referencial teórico, (2) objetivos, (3) artigos e capítulo publicado e (4) artigo a ser submetido.

2 REFERENCIAL TEÓRICO

2.1 Células Neurais e Suas Patologias

O termo “neuroglia” (neuro cola) foi introduzido há 150 anos pelo patologista alemão Rudolf Virchow. No final do século XIX, devido ao grande impulso no desenvolvimento e aplicação dos microscópios, foi possível a identificação das unidades estruturais e funcionais do sistema nervoso central (SNC) formado pelos neurônios e os gliócitos ou células gliais. Classicamente, o neurônio é classificado como a unidade morfofuncional deste sistema e a glia era considerada apenas como unidade de apoio, dando sustentação aos neurônios e auxiliando seu funcionamento. Com os recentes avanços da neurociência, foi descoberto que além do trabalho básico da glia anteriormente citado neste texto, estas células são responsáveis pela transmissão de sinais químicos nas sinapses, orientação do crescimento e da migração dos neurônios durante o desenvolvimento, participa da comunicação entre eles na vida adulta, e da defesa e reconhecimento de patologias. Atualmente o termo “neuroglia” ou simplesmente “glia” é utilizado para designar o coletivo de gliócitos (LENT, 2002; WANG; BORDEY, 2008).

Estima-se que haja no sistema nervoso central cerca de 10 células glia para cada neurônio, mas devido ao seu tamanho reduzido, elas ocupam apenas a metade do volume do tecido nervoso (GOMES; TORTELLI; DINIZ, 2013). Atualmente a neuroglia pode ser dividida em dois grupos que são distintos em sua morfologia e função desempenhada, a macroglia, que é de origem ectodermal e a microglia de origem mesodermal. Elas diferem em forma e função e são classificadas em: microglia, astrócitos, oligodendrócitos e células de Schwann. A classificação dos tipos celulares neurogliais se deve muito ao trabalho extenso e as descrições detalhadas sobre essas células, feito por Ramon e Cajal (SOMJEN, 1998)(GOMES; TORTELLI; DINIZ, 2013).

A microglia, que foi descrita primeiramente por Pío Del Río Hortega em 1932, possui um corpo pequeno e alongado, mas com poucos prolongamentos que se ramificam moderadamente, e são representantes imunitários do sistema nervoso, pois desempenham funções de proteção

contra agentes agressores, absorção de partes de neurônios que degeneram ou que morrem por apoptose ou até da regeneração de algumas lesões. Por este motivo, as glias são conhecidas como as células polivalentes do sistema nervoso (LENT, 2002). Geralmente a microglia é recrutada logo após uma infecção, lesão ou até mesmo nas doenças degenerativas do SN.

Os astrócitos são as principais fontes de crescimento para os neurônios e estão presentes em diversas regiões do SNC. Eles possuem grande número de prolongamentos que emergem do soma e se ramificam profundamente, formando uma grande arborização e assim recobrem os vasos sanguíneos participando da barreira hematoencefálica, são envolvidos na sinapse e participam da troca de moléculas entre o líquido cefalorraquidiano e o tecido nervoso. Por outro lado, os oligodendrócitos também possuem prolongamentos que emergem do soma, mas estes não são tão numerosos, nem ramificados como no caso dos astrócitos. São estes que formam as bainhas de mielina quando se enrolam em torno dos axônios centrais (GOMES; TORTELLI; DINIZ, 2013).

Além das caracterizações morfológicas de cada uma dessas células, existem marcadores específicos para elas, que são, como no caso dos astrócitos, a proteína ácida fibrilar glial (GFAP), que é expressa exclusivamente neste tipo de célula, e pode ser localizada no astrócito através de anticorpos monoclonais (anti-GFAP). No caso dos oligodendrócitos, existe a proteína chamada Rip, e na microglia existe uma proteína que é expressa na sua superfície chamada isolectina b4 (ENG; GHIRNIKAR; LEE, 2000)(WANG; BORDEY, 2008).

Recentemente, neurocientistas da Universidade Rockefeller provaram com um estudo feito com a *C. elegans*, uma minhoca muito usada como modelo experimental em diversas áreas de pesquisa, que sem as células gliais, os neurônios sensoriais ficam incapazes de captar estímulos. Este estudo mostra a glia com uma função de suporte assim como também envolvida na sinalização neuronal (REICHENBACH; PANNICKE, 2008).

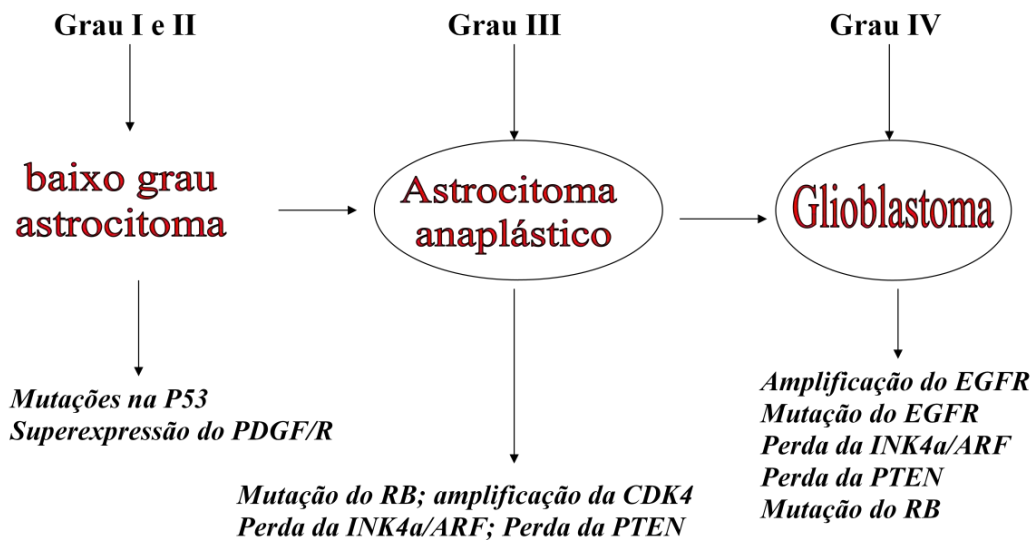
As células gliais podem sofrer algumas mutações as quais dão origem aos tumores gliais, dentre os quais 70% originam de astrócitos. Algumas dessas mutações acontece como uma ativação continuada do receptor do sinal extracelular da proteína do fator de crescimento epidérmico (EGF), através da deleção de parte do domínio extracelular e estes receptores, uma

vez mutados, ainda formam dímeros ativos mesmo na ausência da molécula sinalizadora EGF. Esta mutação é uma das variações mais encontradas em glioblastomas (ALBERTS et al., 2010). As ações desses fatores permitem a proliferação e migração das células tumorais através da modulação de elementos de matriz extracelular, aumentando o estímulo à proliferação microvascular, levando ao aumento do aporte sanguíneo e consequentemente da oxigenação e nutrição da massa tumoral. Desenvolver melhores marcadores para as células tumorais, como por exemplo, novos elementos do citoesqueleto, como a sinemina, é importante para ajudar a classificar melhor o tumor e, portanto, aperfeiçoar o diagnóstico e a intervenção terapêutica.

Os tumores cerebrais de origem neuroepitelial que se desenvolvem a partir de células gliais são chamados de gliomas, que podem também ser chamados de astrocitomas (a partir de astrócitos) e os oligodendrogliomas e ependimomas. O glioblastoma, mais conhecido como glioblastoma multiforme (GBM) é o tipo de astrocitoma de crescimento mais rápido, mais invasivo, e com tendências para metástases invadindo o tecido normal do cérebro e contém áreas de células mortas no centro do tumor. Este tumor é o tipo mais comum de tumor cerebral maligno em adultos e representa cerca de 50% a 60% dos casos (CHARLES et al., 2011). Pode ocorrer em qualquer idade, mas tem uma maior probabilidade entre 50 e 70 anos e ocorre com mais frequência em homens. Este tumor pode ser classificado em primário ou secundário, no primeiro caso, é quando o GBM tem uma origem no SNC sem mostrar nenhuma evidência de lesão pré-existente e acontece mais frequentemente em adultos de faixa etária mais avançada. Por outro lado, os GBM secundários se originam de uma reincidência de um tumor astrocitoma grau II ou III e atingem jovens adultos. Geralmente estes tumores são localizados nos hemisférios cerebrais (SMITH; IRONSIDE, 2007).

Segundo a Organização Mundial da Saúde (OMS), clinicamente os astrocitomas são classificados em quatro graus distintos, sendo o GBM o mais maligno e invasivo entre eles. Quando diagnosticado, o paciente tem de 6 meses a 1 ano de vida e quando passa por processos cirúrgicos para retirada total do mesmo, este tumor tem um alto grau de reincidência (WORLD HEALTH ORGANIZATION, 2011). Na Figura 1 observam-se as mutações existentes e como elas se relacionam na classificação dos tumores cerebrais.

Figura 1. Classificação dos tumores cerebrais pela Organização Mundial de Saúde (OMS).



Onde: P53 – proteína citoplasmática com 53 KDa; PDGF/R - fator de crescimento derivado da plaqueta (ligante) ou o seu receptor (*platelet-derived growth factor receptor*); RB – proteína do retinoblastoma (*retinoblastoma protein*); ARF – ou p14ARF proteína supressora de tumor codificada pelo locus INK4a/ARF; CDK4 – proteína quinase dependente de ciclina; EGFR – receptor epidermal de fator de crescimento; PTEN - gene supressor de tumor.

2.2 Sondas para Histopatologia: aplicação dos Pontos Quânticos ou “Quantum Dots”

Apesar dos avanços cirúrgicos e recentes progressos nas terapias adjuvantes, o prognóstico de pacientes com GBM ainda é muito pouco conhecido e a deterioração sofrida pelos pacientes por causa da progressão do tumor é muito alta. A remoção completa do tumor durante a cirurgia é muito difícil devido à dificuldade para o cirurgião diferenciar o tumor celular (massa tumoral) do tecido tumoral no microambiente. Por isso a remoção incompleta ocorre com bastante frequência e a recorrência do tumor é alta.

Objetivando melhorar esta diferenciação entre tumor celular e periferia tumoral, como também diferenciar as células tumorais das células normais, Jovin e colaboradores começaram a

explorar a bioconjugação por adsorção e por reações de acoplamento, onde QDs de CdSe ligados a EGF ou a anti-EGFR (Her1) são usados para marcação de tumores gliais com alta sensibilidade e especificidade em culturas de células, modelos de ratos e biópsias humanas (ARNDT-JOVIN et al., 2009). A Figura 2 mostra uma biópsia de tumor cerebral humano e o tecido tumoral adjacente ao local onde o tumor estava localizado (mostrado com as setas). A localização tumoral foi ilustrado com ressonância magnética de imagem (MRI, *magnetic resonance imaging*).

Figura 2. Imagem de um corte transversal de cérebro humano obtida por ressonância magnética de imagem. As setas evidenciam a localização de um GBM humano classificado como Grau 4 [retirado de (ARNDT-JOVIN et al., 2009)].

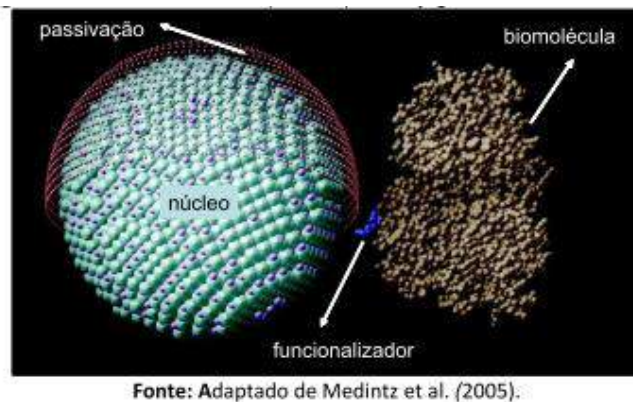


Um dos primeiros trabalhos sobre a preparação e estudos das propriedades de nanocristais fluorescentes de semicondutores do tipo II-VI conhecidos como *quantum dots*, descrevendo a síntese e a caracterização óptica dos compostos, aconteceu no início da década de 80, mas somente em 1998, com os trabalhos independentes do grupo do Prof. Paul Alivisatos (University of Berkeley, EUA) e do grupo do Prof. Shuming Nie (Massachusetts Institute of Technology, EUA) que se começou a ideia do uso dos QDs como potenciais marcadores fluorescentes para sistemas biológicos (BRUCHEZ JR., 1998)(PENG; WICKHAM; ALIVISATOS, 1998)

Nas últimas décadas, um aumento exponencial no uso de QDs como sondas para diagnósticos de doenças tem sido observado, devido às grandes vantagens exibidas por esses nanocristais de semicondutores frente aos corantes orgânicos convencionais, que sofrem fotodegradação rapidamente e alguns são tóxicos em meio celular. Isso também ocorre devido ao melhoramento dos equipamentos para microscopia por fluorescência, que tem como vantagem a aquisição de imagens quase que em tempo real, como também do avanço nas técnicas de citometria de fluxo entre outras (AL-HAJAJ et al., 2011).

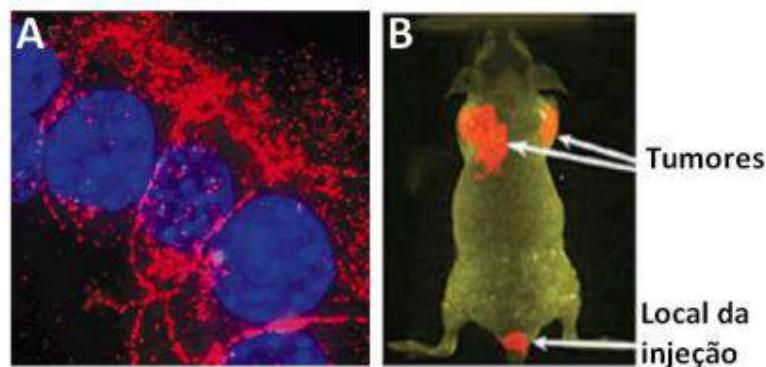
Atualmente existem várias aplicações dos QDs em marcações celulares *in vitro* e *in vivo*, como também é bem vasto seu uso em diagnóstico, devido ao fato de estes nanocristais apresentarem consideráveis vantagens tais como: (i) propriedades ópticas dos QDs (absorção e emissão) que mudam de acordo com o tamanho deles; (ii) largos espectros de absorção eletrônica fazendo com que com uma única fonte de luz se consiga excitar a luminescência destas nanopartículas, (iii) possibilidade de sondas que emita em todas as regiões de interesse do espectro eletromagnético (i.e. ultravioleta próximo, visível e infravermelho próximo); (iv). suspensões de QDs não sofrem fotodegradação, (v) possuem um estreito espectro de emissão (larguras de banda < 70 nm); (vi) superfícies quimicamente ativas possuindo grande capacidade de interação com material biológico; (vii) podem ser utilizados em ensaios *in vivo* e *in vitro* e por um tempo de incubação e análise mais longo. A Figura 3 mostra a estrutura de um *quantum dot* de semicondutor e as possíveis modificações na superfície do mesmo, como por exemplo, funcionalização ou bioconjugação para se obter uma melhoria nas propriedades ópticas e variação nas aplicações destes nanocristais (FONTES et al., 2012).

Figura 3 Esquema de um nanocristal de semiconductor (QD) funcionalizado com uma proteína.



Dentre outros exemplos na literatura, True e colaboradores mostraram em 2007 que os *quantum dots* começaram a ter um papel muito importante na patologia molecular, sendo usados como sondas fluorescentes com múltipla marcação de tumores malignos. Este trabalho reportou a comparação entre metodologias que utilizam marcadores como fluoróforos orgânicos, ensaios imunoenzimáticos, QDs, nanopartículas de ouro e prata, os quais permitem análise *in situ* de tecido tumoral. Dentre estes marcadores, os QDs foram destacados pela alta capacidade de multi marcação, pela alta capacidade de quantificação e pela alta sensibilidade na detecção (GAO et al., 2004)(TRUE; GAO, 2007) . Gao e colaboradores conseguiram marcar um tumor *in vivo* utilizando QDs que possuem emissão no vermelho (Figura 4).

Figura 4. (A) O tecido mamário, onde os QDs (vermelhos) se ligam especificamente a receptores Her2. (B) Visualização dos tumores *in vivo*

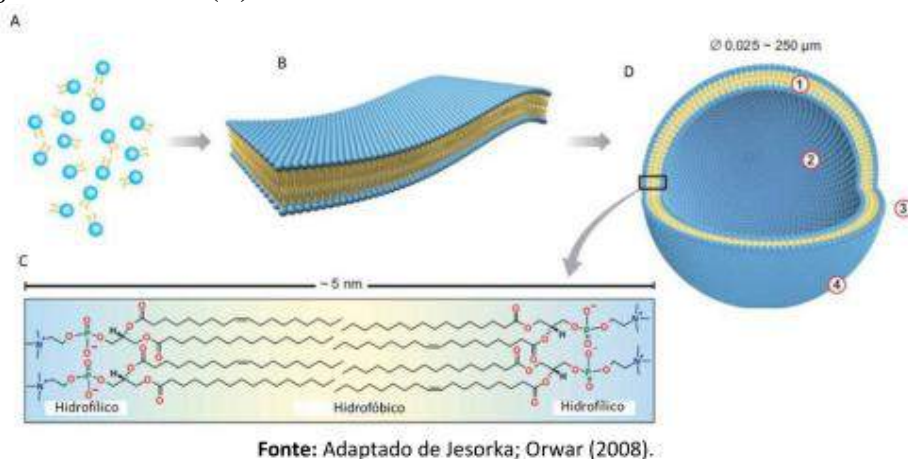


Fonte: Adaptado de Gao et al. (2004).

Uma outra forma de entrega destes pontos quânticos para dentro das células ou tecidos é através do uso dos lipossomas, que são estruturas esféricas, onde a fase aquosa é cercada por uma camada ou bicamada composta por fosfolipídeos em forma de vesículas, sendo muito utilizadas como modelo simplificado de membrana e para o encapsulamento de substâncias ativas hidrofílicas e lipofílicas. As substâncias hidrofílicas se encontram dentro das vesículas (no compartimento aquoso) enquanto que as lipofílicas encontram-se inseridas ou adsorvidas na bicamada lipídica (BATISTA; CARVALHO; MAGALHÃES, 2007). A escolha do(s) fosfolipídio(s) formador(es) dos lipossomas depende muito da aplicação que se quer obter com o uso das vesículas.

A Figura 5 mostra a estrutura química dos fosfolipídeos, os quais possuem uma cabeça polar (que confere o caráter hidrofílico) e duas caudas de hidrocarboneto hidrofóbicas (característica que confere a dupla camada lipídica). As caudas são normalmente ácidos graxos com diferenças no comprimento e na presença ou não de duplas ligações, o que influi na fluidez da membrana. O esquema ilustrado na Figura 5 demonstra a formação da vesícula lipossomal mostrando o interior hidrofílico (JESORKA; ORWAR, 2008).

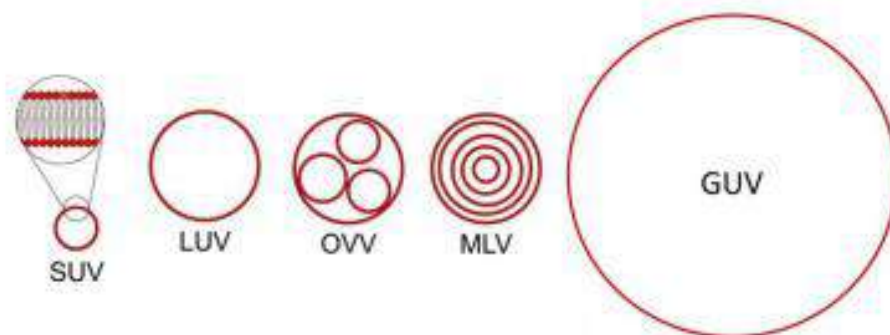
Figura 5. Sequência de formação de lipossomas: (A) fosfolipídeos, (B) formação da bicamada, vesícula formada (D), onde há o rearranjo da bicamada em solução para não expor a região hidrofóbica (C).



Morfologicamente, os lipossomas podem ser classificados de acordo com o número de camadas que possuem. Neste caso podem ser unilamelares, com uma única camada, ou

multilamelares (MLVs), que apresentam mais de uma camada. As unilamelares podem ser classificadas de acordo com o tamanho sendo, portanto caracterizadas como lipossomas unilamelares pequenos (SUVs), lipossomas unilamelares grandes (LUVs) e finalmente os lipossomas unilamelares gigantes (GUVs), como ilustrado na Figura 6. Outra forma de classificação destas vesículas é de acordo com o método de preparação das mesmas, que pode ser obtenção através da evaporação em fase reversa (REV), obtidas em prensa de French (FPV), como também aquelas obtidas por injeção de éter (EIV) (BATISTA; CARVALHO; MAGALHÃES, 2007; LASIC, 1998).

Figura 6 Morfologia dos lipossomas de acordo com o tamanho e com a quantidade de camadas. SUVs, LUVs e GUVs possuem uma única bicamada. Os OVVs possuem outras vesículas no seu interior e o MLVs possuem multicamadas.



Com o avanço nos estudos e nas aplicações dos lipossomas, podendo também ser classificados de acordo com as interações com sistemas biológicos (TORCHILIN, 2005) (AL-JAMAL et al., 2009). Neste caso, os lipossomas podem ser convencionais, de longa duração (Furtivos ou Stealth®), sítio específico ou direcionados e os lipossomas polimórficos.

Os lipossomas convencionais geralmente são formados por fosfolipídeos e colesterol e às vezes pode ter outro fosfolipídeo positiva ou negativamente carregado, evitando assim o processo de agregação das vesículas quando em formação, dando origem a vesículas mais estáveis quando em suspensão. No entanto, o que se observa com o uso deste tipo de lipossoma, é o reconhecimento pelas células fagocíticas e a rápida eliminação através da circulação (BATISTA; CARVALHO; MAGALHÃES, 2007).

Objetivando uma longa duração dos lipossomas na corrente sanguínea e para estes não serem reconhecido pela opsoninas e não serem fagocitados, em geral os lipossomas são revestidos com componentes hidrofílicos naturais ou com polímeros hidrofílicos sintéticos, como por exemplo, o polietilenoglicol (PEG). Este tipo de lipossoma também é chamado furtivo. Existem também os lipossomas sítios específicos ou direcionados, que são aqueles que interagem especificamente com uma célula alvo, ou que reconhecem receptores de membrana. Estes podem ser classificados em: (i) imunolipossomas (contêm um anticorpo na superfície) (AL-JAMAL et al., 2009), (ii) lipossomas carreadores de proteínas e lipídeos e, também, (iii) virossomas que contém hemaglutinina na superfície.

Atualmente existem vários estudos utilizando lipossomas polimórficos. Estes são caracterizados por sofrerem modificação estrutural induzida por uma alteração no pH da solução, temperatura ou até mesmo mudança na carga eletrostática na sua estrutura e assim se tornam bastante reativos. Os imunolipossomas e lipossomas catiônicos estão sendo muito estudados como veículos e entrega direcionada de fármacos e QDs, como também nas terapias gênicas utilizando RNAs e DNAs virais (AL-JAMAL et al., 2009)(WENG et al., 2008)(PERRIE; GREGORIADIS, 2000).

No caso dos lipossomas fusogênicos, estes podem fundir a sua bicamada com a membrana celular e com isso entregar fármacos e nanopartículas conjugadas ou não, no interior das células, ultrapassando assim o efeito hidrofóbico da bicamada (LIRA et al., 2013).

A motivação deste trabalho encontra-se no uso dos QDs conjugados com o anticorpo anti- proteína glial fibrilar ácida (GFAP) ou encapsulados em lipossomas para entrega e marcação de tumores cerebrais, pois até esta data, ainda não existem trabalhos na literatura que relatam a entrega destes sistemas nanoestruturados em pacientes com câncer cerebral do tipo glioblastoma *in vivo*. Com isso pretendemos desenvolver uma sonda fluorescente para marcação de tecidos patológicos como também ajudar o neurocirurgião na identificação dos tumores e completa remoção dos mesmos, evitando com isso a reincidência tumoral.

3 OBJETIVOS GERAL E ESPECÍFICOS

3.1 Objetivo Geral

Desenvolver uma sonda histopatológica baseada em pontos quânticos de telureto de cádmio para a detecção e diagnóstico *in vivo* de tumores cerebrais do tipo glioblastoma multiforme.

3.2 Objetivos Específicos

- Sintetizar os pontos quânticos de CdTe (telureto de cádmio) funcionalizados com diferentes funcionalizantes alquil-tióis em água e caracterizar estes QDs óptica- e estruturalmente.
- Realizar os ensaios de toxicidade com MTT dos pontos quânticos de CdTe nas células de tumores humanos da linhagem U87.
- Conjuguar quimicamente estes pontos quânticos com o anticorpo anti-GFAP e caracterizar opticamente através do espectro de absorção e emissão, como também medir a eficiência da conjugação através de leitura de placa.
- Preparar lipossomas a partir da fosfatidilcolina e do 1,2-dioleoyl-3-trimetilammonium-propane (DOTAP) e encapsular os pontos quânticos. Caracterizar estes sistemas por microscopia de fluorescência, microscopia eletrônica de transmissão como também pela medida do tamanho e do potencial zeta.
- Cultivar astrócitos em cultura primária, e as células de tumores humanos da linhagem U87
- Desenvolver um protocolo de marcação dos astrócitos e das células tumorais com os pontos quânticos sem e com anticorpo anti-GFAP. Caracterizar estas marcações através de microscopia de fluorescência.
- Desenvolver modelo xenográfico em camundongos suíços para crescimento dos tumores de glioblastoma. Marcação dos tumores com os pontos quânticos.

- Realizar identificação histológica dos cortes cerebrais utilizando-se a coloração hematoxilina e eosina e identificação de tecido tumoral por microscopia de fluorescência.

4 RESULTADOS

Os resultados desta tese são descritos em cada artigo anexados nos apêndices B à D.

Os resultados do artigo do apêndice B mostram a síntese aquosa dos QDs CdTe estabilizado com MPA realizada com eficiência e com caracterização feita através dos espectros de absorção e emissão como também difração de raio-x confirmando que estes QDs possuem $d=2.6$ nm com uma máximo de emissão em 551 nm e FWHM= 50 nm. QDs foram utilizados para marcação de PBMCs permeabilizadas artificialmente. Estes QDs estavam localizados no citoplasma sugerindo que eles entraram no interior das células de forma homogênea e interagiram com algumas estruturas intracelulares, mostrando assim interações não-específicas. Potencial zeta antes e depois da incubação também foram medidos e estes resultados corroboram mostrando uma interação entre estes QDs e as PBMCs permeabilizadas.

O artigo do apêndice C retrata o estudo da entrega dos QDs CdTe estabilizados com MPA dentro de células troncos do cordão umbilical de humanos feitos através do uso dos lipossomas. O encapsulamento destes QDs em lipossomas fusogênicos contendo DOTAP foi realizado com sucesso através do método de congelamento e descongelamento. DOTAP, um fosfolípido positivo, foi utilizado neste estudo para modificar o potencial negativo de membrana ajudando assim na entrega dos QDs no interior das células. Este método de encapsulamento de QDs não foi eficiente para a obtenção de imunolipossomas pois o mesmo é muito forte quando utilizado com anticorpos modificando as propriedades desse material. Futuros estudos são necessários para um maior entendimento dessas interações entre QDs e células viáveis como também para o esclarecimento das vias de entrega utilizadas por esses nanocristais.

Os resultados obtidos no manuscrito do apêndice D ainda estão sendo submetidos. Neste trabalho a síntese aquosa dos QDs CdTe estabilizados com AMS e a bioconjugação destes QDs com o anticorpo anti-GFAP foram realizadas com sucesso. O estudo da toxicidade destes QDs foi realizado *in vitro* através do MTT em astrócitos do cérebro de camundongos machos como também em células U87 mostrando uma decrescente viabilidade celular a partir de 1 hora de incubação. QDs CdTe com AMS foram entregues em um tumor glioblastoma U87

xenotransplantado e através das caracterizações das colorações histopatológicas, microscopia de fluorescência e imunohistoquímica pode-se confirmar esta entrega específica. Estes QDs são de fácil preparação e de baixo custo e são disponíveis para serem utilizados como sondas histopatológicas em ajuda durante a cirurgia para uma melhor acessividade ao tumor glioblastoma.

5 CONCLUSÕES E PERSPECTIVAS

5.1 Conclusões

Foram sintetizados pontos quânticos de telureto de cádmio estabilizados com ácido mercaptosuccínico e mercaptopropiônico de tamanhos entre 2.8 a 3.3 nm e todos os QDs possuem arranjo cúbico tipo blenda de zinco.

A partir dos ensaios de toxicidade dos QDs, os mesmos mostraram-se tóxicos a partir de 1 hora de incubação com os astrócitos como também quando incubados com as células U87.

Estes pontos quânticos foram encapsulados em lipossomas contendo fosfatidilcolina com DOTAP com sucesso utilizando-se o método de congelamento e descongelamento.

Pontos quânticos de Telureto de Cádmio (CdTe) bioconjugados com o anticorpo GFAP mostraram-se eficientes como sonda fluorescente e específica para detecção de células tumorais U87 *in vitro* e *in vivo*.

Durante a realização deste trabalho houveram algumas dificuldades no encapsulamento destes pontos quânticos em lipossomas neutros e catiônicos, pois com o uso deles não foi evidenciada a liberação destes marcadores nas células tanto *in vitro* quanto *in vivo*. Estudos futuros são necessários para explorar esta outra características destes nanocristais.

5.2 Perspectivas

As perspectivas deste trabalho consistem em realizar estudos de toxicidade dos conjugados CdTe-MSA-anti-GFAP e síntese de QDs tipo CdTe com diferentes funcionalizantes com menor potencial tóxico. Como também repetir os experimentos *in vitro* com a linhagem celular de tumor humano U87 e GL261 (tumor de rato) utilizando diferentes QDs. Outro ponto importante é a preparação do imunolipossoma por outros métodos para entrega específica dos

QDs conjugados e isolados e assim testar as mesmas condições dos experimentos in vivo utilizando camundongos nude. Testar QDs conjugados com EGF com emissão no verde e também utilizar o CdTe-MSA com emissão no vermelho para realizar uma dupla marcação.

REFERÊNCIAS

- ALBERTS, B. et al. **Biologia Molecular da Célula**. 5a Ed ed. Porto Alegre RS: Artmed, 2010.
- AL-HAJAJ, N. A et al. Short ligands affect modes of QD uptake and elimination in human cells. **ACS nano**, v. 5, n. 6, p. 4909–18, 28 jun. 2011.
- AL-JAMAL, W. T. et al. Tumor targeting of functionalized quantum dot-liposome hybrids by intravenous administration. **Molecular pharmaceuticals**, v. 6, n. 2, p. 520–30, 2009.
- AMERICAN BRAIN TUMOR ASSOCIATION. **Brain Tumor Statistics**. Disponível em: <<http://www.abta.org/about-us/news/brain-tumor-statistics/>>. Acesso em: 16 mar. 2014.
- ARNDT-JOVIN, D. J. et al. Tumor-targeted quantum dots can help surgeons find tumor boundaries. **IEEE transactions on nanobioscience**, v. 8, n. 1, p. 65–71, mar. 2009.
- BATISTA, C. M.; CARVALHO, C. M. B. DE; MAGALHÃES, N. S. S. Lipossomas e suas aplicações terapêuticas: estado da arte. **Revista Brasileira de Ciências Farmacêuticas**, v. 43, n. 2, p. 167–179, jun. 2007.
- BRUCHEZ JR., M. Semiconductor Nanocrystals as Fluorescent Biological Labels. **Science**, v. 281, n. 5385, p. 2013–2016, 25 set. 1998.
- CHARLES, N. A et al. The brain tumor microenvironment. **Glia**, v. 59, n. 8, p. 1169–80, ago. 2011.
- ENG, L. F.; GHIRNIKAR, R. S.; LEE, Y. L. Glial fibrillary acidic protein: GFAP-thirty-one years (1969-2000). **Neurochemical research**, v. 25, n. 9-10, p. 1439–51, out. 2000.
- FONTES, A. et al. Quantum Dots in Biomedical Research. In: RADOVAN HUDAK, M. P. AND J. M. (Ed.). . **Biomedical Engineering-Technical Applications in Medicine**. Rijeka, Croatia: InTech, 2012. v. 232p. 269–290.
- GAO, X. et al. In vivo cancer targeting and imaging with semiconductor quantum dots. **Nature biotechnology**, v. 22, n. 8, p. 969–76, ago. 2004.
- GOMES, F. C. A.; TORTELLI, V. P.; DINIZ, L. Glia: dos velhos conceitos às novas funções de hoje e as que ainda virão. **Estudos Avançados**, v. 27, n. 77, p. 61–84, 2013.
- INSTITUTO NACIONAL DE CÂNCER. **Câncer no Brasil**. [s.l: s.n.].
- INSTITUTO NACIONAL DE CÂNCER. **Incidência de Câncer no Brasil, 2014, Estimativa**. Disponível em: <<http://www.inca.gov.br/estimativa/2014/estimativa-24012014.pdf>>. Acesso em: 16 mar. 2014.

- JESORKA, A.; ORWAR, O. Liposomes: technologies and analytical applications. **Annual review of analytical chemistry (Palo Alto, Calif.)**, v. 1, p. 801–32, jan. 2008.
- LASIC, D. Novel applications of liposomes. **Trends in Biotechnology**, v. 16, n. 7, p. 307–321, 1 jul. 1998.
- LENT, R. **Cem Bilhões de Neurônios: Conceitos Fundamentais de Neurociências**. 2nd. ed. São Paulo: Atheneu, 2002.
- LIRA, R. B. et al. Studies on intracellular delivery of carboxyl-coated CdTe quantum dots mediated by fusogenic liposomes. **Journal of Materials Chemistry B**, v. 1, n. 34, p. 4297, 2013.
- NATIONAL INSTITUTE OF CANCER. **Report to nation finds continued declines in many cancer rates**. Disponível em: <http://www.cancer.gov/newscenter/pressreleases/2011/ReportNation2011Release>. Acesso em: 20 set. 2011.
- OMURO, A. M. et al. Pitfalls in the diagnosis of brain tumours. **Lancet neurology**, v. 5, n. 11, p. 937–48, nov. 2006.
- PENG, X.; WICKHAM, J.; ALIVISATOS, A. P. Kinetics of II-VI and III-V Colloidal Semiconductor Nanocrystal Growth: “Focusing” of Size Distributions. **Journal of the American Chemical Society**, v. 120, n. 21, p. 5343–5344, jun. 1998.
- PERRIE, Y.; GREGORIADIS, G. Liposome-entrapped plasmid DNA: characterisation studies. **Biochimica et biophysica acta**, v. 1475, n. 2, p. 125–32, 3 jul. 2000.
- REICHENBACH, A.; PANNICKE, T. Neuroscience. A new glance at glia. **Science (New York, N.Y.)**, v. 322, n. 5902, p. 693–4, 31 out. 2008.
- SMITH, C.; IRONSIDE, J. W. Diagnosis and pathogenesis of gliomas. **Current Diagnostic Pathology**, v. 13, n. 3, p. 180–192, jun. 2007.
- SOMJEN, G. G. Nervenkitz: Notes on the history of the concept of neuroglia. **Glia**, v. 1, n. 1, p. 2–9, 1998.
- TORCHILIN, V. P. Recent advances with liposomes as pharmaceutical carrier. **Nature Rev. Drug Disc.**, v. 4, p. 145–160, 2005.
- TRUE, L. D.; GAO, X. Quantum dots for molecular pathology: their time has arrived. **The Journal of molecular diagnostics : JMD**, v. 9, n. 1, p. 7–11, mar. 2007.
- WANG, D. D.; BORDEY, A. The astrocyte odyssey. **Progress in neurobiology**, v. 86, n. 4, p. 342–67, 11 dez. 2008.

WENG, K. C. et al. Targeted Tumor Cell Internalization and Imaging of Multifunctional Quantum Dot-Conjugated Immunoliposomes in Vitro and in Vivo 2008. **Nano**, 2008.

WORLD HEALTH ORGANIZATION. **WHO | World Health Organization**. Disponível em: <<http://www.who.int/en/>>. Acesso em: 15 set. 2011.

APÊNDICES

Apêndice A: Quantum Dots in Biomedical Research

Livro: "Biomedical Engineering - Technical Applications in Medicine"

Classificação Qualis (Farmácia): N/A

Autores: Adriana Fontes, Rafael Bezerra de Lira, Maria Aparecida Barreto Lopes Seabra, Thiago Gomes da Silva, Antônio Gomes de Castro Neto and Beate Saegesser Santos

Ano: 2012

Quantum Dots in Biomedical Research

Adriana Fontes, Rafael Bezerra de Lira,
Maria Aparecida Barreto Lopes Seabra, Thiago Gomes da Silva,
Antônio Gomes de Castro Neto and Beate Saegesser Santos

Additional information is available at the end of the chapter

<http://dx.doi.org/10.5772/50214>

1. Introduction

Quantum dots (QDs) are colloidal semiconductor nanocrystals which have unique optical properties due to their three dimensional quantum confinement regime. The quantum confinement may be explained as follows: in a semiconductor bulk material the valence and conduction band are separated by a band gap (E_g). After light absorption, an electron (e^-) can be excited from the valence band to the conduction band, leaving a hole (h^+) in the valence band. When the electron returns to the valence band, fluorescence is emitted. During the small time scale of the light absorption the e^- and h^+ perceive one another and do not move so independently due to Coulomb attraction (Brus, 1984). The e^- - h^+ pair may be observed as an Hydrogen-like species called exciton and the distance between them is called the exciton Bohr radius (a_B). When the three dimensions of the semiconductor material are reduced to few nanometers and the particles become smaller than the Bohr radius, one can say that they are in quantum confinement regimen and in this situation these nanoparticles are named quantum dots (QDs). For example, the exciton Bohr radius of CdS and CdSe bulk materials presents a size of $a_B = 3$ to 5 nm.

In this way, QDs can be defined as colloidal particles made of semiconductor materials with diameters ranging typically from 2 to 10 nm. The semiconductor particle (named "core") is usually coated by a layer of another semiconductor material (named "shell") which in general has a greater band gap than the band gap of the core rendering excellent optical properties. The QDs' core is responsible for the fundamental optical properties (i.e. light absorption and emission) and the shell is used to passivate the surface of the core with the goal to improve its optical properties and reduce chemical attack. The shell separates physically the optically active core from its surrounding medium (Dabbousi *et al.*, 1997; Santos *et al.*, 2008a) as depicted in Figure 1. As a consequence, the nanoparticles' optical properties become less sensitivity to changes induced, for example, by the presence of

oxygen or pH in the local environment. At the same time, the shell reduces the number of surface dangling bonds, which can act as trap states for electrons and minimize the QDs fluorescence efficiency.

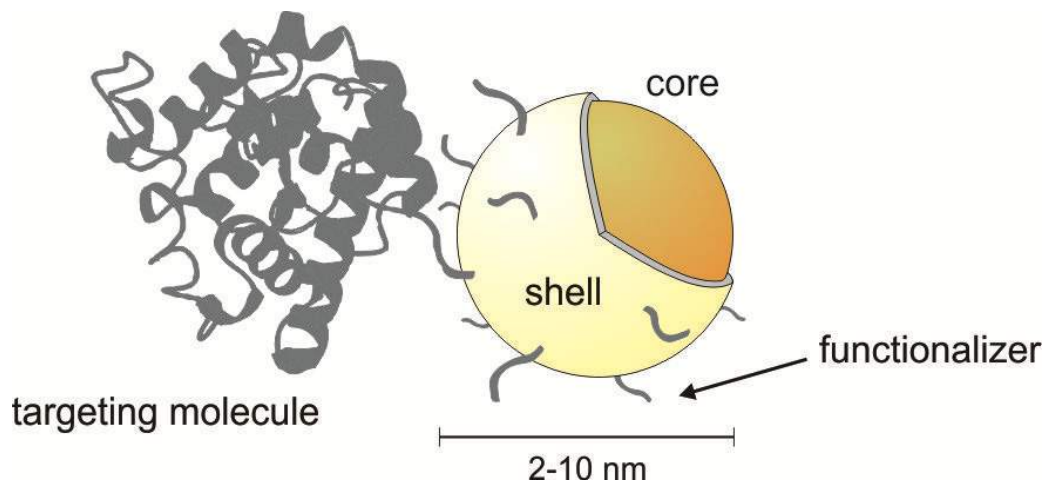


Figure 1. A schematic representation of a functionalized core-shell quantum dot bound to a biomolecule.

For biomedical purposes, in which fluorescence in the visible region is usually required, both core and shell are composed of elements from the II B and VI A groups of the Periodic Table. The major examples are CdSe/ZnS, CdTe/CdS and ZnSe/ZnS QDs (Dabbousi *et al.*, 1997; Santos *et al.*, 2008a). Most QDs crystallize either in the cubic zinc blend or in the hexagonal wurtzite type structure (Yeh *et al.*, 1992).

In nanosized regime many QDs' physico-chemical properties are different from those of the same bulk materials. Since QDs are fluorescent nanoparticles, an example of these changes is the shift of the emission color according to the particle size. In this case, QDs made from the same material, but with different sizes, can present fluorescence light emission in different spectral regions (from the ultraviolet to the infrared light) as represented in Figure 2. This is a consequence of QDs energy level discretization and also of the QDs band gap energy changes according to their size. After absorption, electrons come back to valence band and QDs emission is proportional to the band gap energy. As smaller the QDs are, the higher is the band gap energy and more towards to the blue end is the emission (since the energy is inversely proportional to the wavelength of the light).

Another observed feature for these systems is that the QDs' absorption bands are broad and extend up to the UV region, as observed in Figure 3 (A). The first peak (located at greater wavelength) represents an exciton formed by transitions between discrete states. The width of the first absorption band is related to the size dispersion of the nanoparticles and can give us information about the QDs' average size and nanoparticles concentration (Santos *et al.*, 2008a). On the other hand, the width of the emission spectrum is related to the presence of crystal defects which result in discrete electronic states between the conduction and the valence band. These new electronic states displace the emission towards to the red and broaden the emission band and is related to the passivation shell.

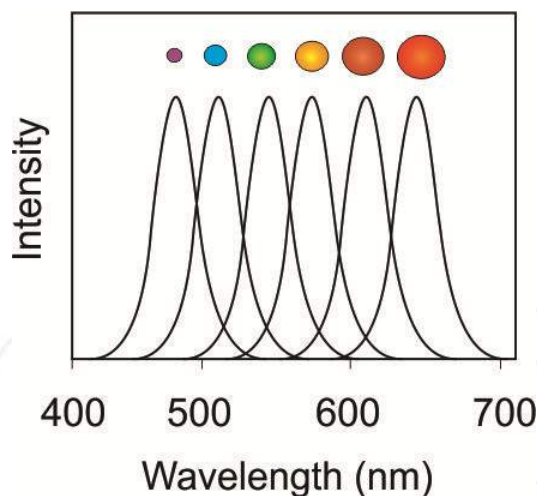


Figure 2. Emission spectra as a function of size for the same quantum dot material. The colored spheres represent the size decrease of the particles.

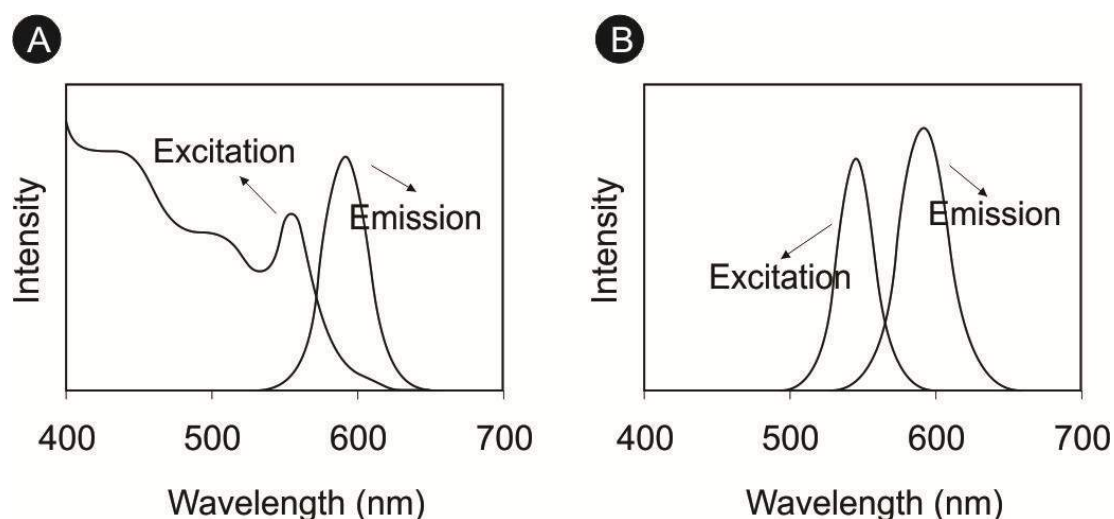


Figure 3. Characteristic absorption and emission band profile of (A) QDs colloidal suspension (A) and (B) a typical organic fluorophore (B).

The QDs' physico-chemical properties have offered considerable advantages and complementary characteristics over the conventional fluorescent dyes. Besides the size tunable emission discussed before, compared to organic fluorophores, the major advantages offered by QDs are:

1. A broad absorption band (Fig. 3A), allowing a flexible cross section for multiphoton microscopy and as well as for Fluorescence Energy Transfer (FRET) processes (Fig. 3A and B compare the characteristic absorption and emission band profiles of QDs and organic fluorophores).
2. An active surface for chemical conjugation. QDs can be conjugated to a variety of proteins or antibodies and become inorganic-biological hybrids nanoparticles that

combine characteristics of both materials, that is, the fluorescence properties of QDs with the biochemical functions of the attached biomolecules (Fig. 1).

3. High resistance to photobleaching: the most important advantage of QDs over organic dyes allowing long term observation of these fluorescent nano-probes.

Colloidal QDs can be synthesized in organic or aqueous medium. When compared to organometallic routes, water-based QDs syntheses are cheaper, less toxic and intrinsically biocompatible to applications in biomedical fields (Santos *et al.*, 2008a). The colloidal synthesis generally involves several consecutive stages: (i) nucleation from an initially homogeneous solution, (ii) growth of the preformed crystal nuclei into isolated particles, reaching the desired size from the reaction mixture and (iii) post preparative treatments, such as colloidal purification, size precipitation and UV light exposure.

During the colloidal synthesis QDs end up coated by organic or inorganic molecules (called surfactants or stabilizers), which keep the nanocrystals away from each other preventing agglomeration and precipitation (Brus, 1984; Santos *et al.*, 2008a) (Figure 1). In some cases, as for CdTe QDs for example, the surfactant molecules may also act as precursors of the passivation shell (Menezes *et al.*, 2005). For the direct aqueous synthetic procedures the main classes of organic molecules used as surfactants are alkyl-thiol molecules such as mercaptopropionic acid - MPA, mercaptoacetic acid - MAA and mercaptosuccinic acid - MSA, Dihydrolipoic acid - DHLA, cysteine - CYS, cysteamine - CYSAM and different mercaptodithiols. The carboxyl, thiol or amine terminals of these molecules can be used as chemical bridges to conjugate biomolecules (such as proteins and biopolymers) which confer more specificity for biological applications. The chemical binding of such biomolecules to the surface of the QDs is a process defined as bioconjugation. It can be accomplished by simple adsorption (of stabilizing agent such as: MPA, MSA or cysteine) to the biomolecule or by covalent attachment. Currently, bioconjugation occurs between carboxyl-amine (through EDC and Sulfo-NHS) groups, amine-amine (by glutaraldehyde), disulfide bonds and streptavidin-biotin interactions (Goldman *et al.*, 2002).

For the non-aqueous synthetic routes, nucleation and growth of QDs occur in the solution phase in the presence of organic surfactant molecules, which dynamically adhere to the surface of growing crystals. Typical surfactants include long-chain carboxylic and phosphonic acids (e.g., oleic acid and *n*-octadecylphosphonic acid), alkanethiols (e.g., dodecanethiol), alkyl phosphines, alkylphosphine oxides (classical examples are trioctylphosphine, TOP, and trioctylphosphine oxide, TOPO), and alkylamines such as hexadecylamine (Yin & Alivisatos, 2005). In order to be applied to biological systems as active fluorophores these nanocrystals must be extracted from the organic phase to an aqueous phase. An alternative method of dispersing non-aqueous QDs is to form a hydrophilic coating that carries along with it a layer of hydration consisting of hydrogen-bonded water molecules. This often is accomplished by using hydroxyl bearing polymers or Polyethylene glycol (PEG) modifications. These also prevent aggregation due to the high energy needed to remove the bound water layer.

2. Applications of quantum dots in biomedical sciences

Since the first mention in the literature, in 1998, QDs have been studied extensively and the applications of these fluorescent nanocrystals range from imaging fixed and live cells all the way to fluoroimmunoassays rendering innovative diagnostic methodologies (Bruchez Jr. *et al.*, 1998; Chan & Nie, 1998). QDs have been used in many different studies, such as a probe in DNA hybridization, in receptor mediated endocytosis, monitoring of parasite metabolism and visualization of tissue and cellular structures in real time. Due to their photostability and low cytotoxicity the QDs are starting to be used as fluorophores for *in vivo* applications, but there is still a great discussion about their safe use. When injected in the initial stage of embryonic development of *Xenopus embryos*, for instance, the QDs demonstrated to be stable, non-toxic and resistant to photobleaching (Dubertret *et al.*, 2002). This experiment also showed its potential in monitoring the development and cellular differentiation processes that occur during embryogenesis. The use of QDs as fluorophores is important for the real time diagnosis of tumors. Preliminary experiments with QDs emitting in the near infrared conducted in animals have shown promising results in the sensitive detection of cancerous tumors and *in vivo* systems (Cai *et al.*, 2006; Gao *et al.*, 2010). The prospects of the applications of QDs, especially those free of heavy metals such as zinc based QDs, make them even more promising for its current use in the near future. Moreover, cells labeled with QDs can be injected in small animals and the fluorescence can be used to follow a particular pathway in the organism, such as the carcinogenesis process, helping to understand the process and discover new kinds of treatments (Noh *et al.*, 2008).

2.1. Quantum dots as fluorophores for imaging and detection purposes

2.1.1. Non-specific labeling

The staining of a biological sample can occur even when the reporting probe is not designed to interact with a specific molecule. Untargeted labeling of the probe with the (biological) material is defined as a *non-specific interaction*, and can be usually mediated by hydrophobic and/or electrostatic interactions between the surface molecules of the particles with molecules in suspension or on the anchoring surface such as cellular plasma membrane or even by internalization process (Biju *et al.*, 2010).

In the past years, when the use of QDs in biomedical research was still at the beginning, passive labeling (simple staining of biological samples) was of great interest since researchers aimed to study the probe itself as a potential dye. In such applications, labeling could give information about bioavailability and more importantly about the optical properties of these nanoparticles in biological conditions. It has been shown that the simple incubation with a biological specimen may have the potential to stain it, revealing its structural features or even their biological behavior. We observed this feature for instance in the non-targeted glutaraldehyde-capped CdS/Cd(OH)₂ QDs staining of different neural cell lines, normal and cancerous cells (Santos *et al.*, 2008b) as demonstrated in the staining pattern observed in Figure 4 (A – D). For these systems the unrestricted labeling/internalization allows the identification of minor details of the cellular architecture, such as cell-cell contacts, axons and

intracellular organelles, as shown on the images of Fig. 4A and Fig. 4B. Moreover, these QDs are taken up at different rates depending on cellular stage as for normal glial or glioblastoma cells (Farias *et al.*, 2006) – Figures 4C and 4D, respectively. Therefore, passive labeling can be a useful strategy when one aims to label the whole biological sample or to study differences in the behavior of normal *versus* cancer cells in diagnostic purposes.

2.1.2. Internalization of quantum dots by live cells

In general, the binding of non-targeted particles with living cells results in internalization of the particles. This process may be accomplished by different routes, which depend either on the particle properties (size, shape, surface functionalization, surface charge and the combination of these properties) or on the cell type (i.e. lineage, metabolic state, cell cycle stage, normal or cancerous cells). The first assumption was that the main internalization process resulted from endocytosis. One of the first reports to show that internalization of these nanoparticles occurs by endocytosis was described by Jaiswal *et al.* (Jaiswal *et al.*, 2003), where human cancer (HeLa) cells and *Dictyostelium discoideum* amoeba cells internalize negatively-charged DHLA-capped QDs, a process inhibited by low temperature treatment and co-localized with endosome markers.

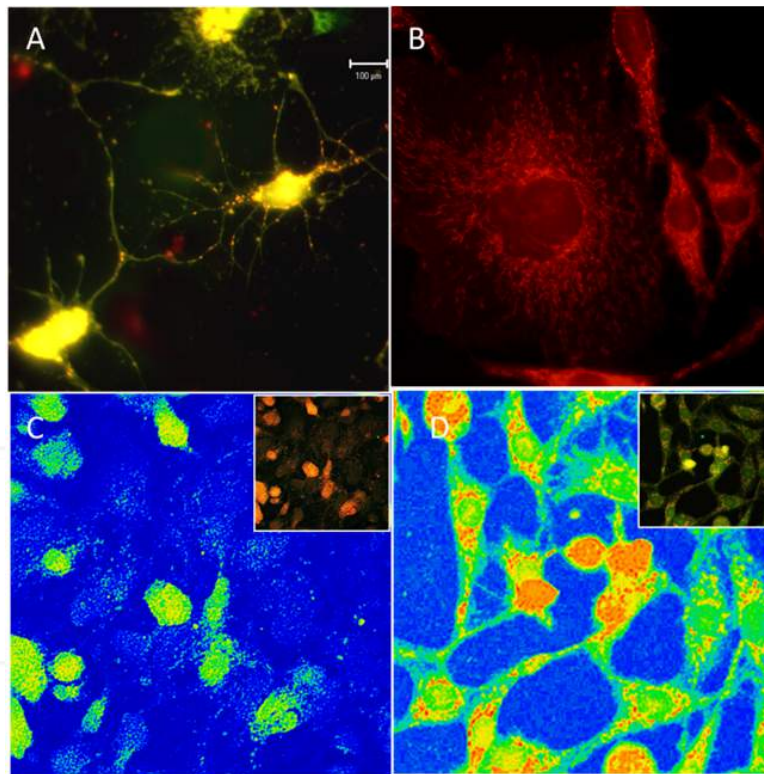


Figure 4. Non-targeted glutaraldehyde-capped CdS/Cd(OH)_2 labeling of live neuron live cells (A) and live glioblastoma cells (B). It is possible to observe the cell body and axons in living neurons and intravesicular structures in glioblastomas. Intensity map images of glial (C) and glioblastomas (D) incubated for three minutes with these QDs. Insets are the corresponding fluorescence images. (Santos *et al.*, 2008a).

Molecule specific endocytosis is known as receptor-mediated endocytosis which are clathrin or caveolae-mediated endocytosis, or clathrin/caveolae independent endocytosis. It is probably the major pathway where QDs are uptaken by cells. It seems that lipid rafts localized within the plasma membrane plays an important role in the QDs uptake as well. These rafts provide a support for the assembly of many receptors, adaptors as well as proteins involved in a signaling complex such as caveolae and clathrin. (Nichols, 2003a; Nichols 2003b)

In 2011, Maysinger and collaborators synthesized QDs with almost the same hydrodynamic size (between 8-10 nm) and functionalized with different short ligands such as cysteine, cysteamine, dihydrolipoic acid and mercaptopropionic acid (Al-Hajaj *et al*, 2011). These QDs were tested in human embryonic kidney cells (Hek 293) and human hepatocellular carcinoma cells (Hep G2) in order to achieve information about these QDs uptake and elimination. They showed that most of the QDs with the same size but different surface properties were uptaken through lipid raft-mediated endocytosis with the contribution of the XAG transport system (responsible for the carrier-mediated Na(+)-independent transport of anionic amino acids such as glutamate and aspartate across the plasma membrane of cells) which takes up cysteine, glutamate and aspartate. The contribution of a P-glycoprotein transporter on QD efflux was also demonstrated during the experiments. Figure 5 shows the hypotheses about QDs internalization and elimination.

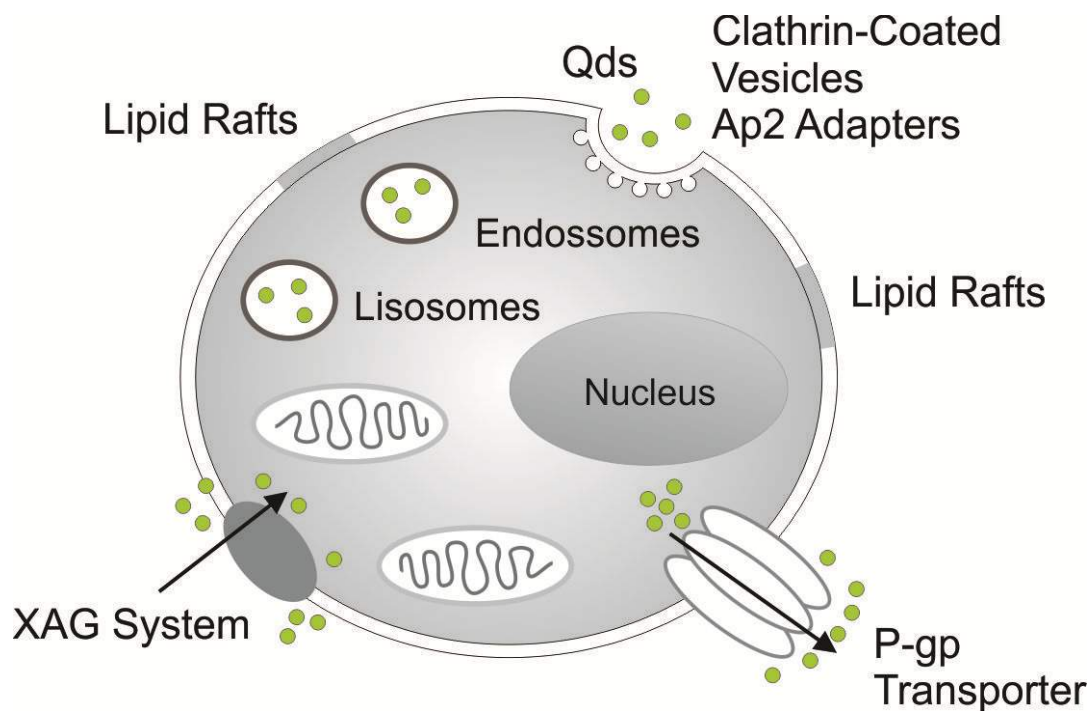


Figure 5. Representation of all the cell signaling mechanisms Studied by using QDs (Al-Hajaj *et al*, 2011).

These results corroborated with those obtained from Chan's (Jiang *et al.*, 2008), where they showed the size dependent internalization of particles using both pathways clathrin- and caveolae- mediated endocytosis. It has been shown that particles with a diameter of $d = 40$ -

50 nm are endocytosed more efficiently than those larger or smaller (Jiang *et al.*, 2008). Sizes also dictates the final location of the particles (i.e. cytosol, nucleus), being able or not to cross their natural cellular barriers (Williams *et al.*, 2009), which is on the other hand cell-type dependent (Williams *et al.*, 2009).

However, QDs internalization by cells not only depends on their size. Although size is an important parameter, charge is thought as one of the most important parameter controlling cell-QD interactions (Conroy *et al.*, 2008). An interesting finding of charge-mediated internalization and interactions with intracellular structures was found by Conroy *et al.* (Conroy *et al.*, 2008), who demonstrated that these carboxyl-coated (negative) QDs but not amine-coated (positive) are able to enter macrophage-like cells and bound nuclear structures rich in the positive histone proteins. In fact, such interactions were sufficiently strong to change QDs' optical and colloidal properties even in cell-free conditions (Conroy *et al.*, 2008).

Lira *et al* have recently shown that even in the same cell population, carboxyl-coated QDs have differential access to intracellular compartments and when they reach the nucleus, they actually bind nuclear/nucleolar structures, as shown in Figure 6 for permeabilized human-derived peripheral blood cells (Lira *et al.*, 2012). Figure 6 shows that the intracellular localization of these carboxyl-QDs for same cell population may differ from cell to cell. Depending on the cell, QDs could or not reach the nucleus (square 1 and 2, respectively). As will be discussed, the surface charge plays a critical role on such interactions. Although the internalization efficiency is significantly higher for positively-charged materials due to the

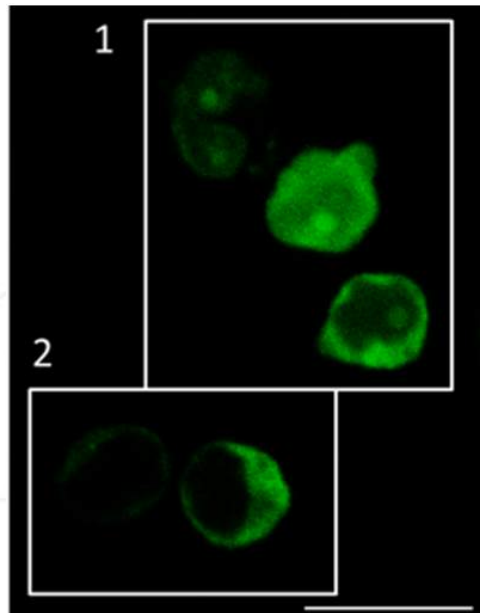


Figure 6. Non-specific labeling of fixed peripheral blood mononuclear cells. The image shows an optical field where CdTe/CdS QDs can reach only the cytoplasm (square 2) or can cross the nuclear membrane and reach the nucleus (square 1). In the nucleus, these nanoparticles bind with high affinity nuclear structures such as nucleoli (Lira *et al.*, 2012).

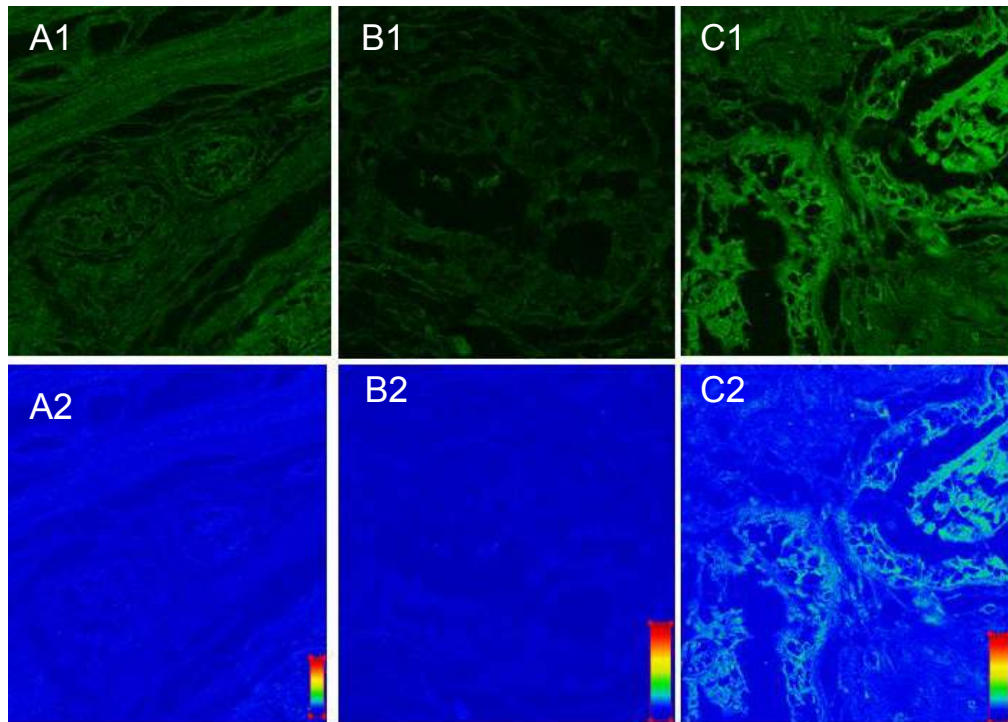


Figure 7. Human mammary tissue diagnosed as Fibroadenoma (Fib). (A1) Fib treated with Evan's Blue solution (EB); (B1) Fib incubated with QDs diluted in EB (QD-FIB-EB); (C1) Fib incubated with QD-Con-A conjugate diluted in EB (QD-Con-A-FIB-EB). A2, B2 and C2 are the intensity maps of A1, B1 and C1, respectively. The bright pattern observed in (1c) is related to regions of high glucose/mannose expression in the tissue (Santos *et al.*, 2006).

interactions with the negative cell surface, it is believed that cationic sites on the negatively charged cell surface can mediate the interaction of negative nanomaterials (Ghinea *et al.*, 2009) eventually leading to internalization by cells.

2.1.3. Some examples of specific labeling

The capacity of QDs for specific labeling cells and tissues depends on the bioconjugation. Santos *et al.*, for example, reported the use of CdS/Cd(OH)₂ QDs functionalized with glutaraldehyde and conjugated to concanavalin-A (Con-A) lectin (Santos *et al.*, 2006) to investigate cell alterations regarding carbohydrate profile in human mammary tissues diagnosed as fibroadenoma (benigne tumor). Con-A lectin is a protein which binds specifically to glucose/mannose residues expressed in the plasma membrane. Figure 7 shows the QD-Con-A more expressive staining of mammary tissue diagnosed with Fibroadenoma

Con-A was used also in another work for cellular labeling of *Candida albicans* with CdTe/CdS QDs conjugated or not to Con-A (Kato *et al.*, 2012). Fluorescence microscopy analysis of the yeast cells showed that the non-functionalized QDs do not label *C. albicans* cells, however for the QD conjugated to Con-A the cells showed a fluorescence profile indicating that the cell wall was preferentially marked.

In another work of the same group it was also used CdS/Cd(OH)₂ QDs functionalized with glutaraldehyde as efficient fluorescent labels for living human red blood cells (Santos *et al.*, 2008a), the aim of this investigation was to determine the antigen-A expression in subgroups of group A erythrocytes.

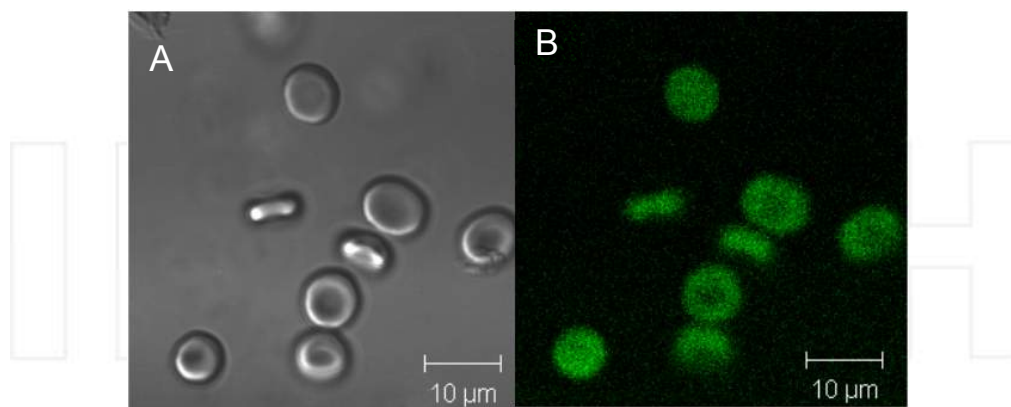


Figure 8. Microscopic confocal images obtained for QDs/anti-A marking living A+ erythrocytes. A is the DIC observation of the marked red blood cells and (B) is the marking pattern when excited at 488 nm (Santos *et al.*, 2008a).

2.1.4. Quantum dots for intracellular delivery

QDs can be used as a probe for monitoring protein dynamics in live cells, allowing the study of their traffic down to a single molecule (Pinaud *et al.*, 2010), taking advantages of the most striking properties as a fluorescent probe, which is long term imaging for prolonged periods of time (Courty *et al.*, 2006). However, traffic of molecular dynamics, especially in live cells, are almost exclusively carried out for surface molecules – membrane proteins, accessible by the external side of the cells. This limitation arise mainly due to the incapacity of water dispersed QDs to cross the lipid bilayers by simple diffusion (only few works report tracking of intracellular molecules) (Chen & Gerion, 2004).

a. Physical methods

The physical methods to deliver aqueous compounds into cells are of special interest since the precise control over the cell (extent of delivery over the population) and the amount of materials can be reached in most cases. These are mainly based on microinjection and electroporation. In fact these two traditional and well recognized methods are among the most efficient methods to deliver QDs into cells. The electroporation is based on the application of one or more strong electrical pulses, which is thought to create localized pores in the membrane bilayer for enhancing its permeability – Figure 9A. Using electroporation, Chen and Gerion delivered QDs into HeLa cells (Chen & Gerion, 2004). The QDs were able to be recognized by the cellular machinery and enter the cell nucleus in living cells, although in a fraction of the total number of cells and as agglomerated particles. In fact, nanoparticle aggregates of up to 500 nm have been reported to be produced later after the application of electric pulses, even for protein-

conjugated QDs. However, if agglomeration does not matter, as in the case of simple cell labeling, electroporation can be well suited. In fact, cells filled with QDs after electroporation can be readily seen in living mice for cell tracking purposes (Yoo *et al.*, 2010).

Figure 9 shows schematic representations of the most common strategies for intracellular delivery of membrane-impermeable materials. Figure 9A and B represent physical processes while Fig. 9C and D are chemical methods. In electroporation, cells are exposed to an electric field and a single or multiple pulses are applied, creating pores that allow the passage of materials to the cell interior. In the microinjection (Figure 9B), a micropipette delivers precise amounts of fluids inside any compartment of the cells. In Fig. 9C, the conjugation of QDs with Cell Penetrating Peptides (CPPs) (discussed later) can deliver them into cells by direct membrane entrance (as shown in the scheme of Figure 9C) or by endocytosis. Also by endocytosis, polycation-coated QDs (green spheres) trigger “proton-sponge effect”, (discussed later) releasing endo/lysosomal content into the cytosol. In Figure 9D, binding of negative cargos to lipoplex systems results in endocytosis likely due to charge interactions with negative plasma membrane. After internalization, charge neutralization seems to release the cargo from the lipid system.

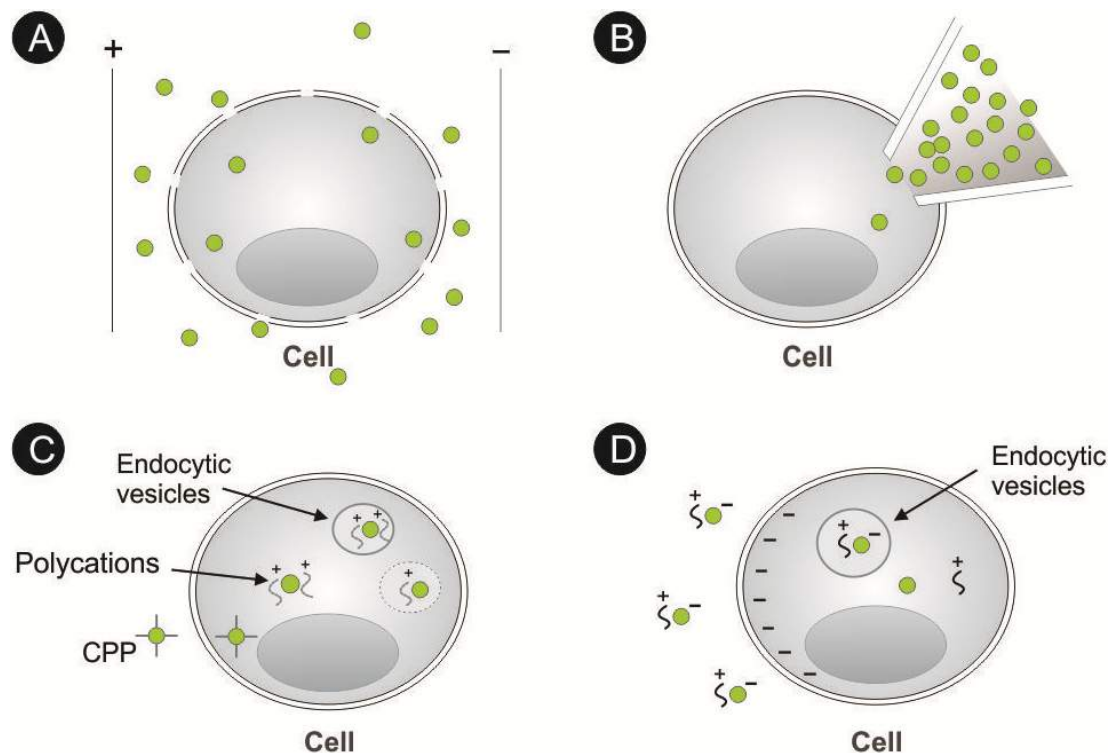


Figure 9. Schematic representations of four types of processes used in the internalization of QDs: electroporation (A); microinjection (B); CPP and polycation-mediated internalization (C) and lipoplex mediated process (D).

Another physical method for intracellular delivery of membrane impermeable materials is microinjection. This technique is based on the insertion of precise volumes inside an aqueous

compartment (such a cell) by micropipettes – Figure 9B. Since the first attempts of using QDs as fluorescent probes, microinjection is recognized as a potent method to insert these particles in intracellular media. One example of the application of microinjection it is the use of micelle-capped QDs as an agent to follow the development of tissues derived from a single cell in living *Xenopus embryos* after transfection (Dubertret *et al.*, 2002) or dynamics changes during the vasculature development in Zebrafish (Rieger *et al.*, 2005).

Although their recognized efficiency, both methods suffer from some drawbacks. Electroporation not only cause QDs to aggregate, but may seriously compromise cellular viability. On the other hand, microinjection is technically and costly demanding, requiring specialized equipment and, as a serial technique it has poor statistical significance.

b. Chemical methods

Chemical approaches represent a wealthy range of strategies for intracellular delivery of membrane impermeable materials, and include covering cargos' surface or couple/bind them to a vehicle, promoting the labels enter into cytoplasm of a large number of cells simultaneously in a straightforward way. Moreover, it can actually be used in living animals - the methods described above can only be used in such applications in very specific conditions.

Many methods to allow QDs to reach the cell cytosol are based on the conjugation of surface of nanoparticles to interact or to be recognized by cells until they reach the cytoplasm by different means. One of the most effective chemical methods for nanoparticle delivery into cells is the conjugation with Cell Penetrating Peptides (CPPs). A number of publications report such a class of molecules for this purpose, in which the mechanism of cell entry is similar to endocytosis (Thorén *et al.*, 2004) rather than direct bypass through the lipid bilayer, although the consensus for the real pathway is still controversial. If trafficked into cells by endocytosis, these QDs bioconjugates need to be released from endo/lysosomal compartments to reach their targets (if such target is some intracellular organelles, for example).

A wide range of molecules can be conjugated to QDs' surface to be specifically delivered to cells (toxins, sugars, polymers and so on); however most of them lead to receptor-mediated endocytosis, which predominantly result in entrapment into endocytic vesicles. For this reason, we will not address here intracellular delivery of QDs by molecules which do not explicitly release these particles freely in cytosol.

Other chemical modifications can result in intracellular release after nanoparticle endocytosis rather than simple membrane permeation – as proposed for CPPs. One of such approaches is to cover QDs' surface with osmotic active polymers such as polyethyleneimine. After endocytosis, such polycations are capable of sequestering protons by H^+ -pumps in the endo/lysosomal membrane, which in turn force the entrance of Cl^- ions and water to balance osmotic effects (this is the reason why this approach is called the “proton-sponge effect”). As a consequence, it leads vesicle rupture and releases endocytosed materials into the cell cytosol. Using this approach, Yezhelyev *et al.* delivered siRNA conjugated-QDs to breast cancer cells (Yezhelyev *et al.*, 2008). The functionality of the system was showed by a

remarked reduction in cyclophilin B protein expression after gene silencing. One similar approach is the osmotic lysis, where endo/lysosomal vesicles are also ruptured, now by submitting cells to hypotonic solutions. In fact, it was the method used to track for the first time an intracellular protein in living cells using QDs (Courty *et al.*, 2006) where kinesin from *Drosophila* were delivered and tracked in HeLa cells. Lately, Nelson *et al.* reported a detailed study on the movement of Myosin Va (a molecular motor which tracks over actin filaments) inside COS-7 cells (Nelson *et al.*, 2009). However, lysosome lysis might be harmful to cells as some acidic proteins such as proteases are released in the cytosol, which may degrade the constituents in there.

c. Quantum dots encapsulation

Quantum Dots can be entrapped in a vehicle for its delivery instead of being conjugated to transporter molecules, a strategy that can be also suited for intracellular delivery after endocytic uptake. It is quite advantageous because it allows the conjugation of targeting moieties (i.e. antibodies, ligands) on the surface of the nanoparticles, which was otherwise occupied by the targeting transporter molecules (as in the case of CPPs peptides and polymers). Moreover, it can avoid the rupture of acidic intracellular vesicles, which has the tendency to cause cytotoxicity effects. The encapsulating vehicles can be classified in two major groups, named polymeric and lipid delivering systems. QDs were encapsulated in functionalized polymeric poly(lactic-co-glycolic acid) (PLGA) nanospheres and delivered into the cell cytosol after endocytosis of the complex (Kim *et al.*, 2008). After preferential endocytosis of antibody-coated polymer nanospheres into ErbB2 over expressing cancer cells, the polymer were degraded in the acidic intracellular compartments releasing the bioconjugated QDs, which in turn could reach and label intracellular structures such as mitochondria and actin filaments.

Another approach is using micelles. An advantage of encapsulating QDs in lipid micelles relies on the small size of the resulting probe, up to 25 nm (Carion *et al.*, 2007). Taking advantages on the physical-chemical and photostability of these QD-containing micelles, the group who reported this system for the first time could track cell lineage developments in live *Xenopus embryos* (Dubertret *et al.*, 2002). This breakthrough report was one of the first reports on the use of QDs for in vivo imaging.

Among the vehicles composed of lipids, probably the most popular is liposomes (Valenzuela, 2007; Al-Jamal & Kostarelos, 2007). Liposomes are lipid vesicles containing one (or more) lipid bilayer(s) enclosing an aqueous compartment and that can entrap hydrophilic and/or hydrophobic materials during its formation (Valenzuela, 2007). As in the case of micelles (or any other encapsulation system), their interaction with biological species depends on the physical-chemical properties, which can be fine-tuned. In fact, Yang *et al.* (Yang *et al.*, 2009) encapsulated water aqueous CdTe QDs in folate-conjugated liposomes and showed that these vesicles can be directed to folate-overexpressing cancer cells and be monitored by QDs fluorescence. The resulting system is resistant to optical and chemical degradation, with lower toxic effects.

QDs can also be delivered to cells by commercial cationic liposomes, the lipofection system (Fig. 9D). Lipoplex are positively-charged lipidic vesicles (mainly liposomes) able to bind

negative particles, including oligonucleotides and QDs, which mediate charge interactions with cells, leading to endocytosis of the resulting system and eventually the release of cargos inside the cell. In such an application, Yoo *et al.* (Yoo *et al.*, 2008) reported for the first time the use of these lipid vesicles as QD vehicles for protein tracking inside living cells. In contrast to earlier works, their bioconjugated QDs could escape from cellular vesicles and reach the cytosol, where they could be used to track the movements of actin, kinesin and tubulin proteins. Although the mechanism of endosomal release of materials delivered by cationic liposomes is not known, it is believed that charges play important roles in membrane destabilization, which could explain the successful applications of such liposomes. However cytosolic release is not the main fate of delivered moieties in most applications of cationic liposomes, as exemplified above. It is important to note that lipofection delivery is not based on encapsulation; it is rather based on electrostatic interactions with negatively-charged cargos.

2.2. Quantum dots as probes in other bioassays

An increasing interest in using QDs as more than passive/active labels is reflected by the great number of published data in the literature in the past decade. There is a growing research community that recognizes that the fluorescent QDs may be extensively applied as a central component of nano-probes (Algar & Krull, 2008). We may classify among all the suggested applications the following: Fluorescence Resonance Energy Transfer (FRET) for bioassays, optical biosensors and Photodynamic Therapy (PDT).

In all these applications, the QDs act as scaffolds for the assembly of biomolecular probes while its fluorescence is modulated by biorecognition events. In the particular case of FRET-QDs studies, a broad absorption band combined with a size-tunable fluorescence and larger physical size (when compared to conventional dyes) allow: (i) optimization of the spectral overlap with any potential FRET acceptor; (ii) excitation at a wavelength far from the acceptor absorption peak (minimizing acceptor direct excitation); QDs can be excited over a range of wavelengths in the blue-ultraviolet region of the spectrum to allow minimization of the direct excitation of acceptors and (iii) the ability to assemble multiple acceptors around a QD core to increase the overall FRET efficiency (Algar & Krull, 2008; Bakalova *et al.*, 2004; Juzenasa *et al.*, 2008; Medintz & Mattoussi, 2009; Tekdas *et al.*, 2012). The use of fluorescence resonance energy transfer (FRET) as a mechanism of tuning QDs' fluorescence is particularly advantageous and due to their high photostability QDs are ideal donors (Algar & Krull, 2008; Bakalova *et al.*, 2004; Medintz & Mattoussi, 2009). Moreover, the potentially high quantum yield of QDs helps to maximize Förster distances, while the narrow emission can be tuned to optimize spectral overlap and reduce crosstalk between donor and acceptor (Algar & Krull, 2008; Medintz & Mattoussi, 2009).

The great potential of FRET-QDs applications may be exemplified by several reports. For instance, Stringer *et al.* developed a biosensor that is able to detect troponin I to diagnose early injuries of cardiac muscles (Stringer *et al.*, 2008) and also to detect small amounts of nitrated ceruloplasmin (a significant biomarker for cardiovascular disease, lung cancer, and

stress response to smoking) (Pyo & Yoo, 2012). Another interesting application is described by Krull *et al.* which performed solid-phase hybridization assays aiming multiplexed nucleic acid diagnostics using QDs as donors in FRET processes (Algar & Krull, 2008; Medintz & Mattoussi, 2009). They developed multiplexed assays using immobilized QDs as both FRET donors and scaffolds for the immobilization of oligonucleotides probes, where the association of fluorescent acceptor dyes with sequence-specific hybridization events provided the basis for transduction. QD donors were paired with one or more acceptor dyes, and the ratios of QD fluorescence and FRET-sensitized acceptor fluorescence provided an analytical signal. The basic idea is depicted in Figure 10.

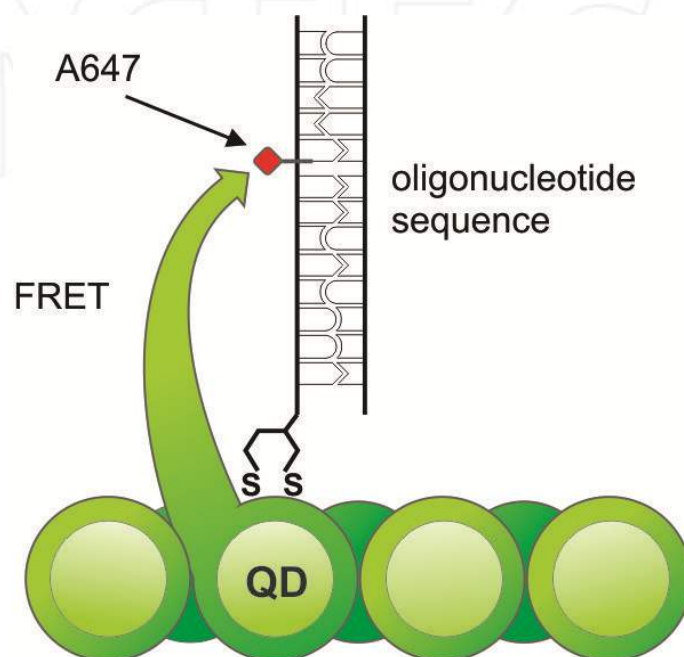


Figure 10. Schematic representation of a FRET process. Immobilized QDs are derivatized with dithiol-terminated probe oligonucleotides and under light excitation the QDs are involved in the emission of the Alexa Fluor 647 dye bound to a determined oligonucleotides sequence (Algar & Krull, 2008; Medintz & Mattoussi, 2009).

QDs may also play a critical role as energy acceptors in bioluminescence resonance energy transfer (BRET) processes, with a bioluminescent protein as the energy donor. BRET resembles FRET in many aspects except that it does not require external light source for the donor excitation. The broad excitation spectra and large Stokes shift of QDs allow them to be excited by nearly all the bioluminescent proteins in BRET assemblies. Feasibility of QDs as the BRET acceptor for a mutant of Renilla luciferase (Luc8 with improved chemical stability and light efficiency) has been recently realized both *in vitro* and *in vivo* (Samia *et al.*, 2006).

More recently QDs have also been applied in photodynamic therapy (PDT) related processes (Juzenasa *et al.*, 2008). This could be done due to the combination of the unique optical properties of these nanostructured systems with their active chemical surfaces. PDT

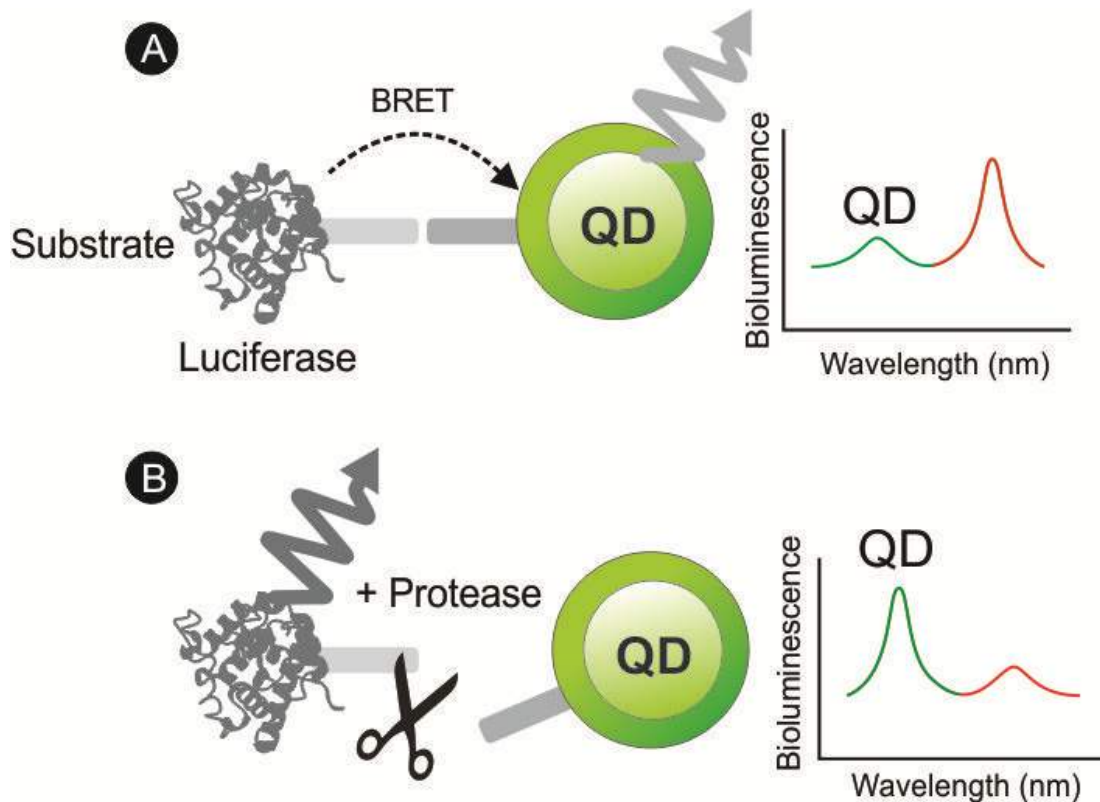


Figure 11. Schematic representation of BRET-QDs sensor applied to detect protease activity. In this assembly QD and luciferase protein are closely linked together through a peptide substrate. In process (A) QD fluorescence induced by the BRET process is observed and in the presence of a protease (B) the BRET process is disrupted leading to a loss of bioluminescence-induced QD emission (Xia & Rao, 2009).

causes cell death (by necrosis or apoptosis) when singlet oxygen and other reactive species of oxygen (ROS) are produced while photosensitizers are stimulated by light. In PDT studies QDs may work as energy donors for traditional photosensitizers or interacting directly with molecular oxygen by mechanisms of energy transfers to generate singlet oxygen as described in Figure 12. PDT based QDs have been used both for treatment of skin lesions and for the treatment of skin cancers (Xia & Rao, 2009). QDs conjugated with Pc4, a known photosensitizing protein, were excited at 488 nm and by energy transfer mechanisms the protein was excited indirectly, emitting at 680 nm. In other words, the QDs, when excited, emit in a wavelength which excites the protein (Xia & Rao, 2009).

3. Some drawbacks of quantum dots

Non-specific interactions are a common phenomenon on the application of biological probes. Besides some benefits, these interactions are commonly a negative feature. An incomplete conjugation may result in residual non-conjugated QDs in the same colloidal suspension which can bind or interact non-specifically with the biological system and interfere in the desired results interfering in the specificity of the original applications.

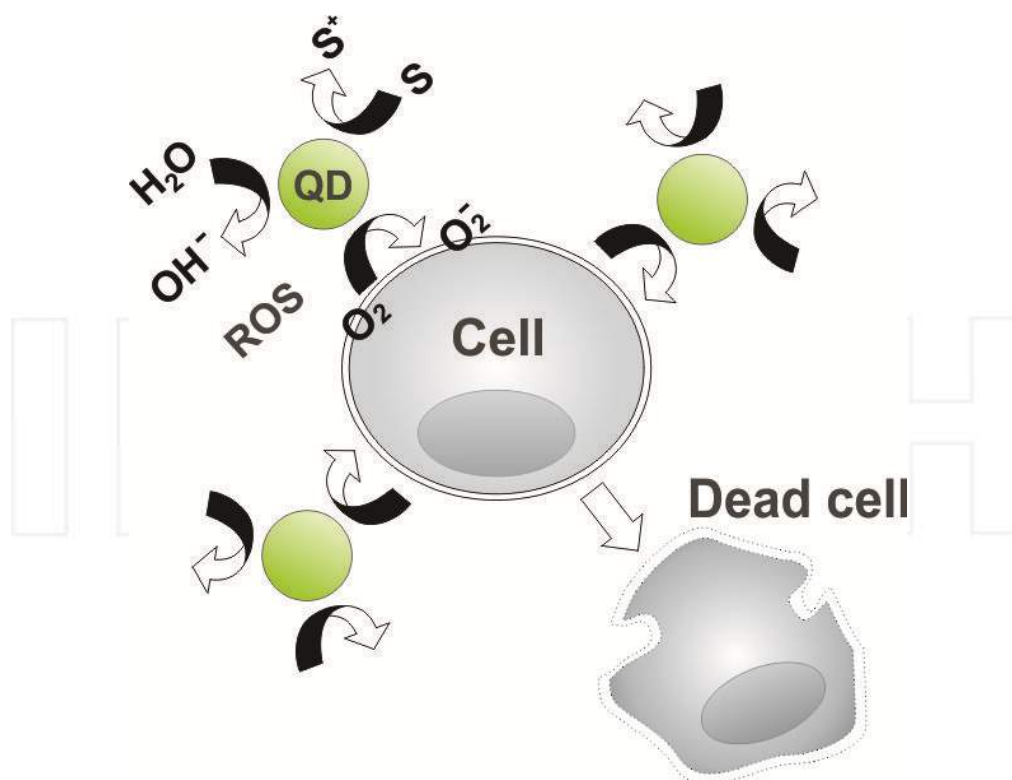


Figure 12. The basic process in the production of ROS species in cell PDT using QDs as producers of O_2^- .

The most common strategy to overcome non-specific labelling relies in covering the QDs surface with polar polymer molecules, such as polyethylene glycol (PEG). This is because such polymers are biologically “inert” and hinder electrostatic interactions of nanoparticle surface against cell surface or molecules in suspension. Pegylated nanoparticles are therefore less prone to aggregation (that is, much more stable) and virtually binding-free. Moreover, they can allow further conjugation with functional biomolecules, include proteins and antibodies (Hezinger *et al.*, 2007; Medintz *et al.*, 2005). Pegylated bioconjugated QDs are then able to bind specifically their targets, being stable and virtually free of non-specific interactions. Pegylation, however, is not universally inert. We have demonstrated that PEG-coated $CdS/Cd(OH)_2$ QDs are able to bind live parasites cells, triggering endocytosis by specialized endocytic pathways such as those using the flagellar pocket (Chaves *et al.*, 2008).

Understanding the interactions of nanoparticles and biological specimens, specially cells, is of great interest since one can therefore modulate specific cellular processes. Unrestricted interactions of any kind of materials, including QDs, have the potential to be toxic, especially at higher concentration and/or with enhanced adsorption/internalization. Beyond the changes over cell function, more evident effects are prone to be caused by QDs, including cellular ones such: (i) changes in cell morphology (Chang *et al.*, 2009), (ii) oxidative stress (Lovrić, *et al.*, 2005), (iii) release of heavy metal compounds (Kirchner *et al.*, 2005) and (iv) genetic and epigenetic damage (Choi *et al.*, 2008), as well as local inflammation in live rats, as we have recently reported.

4. General conclusions

QDs have broad and strong one-photon absorption, narrow and symmetric size-tunable fluorescence bands, and a great resistance to photobleaching, making them an attractive alternative to molecular fluorophores in imaging applications and bioanalytical chemistry assays. This Chapter discusses some current applications of QDs as well as presents some drawbacks that still remain. Taken together, all these findings show that a deeper understanding of the mechanisms underlying QDs-biological systems interactions is helpful in the way that researchers can avoid side effects and improve the quality of labeling of QDs for diagnostics and therapeutic purposes.

Author details

Adriana Fontes, Rafael Bezerra de Lira, Maria Aparecida Barreto Lopes Seabra, Thiago Gomes da Silva, Antônio Gomes de Castro Neto and Beate Saegesser Santos
Biomedical Nanotechnology research group of the Universidade Federal de Pernambuco, Recife, Pernambuco, Brazil

Acknowledgement

The authors are grateful to CAPES, CNPq, FACEPE, HEMOPE, L'óreal, Brazilian Academy of Sciences and UNESCO. This work is also linked to the National Institute of Photonics (INCT-INFO). The authors also wish to thank Pedro Barroca for the schematic drawings.

5. References

- Algar, W. R.; Krull, U. J. (2008) Quantum Dots as Donors in Fluorescence Resonance Energy Transfer for the Bioanalysis of Nucleic Acids, Proteins, and Other Biological Molecules. *Anal. Bioanal. Chem.*, Vol. 391, pp. 1609-1618.
- Algar, W. R.; Tavares, A. J.; Krull, U. J. (2010) Beyond Labels: A Review of the Application of Quantum Dots as Integrated Components of Assays, Bioprobes, and Biosensors Utilizing Optical Transduction. *Anal. Chim. Acta*, Vol. 673, pp. 1-25.
- Al-Hajaj, N.A., Moquin, A., Neibert, K.D., Soliman, G.N., Winnik, F.M., Maysinger, D. (2011) Short Ligands affect Modes of QD uptake and elimination in Human Cells. *ACS Nano*, Vol.6, pp.4909-4918.
- Al-Jamal, W. T.; Kostarelos, K. (2007) Liposome-nanoparticle hybrids for multimodal diagnostic and therapeutic applications. *Nanomedicine*, Vol. 2, pp. 85-98.
- Bakalova, R.; Ohba, H.; Zhelev, Z.; Ishikawa, M.; Baba, Y. (2004) Quantum dots as photosensitizers? *Nature Biotechnology*, Vol. 22, pp. 1360-1361.
- Biju, V.; Itoh, T.; Ishikawa, M. (2010) Delivering quantum dots to cells: bioconjugated quantum dots for targeted and nonspecific extracellular and intracellular imaging. *Chem. Soc. Rev.*, Vol. 39, pp. 3031-3056.

- Brus, L. E. (1984). Electron–electron and electron–hole interactions in small semiconductor crystallites—the size dependence of the lowest excited electronic state. *Journal of Chemical Physics*, Vol. 80, pp. 4403–4409.
- Cai, W.; Shin D.-W.; Chen, K.; Gheysens, O.; Cao, Q.; Wang, S. X.; Gambhir, S. S.; Chen, X. (2006) Peptide-Labeled Near-Infrared Quantum Dots for Imaging Tumor Vasculature in Living Subjects. *Nano Lett.*, Vol. 6, pp 669–676.
- Carion, O.; Mahler, B.; Pons, T.; Dubertret, B. (2007) Synthesis, encapsulation, purification and coupling of single quantum dots in phospholipid micelles for their use in cellular and in vivo imaging. *Nature Protocols*, Vol. 2, pp. 2383–2390.
- Chang, S. Q.; Dai, Y. D.; Kang, B.; Hana, W.; Mao, L.; Chen, D. (2009) UV-enhanced cytotoxicity of thiol-capped CdTe quantum dots in human pancreatic carcinoma cells. *Toxicology Letters*, Vol. 188, pp. 104–111
- Chaves, C. R.; Fontes, A.; Farias, P. M. A.; Santos, B. S.; Menezes, F. D.; Ferreira, R. C.; Cesar, C. L.; Galembeck, A.; Figueiredo, R. C. B. Q. (2008) Application of core–shell PEGylated CdS/Cd(OH)₂ quantum dots as biolabels of *Trypanosoma cruzi* parasites. *Applied Surface Science*, Vol. 255, pp. 728–730.
- Chen, F.; Gerion, D. (2004) Fluorescent CdSe/ZnS Nanocrystal-Peptide Conjugates for Long-term, Nontoxic Imaging and Nuclear Targeting in Living Cells. *Nano Letters*, Vol. 4, pp. 1827–1832.
- Choi, A. O.; Brown, S. E.; Szyf, M.; Maysinger, D. (2008) Quantum dot-induced epigenetic and genotoxic changes in human breast cancer cells. *J Mol Med*, Vol. 86, pp. 291–302.
- Conroy, J.; Byrne, S. J.; Gun'ko, Y. K.; Rakovich, Y. P.; Donegan, J. F.; Davies, A.; Kelleher, D.; Volkov, V., (2008) CdTe Nanoparticles Display Tropism to Core Histones and Histone-Rich Cell Organelles. *Small*, Vol. 4, pp. 2006–2015.
- Courty, S.; Luccardini, C.; Bellaiche, Y.; Cappello, G.; Dahan, M. (2006) Tracking Individual Kinesin Motors in Living Cells Using Single Quantum-Dot Imaging. *Nano Letters*. Vol. 6, pp. 1491–1495.
- Dabbousi, B. O.; Rodriguez, V. J.; Mikulec, F. V.; Heine, J. R.; Mattoussi, H.; Ober, R. (1997). (CdSe) ZnS core-shell quantum dots: synthesis and characterization of a size series of highly luminescent nanocrystallites. *Journal of Physical Chemistry B*, Vol. 101, pp. 9463–9475.
- Dubertret, B.; Skourides, P.; Norris, D. J.; Noireaux, V.; Brivanlou, A. H.; Libchaber, A. (2002) In Vivo Imaging of Quantum Dots Encapsulated in Phospholipid Micelles. *Science*, Vol. 298, pp. 1759–1762.
- Farias, P. M. A.; Santos, B. S.; Menezes, F. D.; Ferreira, R.; Fontes, A.; Carvalho H. F.; Romão L.; Moura-Neto, V.; Amaral, J. C. O. F.; Cesar, C. L.; Figueiredo, R. C. B. Q.; Lorenzato, F. R. B. (2006) Quantum dots as fluorescent bio-labels in cancer diagnostic. *Phys. Stat. Sol. (C)*, Vol. 3, pp. 4001–4008.
- Gao, J.; Chen, X.; Cheng, Z. (2010) Near-infrared quantum dots as optical probes for tumor imaging. *Curr. Top Med Chem.*, Vol. 10, pp. 1147–1157.
- Ghinea, N; Simionescu, N. (1985) Anionized and Cationized Hemeundecapeptides as Probes for Cell Surface Charge and Permeability Studies: Differentiated Labeling of Endothelial Plasmalemmal Vesicles. *The Journal Of Cell Biology Volume*, Vol. 100, pp. 606–612.

- Goldman, E. R.; Anderson, G. P.; Tran, P. T.; Mattoussi, H.; Charles, P. T.; Mauro, J. M. (2002) Conjugation of Luminescent Quantum Dots with Antibodies Using an Engineered Adaptor Protein To Provide New Reagents for Fluoroimmunoassays. *Anal. Chem.*, Vol. 74, pp. 841-847.
- Jaiswal, J. K.; Matoussi, H.; Mauro, J. M.; Simon, S.; (2003). Long-Term Multiple Color Imaging Of Live Cells Using Quantum Dot Bioconjugates. *Nature Biotechnology*, Vol. 21, pp. 47-51.
- Jiang, W.; Kim, Y.; Rutka, S. B. J. T.; Chan, W. C. W. (2008) Nanoparticle-mediated cellular response is size-dependent. *Nature Nanotechnology*, Vol. 3, pp. 145-150.
- Juzenas, P.; Chen, W.; Sun, Y. P.; Coelho, M. A. N.; Generalov, R.; Generalova, N.; Christensen, I. L. (2008) Quantum dots and nanoparticles for photodynamic and radiation therapies of cancer. *Advanced Drug Delivery Reviews*, Vol. 60, pp. 1600-1614.
- Kato, I. T.; Santos, C. C.; Benetti, E.; Tenorio, D. P. L. A.; Cabral Filho, P. E.; Sabino, C. P.; Fontes, A.; Santos, B. S.; Prates, R. A.; Ribeiro, M. S. CdTe/CdS-MPA quantum dots as fluorescent probes to label yeast cells: synthesis, characterization and conjugation with Concanavalin A. (2012) *Photonics West, San Francisco. Proceedings of SPIE - Colloidal Nanocrystals for Biomedical Applications VII*, Vol. 8232, pp. 82320D.
- Kim, B. Y. S.; Jiang, W.; Oreopoulos, J.; Yip, C. M.; Rutka, J. T.; Chan, W. C. W. (2008) Biodegradable Quantum Dot Nanocomposites Enable Live Cell Labeling and Imaging of Cytoplasmic Targets. *Nano Letters*, Vol. 8, pp. 3887-3892.
- Kirchner, C.; Liedl, T.; Pellegrino, S. K. T.; Javier, A. M.; Gaub, H. E.; Stölzle, S.; Fertig, N.; Parak, W. J. (2005) Cytotoxicity of Colloidal CdSe and CdSe/ZnS Nanoparticles. *Nano Letters*, Vol. 5, pp. 331-338
- Lira, R. B.; Cavalcanti, M. B.; Seabra, M. A. B. L.; Silva, D. C. N.; Amaral, A. J.; Santos, B. S.; Fontes, A. (2012) Non-specific interactions of CdTe/Cds Quantum Dots with human blood mononuclear cells. *Micron*, Vol. 43, pp. 621-626.
- Liu, W.; Howarth, M.; Greytak, A. B.; Zheng, Y.; Nocera, D. G.; Ting, A. Y.; Bawendi, M. G. (2008) Compact Biocompatible Quantum Dots Functionalized for Cellular Imaging. *J. Am. Chem. Soc.*, Vol. 130, pp. 1274-1284.
- Liu, W.; Zhang, S.; Wang, L.; Qu, C.; Zhang, C.; Hong, L.; Yuan, L.; Huang, Z.; Wang, Z.; Liu, S.; Jiang, G. (2011) CdSe Quantum Dot (QD)-Induced Morphological and Functional Impairments to Liver in Mice. *PLoS ONE*, Vol. 6, e24406. doi:10.1371/journal.pone.0024406.
- Lovrić, J.; Bazzi, H. S.; Cuie, Y.; Fortin, G. R. A.; Winnik, F. M.; Maysinger, D. (2005) Differences in subcellular distribution and toxicity of green and red emitting CdTe quantum dots. *J Mol Med*, Vol. 83, pp. 377-385.
- Ma-Hock, L.; Brill, S.; Wohlleben, W.; Farias, P. M. A.; Chaves, C. R.; Tenório, D. P. L. A.; Fontes, A.; Santos, B. S.; Landsiedel, R.; Strauss, V.; Treumann, S.; van Ravenzwaay, B. (2012) Short term inhalation toxicity of a liquid aerosol of CdS/Cd(OH)₂ core shell quantum dots in male Wistar rats. *Toxicology Letters*, Vol. 208, pp. 115-124.
- Medintz, I. L.; Mattoussi, H. (200) Quantum Dot-Based Resonance Energy Transfer and Its Growing Application in Biology. *Phys. Chem. Chem. Phys.*, Vol. 11, pp. 17-45.

- Medintz, I. L.; T. Uyeda, H.; Goldman, E. R.; Mattoussi, H. (2005) Quantum dot bioconjugates for imaging, labelling and sensing. *Nature Materials*, Vol. 4, pp. 435-446.
- Menezes, F. D. de; Brasil Jr., A. G.; Moreira, W. L.; Barbosa, L. C.; Cesar, C. L.; Ferreira, R. C. de; Farias, P. M. A. de; Santos, B. S. (2005). CdTe/CdS core shell quantum dots for photonic applications, *Microelectronics Journal*, Vol. 36, pp. 989-991.
- Nelson, S.R.; Ali, M.Y.; Trybus, K.M.; Warshaw, D.M. (2009) Random walk of processive, quantum dot-labeled myosin Va molecules within the actin cortex of COS-7 cells. *Biophys J.*, Vol. 97, pp. 509-518.
- Nichols, B. J. (2003a). Caveosomes and endocytosis of lipid rafts. *J. Cell Sci.*, Vol. 116, pp. 4707-4714.
- Nichols, B. J. (2003b). GM1-containing lipid rafts are depleted within clathrin-coated pits. *Curr. Biol.*, Vol. 13, pp. 686-690.
- Noh, Y.-W.; Lim, Y. T.; Chung, B. H. (2008) Noninvasive imaging of dendritic cell migration into lymph nodes using near-infrared fluorescent semiconductor nanocrystals. *The FASEB Journal*, Vol. 22, pp. 3908-3918.
- Pinaud F.; Clarke S.; Sittner, A.; Dahan, M. (2010) Probing cellular events, one quantum dot at a time. *Nature Methods*, Vol. 7, pp. 275-285.
- Pyo, D., Yoo, J. (2012) New Trends in Fluorescence Immunochromatography. *J. Immunoassay and Immunochemistry*, Vol. 33, pp. 203-222.
- Rieger, S.; Kulkarni, R. P.; Darcy, D.; Fraser S. E.; Koster, R. W. (2005) Quantum Dots Are Powerful Multipurpose Vital Labeling Agents in Zebrafish Embryos. *Developmental Dynamics*, Vol. 234 pp. 670-681.
- Samia, A. C. S.; Dayal, S.; Clemens, B. (2006) Quantum Dot-based Energy Transfer: Perspectives and Potential for Applications in Photodynamic Therapy. *Photochemistry and Photobiology*, Vol. 82, pp. 617-625.
- Santos, B. S., Farias, P. M. A. ; Fontes, A. . Semiconductor Quantum Dots for Biological Applications. In: Mohamed Henine (Editor Chefe). (Org.). *Handbook of Self Assembled Semiconductor Nanostructures Novel Devices in Photonics and Electronics*. Amsterdam: Elsevier, 2008a, p. 773-798.
- Santos, B. S.; Farias, P. M. A.; Menezes, F. D.; Brasil Jr, A. G.; Fontes, A.; Romão, L.; Amaral, J. O.; Moura-Neto, V.; Tenório, D. P. L. A.; Cesar, C. L.; Barbosa, L. C.; Ferreira, R. (2008b) New highly fluorescent biolabels based on II-VI semiconductor hybrid organic-inorganic nanostructures for bioimaging. *Applied Surface Science*, Vol. 255, pp. 790-792.
- Santos, B. S.; Farias, P. M. A. ; Menezes, F. D. ; Ferreira, R. C.; Alves Junior, S.; Figueiredo, R. C. B. Q.; Carvalho Junior, L. B.; Beltrão, E. I. C. (2006) CdS-Cd(OH)₂ core shell quantum dots functionalized with Concanavalin A lectin for recognition of mammary tumors. *Physica Status Solidi. C, Conferences and Critical Reviews*, Vol. 3, pp. 4017-4022.
- Stringer, R. C.; Hoehn, D.; Grant, S. A. (2008) Quantum Dot-Based Biosensor for Detection of Human Cardiac Troponin I Using a Liquid-Core Waveguide. *Sensors Journal, IEEE*, Vol. 8, pp. 295-300.
- Tekdas, D. A.; Durmus, M.; Yanika, H.; Ahsen V., (2012) Photodynamic therapy potential of thiol-stabilized CdTe quantum dot-group 3Aphthalocyanine conjugates (QD-Pc)

- Spectrochim Acta Part A: Molecular and Biomolecular Spectroscopy, Vol. 93, pp. 313–320
- Valenzuela, S., Liposome techniques for synthesis of biomimetic lipid membranes in Ferrari, M.; Martin, D. (Eds). Nanobiotechnology of biomimetic membranes, , New York: Springer, 2008 p. 75-87.
- Verma, A.; Stellacci, F. (2010) Effect of Surface Properties on Nanoparticle–Cell Interactions. *Small*, Vol. 6, pp. 12-21.
- Williams, Y.; Sukhanova, A.; Nowostawska, M.; Davies, A. M.; Mitchell, S.; Oleinikov, V.; Gun'ko, Y.; Nabiev, I.; Kelleher, D.; Volkov, Y. (2009) Probing Cell-Type-Specific Intracellular Nanoscale Barriers Using Size-Tuned Quantum Dots. *Small*, Vol. 5, pp. 2581-2588.
- Xia, Z., Rao, J. (2009) Biosensing and imaging based on bioluminescence resonance energy transfer. *Current Opinion in Biotechnology*, Vol. 20, pp. 1–8.
- Yang, C., Ding, N.; Xu, Y.; Qu, X.; Zhang, J.; Zhao, C.; Hong, L.; Lu, Y.; Xiang, G. (2009) Folate receptor-targeted quantum dot liposomes as fluorescence probes. *Journal of Drug Targeting*, Vol. 17, pp. 502–511.
- Yeh, C. Y.; Lu, Z. W.; Froyen, S.; Zunger, A. (1992). Zinc-blende-wurtzite polytypism in semiconductors. *Physical Review B*, Vol. 46, pp. 10086–10097.
- Yezhelyev, M. V.; QI, L.; O'Regan, R. M.; Nie, S.; Gao, X. (2008) Proton-Sponge Coated Quantum Dots for siRNA Delivery and Intracellular Imaging. *J. Am. Chem. Soc.*, Vol. 130, pp. 9006–9012.
- Yin, Y.; Alivisatos, A. P. (2005) Colloidal nanocrystal synthesis and the organic–inorganic interface. *Nature*, Vol. 437, pp. 664-670.
- Yoo, J. S.; Won, N.; Kim, H. B.; Bang, J.; Kim, S.; Ahn, S.; Soh, K. S. (2010) In vivo imaging of cancer cells with electroporation of quantum dots and multispectral imaging. *Journal of Applied Physics*, Vol. 107, pp. 124702-124710.
- Yoo, J.; Kambara, T.; Gonda, K.; Higuchi, H. (2008) Intracellular imaging of targeted proteins labeled with quantum dots. *Experimental Cell Research*, Vol. 314, pp. 3563-3569.

INTECH

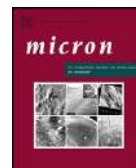
Apêndice B: Non-Specific interactions of CdTe/CdS Quantum Dots with human blood mononuclear cells

Revista: Micron

Classificação Qualis (Farmácia): B2

Autores: Rafael Bezerra de Lira, Mariana B. Cavalcanti, Maria A. B. L. Seabra, Diego C., N. Silva, Ademir J. Amaral, Beate S. Santos, Adriana Fontes

Ano: 2012



Non-specific interactions of CdTe/Cds Quantum Dots with human blood mononuclear cells

Rafael B. Lira^a, Mariana B. Cavalcanti^b, Maria A.B.L. Seabra^c, Diego C.N. Silva^a, Ademir J. Amaral^b, Beate S. Santos^c, Adriana Fontes^{a,*}

^a Departamento de Biofísica e Radiobiologia, Universidade Federal de Pernambuco, Recife, Brazil

^b Departamento de Energia Nuclear, Universidade Federal de Pernambuco, Recife, Brazil

^c Departamento de Ciências Farmacêuticas, Universidade Federal de Pernambuco, Recife, Brazil

ARTICLE INFO

Article history:

Received 20 July 2011

Received in revised form

12 November 2011

Accepted 12 November 2011

Keywords:

Quantum Dots

Fluorescence

Flow cytometry

Non-specific interaction

Zeta potential

ABSTRACT

In order to study biological events, researchers commonly use methods based on fluorescence. These techniques generally use fluorescent probes, commonly small organic molecules or fluorescent proteins. However, these probes still present some drawbacks, limiting the detection. Semiconductor nanocrystals – Quantum Dots (QDs) – have emerged as an alternative tool to conventional fluorescent dyes in biological detection due to its topping properties – wide absorption cross section, brightness and high photostability. Some questions have emerged about the use of QDs for biological applications. Here, we use optical tools to study non-specific interactions between aqueous synthesized QDs and peripheral blood mononuclear cells. By fluorescence microscopy we observed that bare QDs can label cell membrane in live cells and also label intracellular compartments in artificially permeabilized cells, indicating that non-specific labeling of sub-structures inside the cells must be considered when investigating an internal target by specific conjugation. Since fluorescence microscopy and flow cytometry are complementary techniques (fluorescence microscopy provides a morphological image of a few samples and flow cytometry is a powerful technique to quantify biological events in a large number of cells), in this work we also used flow cytometry to investigate non-specific labeling. Moreover, by using optical tweezers, we observed that, after QDs incubation, zeta potentials in live cells changed to a less negative value, which may indicate that oxidative adverse effects were caused by QDs to the cells.

© 2011 Elsevier Ltd. All rights reserved.

1. Introduction

One of the fundamental goals in Biology is the understanding of how biomolecules interact among each other from cells to whole organisms (Michalet et al., 2006). In order to get a better comprehension of these interactions, researchers commonly use techniques based on fluorescence mainly because of its high specificity and sensitivity, even for single molecule detection (Michalet et al., 2006; Giepmans et al., 2006). The evolution of probing tools, including new techniques (such as multiphoton microscopy), new lasers and also new fluorescent probes, allows us to take advantages of the full potential of fluorescence. In fact, the high specificity of fluorescent events is intrinsically linked to the applied fluorescent probes. However, the more conventional fluorophores (i.e. organic dyes) present some critical limitations, such as narrow absorption

and broad emission spectra with short Stokes shift and principally poor photostability (Tsien et al., 2006; Michalet et al., 2005; Genger et al., 2008). This last drawback is very limiting especially for a greater observation time period.

Water synthesized II–VI semiconductor nanocrystals, also known as *Quantum Dots* (QDs), have been extensively used in biological and biomedical fields mainly due to their advantageous optical properties (Michalet et al., 2005; Genger et al., 2008), which include: a broad absorption band (allowing a flexible cross section for multiphoton microscopy), size tunable emission wavelength (fluorescence color depends on the size of QDs), an active surface for molecular conjugation and mainly the high resistance to photobleaching (the best QDs' feature) (Larson et al., 2003; Sperling and Parak, 2010). In general, water-based QDs have been successfully used as fluorescent labels for imaging live cells and small animals (Law et al., 2009), in immunoassays (Tian et al., 2010), in the development of diagnostic methodologies (Yezhelyev et al., 2006) and also for photodynamic therapy (Samia et al., 2006).

In all these applications, QDs conjugated to proteins or antibodies play important roles, because they are inorganic-biological hybrids nanoparticles that combine characteristics of both

* Corresponding author at: Departamento de Biofísica e Radiobiologia, Universidade Federal de Pernambuco, Recife 50670 901, Brazil. Tel.: +55 81 21267818.

E-mail addresses: adriana.fontes@pesquisador.cnpq.br, adri-fontes@uol.com.br (A. Fontes).

materials, that is: the fluorescence properties of QDs with the biochemical functions of the proteins and antibodies. However, an incomplete conjugation may result in residual non-conjugated QDs in the same colloidal suspension which can bind or interact non-specifically with the biological system and interfere in the desired results of the original applications (Smith and Giorgio, 2009). Non-specific interaction is mainly caused by adsorption between the carboxyl groups presented in QDs surface due to the stabilizing agents – such as thioglycolic acid or 3-mercaptopropionic acid used in water dispersion QDs synthesis – and amine groups presented in cells.

In this way, despite the successfully described biological applications of QDs, some drawbacks still exist. Synthesis of high quality water dispersed QDs, stability in aqueous medium, biocompatibility, narrow size distribution and (only) specific interactions with target molecules are characteristically hard tasks to be achieved all together and now are part of a special research topic in the field of QDs biological applications. Moreover, little is still known about the mechanisms which regulate QDs-biological systems interactions and how this can affect cellular functions. As well as in other classes of nanoparticles, QDs cellular uptake is dependent of the nanoparticle surface coating and of the cell type (Kelf et al., 2010) and adverse effects are generally related to cell uptake capacity (Chang et al., 2006). Further, once internalized, QDs can be released from endocytic vesicles and access nuclear structures binding strongly to histone proteins (Nabiev et al., 2007). In order to provide new insights about possible effects associated with non-specific labeling, it is important to evaluate the capacity of the nanoparticles to interact with cells.

In this work we present studies, using different optical techniques, focused on non-specific interactions between water dispersed carboxyl-coated CdTe/CdS QDs and live or permeabilized human peripheral blood mononuclear cells (PBMCs). These cells were chosen because this sample is mainly consisted by lymphocytes, which are more specialized cells that do not perform a very active endocytosis, such as many others mammalian cells. This is an important feature, since unspecific interactions with these cells practically do not depend on the QDs uptake.

Fluorescence microscopy is broadly applied to confirm morphological localization of a fluorescent probe that can label or not a specific cell structure. Although it represents a powerful tool to investigate biological processes it usually lacks statistical analysis. Moreover, QDs have been widely applied for fluorescence microscopy, but they have not been much explored as a potential tool for flow cytometry. Fluorescence microscopy and flow cytometry are complementary techniques, while fluorescence microscopy provides a morphological image of a few samples, flow cytometry is a powerful technique to detect and quantify biological events in a large number of cells. So, in the present study we also performed a more quantitative investigation of the QDs-cells labeling by using not only fluorescence microscopy but also flow cytometry analysis.

Lastly, herein we also investigate QDs incubation effects on the membrane electrical charges of PBMCs through zeta potential measurements performed by using an optical tweezers system (Fontes et al., 2008). We believe that this measurement can be used as a complementary way to analyze adverse effects caused in cells by QDs.

2. Materials and methods

2.1. QDs synthesis and characterization

Water colloidal dispersed CdTe/CdS core/shell QDs were synthesized according to the previously reported method (Gaponik et al., 2002). Briefly, QDs were prepared by the addition of Te^{2-} solution

in a $\text{Cd}(\text{ClO}_4)_2$ 0.01 M solution of pH > 10 in the presence of MPA (3-mercaptopropionic acid) (Sigma Aldrich) as the stabilizing agent in a 2:1:5.7 proportion of Cd:Te:MPA (molar ratio). The reaction proceeds refluxing at 90 °C under argon and constant stirring for 7 h. The Te^{2-} solution was prepared by using metallic tellurium (Sigma Aldrich) and NaBH_4 (Sigma Aldrich), under argon atmosphere. QDs optical characterizations were performed by absorption and emission spectroscopy (using Ocean Optics HR4000 and ISS K2 equipments, respectively). While, QDs structural characterization was performed by X-ray diffractometry (Siemens Nixford D5000, using dried powder samples).

2.2. Mononuclear cell separation and incubation with QDs

PBMCs were obtained according to a previous reported methodology (Cavalcanti et al., 2008). Briefly, PBMCs were isolated by centrifugation (at $400 \times g$ for 35 min) using Ficoll Paque Plus (GE Healthcare). PBMCs were washed twice in PBS (Phosphate Buffered Saline) at pH of 7.4 and resuspended in RPMI medium at 1×10^6 cells/mL. Before incubation, the QDs pH was adjusted to physiological values (7.0–7.4).

In order to study QDs non-specific interactions to live cells, we incubated 900 μL and 950 μL of live PBMCs with 100 μL and 50 μL of QDs (48 μM at original concentration) in serum free RPMI medium for 30 min in a 5% CO_2 atmosphere at 37 °C. The first incubation corresponds to a final QDs concentration of 4.8 μM and the second one of 2.4 μM . After incubation, samples were washed twice times with PBS buffer and resuspended in fresh serum-free RPMI medium. For optical trapping measurements, the same protocol was carried out except that cells were resuspended in compatible blood serum for both control cells (without QDs) and for cells after QDs incubation (by using 2.4 μM).

For cellular permeabilization, PBMCs were resuspended in permeabilizing solution and incubated for 10 min at room temperature. After this step, cells were washed twice using Tween-20 PBS solution (0.5% Tween-20 in PBS) and centrifugated at $400 \times g$ for 5 min.

2.3. Optical tools applied for QDs-cell interactions

Live and permeabilized cells were analyzed by fluorescence microscopy (Leica DMI4000B or Leica SP2-AOBS confocal microscope) and also by flow cell cytometry (FACScalibur, Becton Dickinson). For confocal and cell cytometry analysis the QDs fluorescence excitation was performed by an argon laser ($\lambda = 488 \text{ nm}$). In the cytometry experiments, the emission was detected in FL1 channel ($530 \pm 15 \text{ nm}$). Each analysis included 10,000 events. Control cells (live and permeabilized) were used to define the region for cell gate in the detection system. Computational analysis of cell labeling was performed by using the Cell Quest software version 3.1 (Becton Dickinson). The experiments were performed at least 5 times and each one was done in duplicate.

Membrane electrical charges on live PBMCs with or without (control cells) QDs incubation were analyzed by zeta potential measurements in an optical tweezers system. The optical tweezers system used consisted of a laser beam in the near infrared ($\lambda = 1064 \text{ nm}$ – IPG Photonics) focused on the microscope (Axio-lab – Carl Zeiss) through an objective of 100 \times . The microscope is equipped with a motorized stage (Prior Scientific) and with a real time image capture system integrated to a computer. The zeta potential measurements were performed according to the methodology described in a previous report (Fontes et al., 2008). The PBMCs were submitted to different applied voltages (30, 40, 50, 60, 70 and 80 V) and the optical trap was used to recapture the cell after each voltage. The terminal velocity was measured for each applied voltage and the zeta potential was obtained by using the

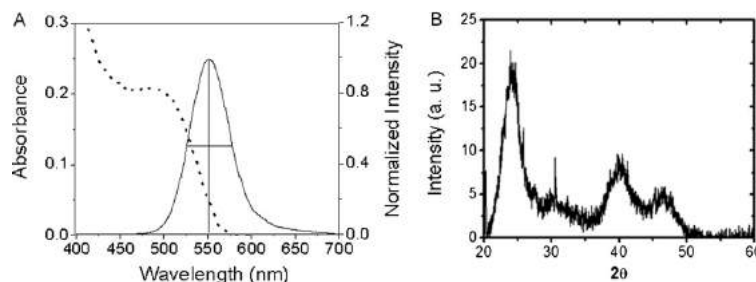


Fig. 1. (A) Absorption (dashed) and emission spectra of typical nanocrystals of CdTe/CdS-MPA (excitation at 365 nm) and (B) CdTe/CdS-MPA X-ray diffraction.

Smoluchowski equation (at least 10 cells were measured by group, with and without QDs) (Fontes et al., 2008).

3. Results and discussion

3.1. QDs synthesis and characterization

Fig. 1 shows the normalized absorption and emission spectra of CdTe/CdS-MPA QDs synthesized for the present study. QDs suspension shows a bright fluorescence emission with maximum at 551 nm and full width at half maximum (FWHM) of 50 nm.

Based on the first absorption peak position, we estimated the average QDs' diameter as $d = 2.3$ nm (Rogach et al., 2007). From the average size and based on QD's first absorption peak, we estimated the original QDs concentration as $48 \mu\text{M}$ (Yu et al., 2003). The QDs structural characterization performed by X-ray powder diffraction (Fig. 1B) confirms the same size range ($d = 2.6$ nm) by applying the Scherrer equation.

3.2. Live PBMCs cells QDs interaction

Fig. 2 shows typical fluorescence microscopy image frames of live PBMCs cells. The diffuse spot-like pattern suggests that bare CdTe/CdS-MPA QDs interact non-specifically to live PBMC cells membrane for the higher concentration used. Other information that supports this observation is that lymphocytes, in general, do not perform a very active internalization such as endocytosis of usual cargos like QDs. We also observe some QDs agglomerates on the cell surface and in the medium. The QD-cells interactions are mainly due to adsorption (induced by electrostatic and hydrophilic/hydrophobic interactions) between amine groups of the cell membrane and carboxyl groups from the QDs' surface.

For a more quantitative analysis, we performed flow cytometry measurements. Fig. 3 shows dot plots for PBMCs cells incubated in conditions similar to those shown in Fig. 2. Fig. 3A and B show that the spots (individual cells) are shifted to the right side, confirming quantitatively that more than 90% of cells were labeled by CdTe/CdS-MPA at both QDs concentrations. Wide distribution of cells in the dot plots (horizontal axes corresponds to FL1 green channel) means that individual cells are differentially labeled by the nanoparticles in the whole cell population as it was also observed in the microscopic images, a common feature for non-specific interactions.

In order to see more clearly the changes in the cell labeling pattern and to better understand non-specific cell interaction, we permeabilized the cells allowing the QDs to cross the plasma membrane. If they were able to enter the cell, we would be able to observe fluorescence throughout the cell rather than only at the surface. Artificially permeabilizing the cells can also be an alternative methodology to stain intracellular structures with

nanoparticles, especially in cells which do not perform active internalization processes.

In fact, Fig. 4 shows that after cellular permeabilization the fluorescence profile has a different staining pattern compared to Fig. 2, suggesting that QDs entered the cell interior almost homogeneously and even interacted with intracellular structures (it was observed for both QDs concentrations). In some cells it was possible to observe QDs distribution in the cytoplasm only, but in other cells it was also possible to see that there were nanoparticles even inside the nucleus (Fig. 4B). The permeabilization acts distinctly in the cytoplasmatic and nuclear membrane in each cell resulting in a different final localization of the QDs and consequently a different staining pattern (Williams et al., 2009).

In more detailed observations one can note that, once QDs cross nuclear membrane they present a high affinity interaction to nuclear structures such as cell nucleolus. Fig. 4B shows representative confocal fluorescence images of nuclear/nucleolar labeling by QDs after nuclear membrane crossing (square 1). In contrast, QDs which did not cross this membrane are located only inside the cell cytosol (square 2). In general, a great number of cells from different experiments displayed nuclear/nucleolar staining. By analyzing the images, we consider that once inside the cells, QDs always interact non-specifically with intracellular structures. In fact, it has been reported that carboxyl coated QDs strongly interact with histone proteins in nucleus (or in free cell conditions) (Conroy et al., 2008), however it is still not known yet why they interact with these structures in the cytosol. As a consequence, non-specific interactions in intracellular compartments have also to be considered when tracking internal targets.

As QDs can also enter and interact with some internal structures rather than just with cell surface, the average fluorescence signal from cells would be higher in permeabilized ones than those without permeabilization treatment. Also it would be expected that a higher number of cells would be labeled, which is true, as shown by the dot plots in Fig. 5. This cellular staining has no dependence from the thiol stabilizing molecule used in QDs synthesis, since mercaptoacetic-acid QDs displayed similar interactions (data not shown). In fact, virtually all cells are labeled with the lower and higher QD concentration used here after permeabilization, as can be seen from dot plots (Fig. 5A and B).

3.3. Zeta potential measurements after cell-QDs incubation

Results reported in the literature on the effects caused by QDs in cells are controversial. While the first reports were based only on morphological changes (Lovrić et al., 2005) more recently ones use metabolic and biochemical assays to study QDs' toxicity (Yana et al., 2011). These last data are directly related to nanoparticle uptake (Chang et al., 2006). Glycoproteins of cell membranes are responsible for the negatively charged membrane surface. This negative cell surface induces the formation of a layer of opposite charges

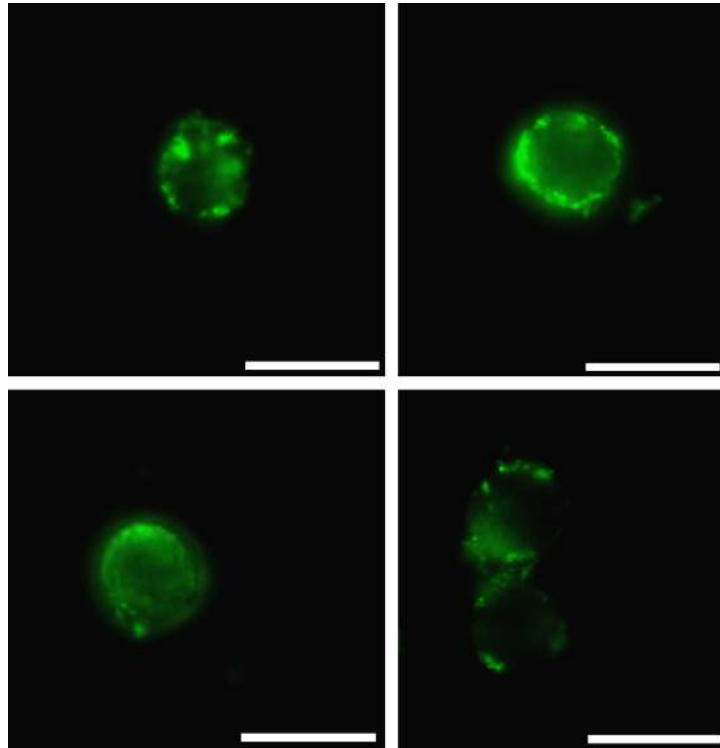


Fig. 2. Non-specific interactions between non-conjugated QDs and live PBMCs cells. These figures represent a frame of common profiles of QDs non-specific labeling presented in these cells. Bars: 12 μm .

consisting of ions rigidly bonded around to the cell and creates a repulsive electrical zeta potential (ζ) between them (Fontes et al., 2008). The zeta potential reflects the membrane electrical charges and can, for example, be used to study cell agglutination (Fontes et al., 2008; Pollack and Reckel, 1977) and also to understand cancer related diseases (Carter and Coffey, 1988).

Here, we evaluate changes on membrane electrical properties through zeta potential (ζ) measurements after live cell incubation with QDs by using optical tweezers measurements. These preliminary results show that control PBMC cells presented an average $\zeta = -14.3 \text{ mV}$ ($\pm 1.8 \text{ mV}$), while those incubated with QDs displayed an average $\zeta = -9.8 \text{ mV}$ ($\pm 1.2 \text{ mV}$).

The zeta potential measurements observed for different carboxyl coated QDs in water are in the range of -20 to -55 mV (Lovrić et al., 2005; Kelf et al., 2010). We would expect that the incorporation of QDs in the cell membrane would shift its zeta potential to a more negative value, but this was not the case. Then, we suggest that the change of the zeta potential to a less negative value is not related to the QDs adsorption to the cell surface. Some works in the literature reported that a decrease of glycoproteins in cell membranes can be related to oxidative stress (Straface et al., 2000). The main responsible for the cell membrane negative charge is the sialic acid presented in glycoproteins and the ζ measurements suggest that the QDs in some way may be collaborating to decrease sialic

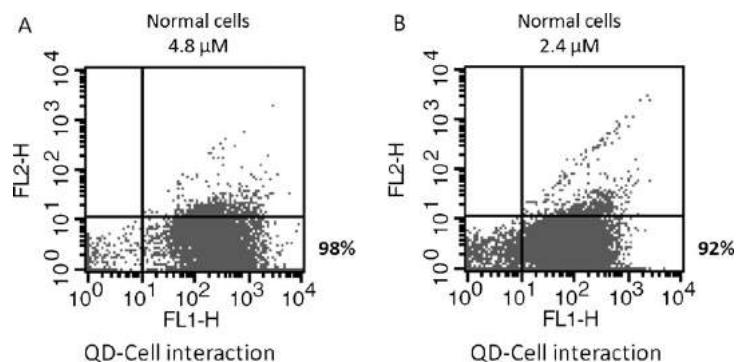


Fig. 3. Dot plots for non-specific cellular labeling of living cells by QDs. The percentage indicates the amount of labeled cells in the concentration used. The analyses show that more than 90% of cells are labeled regardless the two concentrations used.

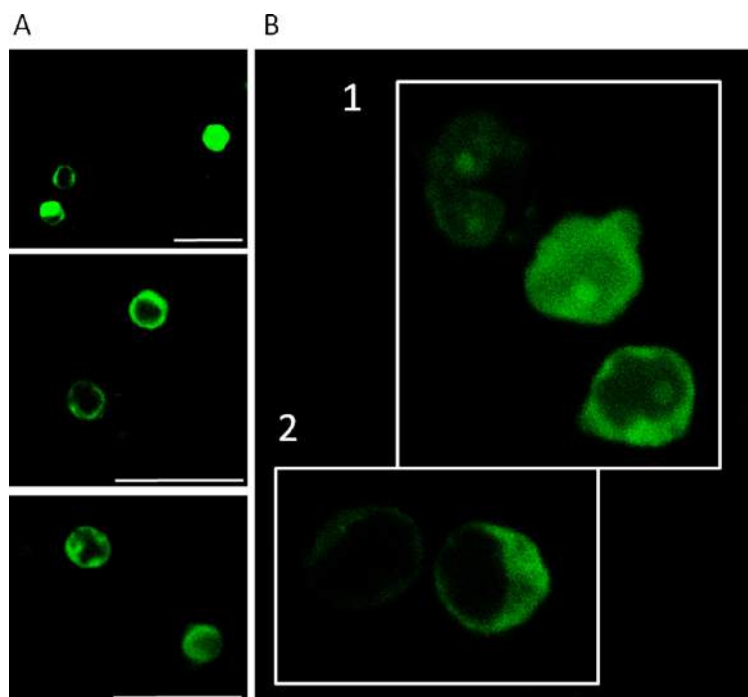


Fig. 4. Non-specific interactions between QDs and intracellular structures in permeabilized PBMCs. After permeabilizing treatment, QDs are able to enter the cells, as shown in typical fluorescence image frames in (A). In (B), QDs can interact with cytoplasmic (square 2) or even nuclear/nucleolar structures (square 1). Bars in A = 25 μm ; Bar in B = 12 μm .

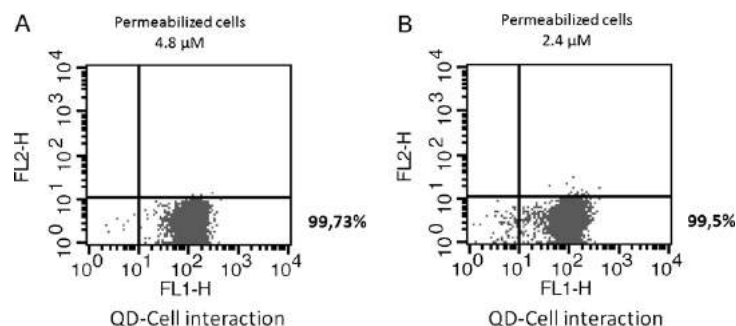


Fig. 5. Dot plots for cellular labeling by CdTe/CdS-MPA QDs after permeabilization. Almost the whole cell population was labeled regardless the concentration used.

acid. Based on this, we suggest that the changes in ζ can be related to membrane oxidative damages caused by the QDs incubation.

4. Conclusions

Water dispersed semiconductor nanocrystals have emerged as an alternative to the traditional hydrophobic QDs where toxic and pyrophoric agents are used. Here, we synthesized fluorescent carboxyl coated CdTe/CdS nanocrystals and evaluated their ability to interact non-specifically with plasma membrane on live PBMCs and also with intracellular compartments in permeabilized PBMCs. Further, we showed that live cell incubation alters cell membrane charges indicating that zeta potential measurements can be used as a complementary analysis of cell membrane integrity to probe eventual adverse oxidative effects caused on cell after QDs incubation or even after the use of other kinds of nanoparticles.

We demonstrate that there are non-specific interactions between bare CdTe/CdS QDs and cells surface and even organelles presented inside PBMCs. Such interactions may interfere in biological conclusions when specific targets have to be detected if a non-effective conjugation processes happened. This is true for these or any other cell lineage when non-specific interaction is significant. These non-specific interactions are results of adsorption (electrostatic and hydrophilic/hydrophobic interactions) between the chemical groups present in the cell membrane and on QDs surface.

Closing, we showed that permeabilized PBMCs presented higher fluorescence pattern than non permeabilized ones, demonstrating an alternative methodology to stain intracellular structures localized in the cytosol or in the nucleus. This work also shows that QDs can become a potential, efficient and low cost diagnostic tool for cytometry, compatible with the lasers and filters used in this kind

of equipment and that studies about non-specific cells-QDs interactions are still necessary to improve biological conclusions when a specific labeling is desired.

Acknowledgements

The authors are grateful to CAPES, CNPq, FACEPE, L'oreal, Brazilian Academy of Sciences and UNESCO. This work is also linked to National Institute of Photonics. We also are grateful to Regina C. Bressan Q. Figueiredo by the microscopy support and to Aggeu Magalhães Institute for flow cytometry analysis.

References

- Carter, H.B., Coffey, D.S., 1988. Cell-surface charge in predicting metastatic potential of aspirated cells from the dunning rat prostatic adenocarcinoma model. *J. Urol.* 140, 173–175.
- Cavalcanti, M.B., Amaral, A.J., Fernandes, T.S., Melo, J.A., Machado, C.G.F., 2008. P53 protein expression levels as bioindicator of individual exposure to ionizing radiation by flow cytometry. *Mol. Cell. Biochem.* 308, 127–131.
- Chang, E., Thekkekk, N., Yu, W.W., Colvin, V.L., Drezek, R., 2006. Evaluation of Quantum Dot cytotoxicity based on intracellular uptake. *Small* 2 (12), 1412–1417.
- Conroy, J., Byrne, S.J., Gun'ko, Y.K., Rakovich, Y.P., Donegan, J.F., Davies, A., Kelleher, D., Volkov, V., 2008. CdTe nanoparticles display tropism to core histones and histone-rich cell organelles. *Small* 4 (11), 2006–2015.
- Fontes, A., Fernandes, H.P., de Thomaz, A.A., Barbosa, L.C., Barjas-Castro, M.L., Cesar, C.L., 2008. Measuring electrical and mechanical properties of red blood cells with double optical tweezers. *J. Biomed. Opt.* 13, 014001.
- Gaponik, N., Talapin, D.V., Rogach, A.L., Hoppe, K., Shevchenko, E.V., Kornowski, A., Eychmüller, A., Weller, H.J., 2002. Thiol-capping of CdTe nanocrystals: an alternative to organometallic synthetic routes. *J. Phys. Chem. B* 106, 7177–7185.
- Genger, U.R., Grabolle, M., Jaricot, S.C., Nitschke, R., Nann, T., 2008. Quantum Dots versus organic dyes as fluorescent labels. *Nat. Methods* 5, 763–775.
- Giepmans, B.N.G., Adams, S.R., Ellisman, M.E., Tsien, R.Y., 2006. The fluorescent toolbox for assessing protein location and function. *Science* 312, 217–224.
- Kelf, T.A., Sreenivasan, V.K.A., Sun, J., Kim, E.J., Goldys, E.M., Zvyagin, A.V., 2010. Non-specific cellular uptake of surface-functionalized quantum dots. *Nanotechnology* 21, 1–8.
- Larson, D.R., Zipfel, W.R., Williams, R.M., Clark, S.W., Bruchez, M.P., Wise, F.W., Webb, W.W., 2003. Water-soluble Quantum Dots for multiphoton fluorescence imaging in vivo. *Science* 300, 1434–1436.
- Law, W.-C., Yong, K.-T., Roy, I., Ding, H., Hu, R., Zhao, W., Prasad, P.N., 2009. Aqueous-Phase Synthesis of Highly Luminescent CdTe/ZnTe Core/Shell Quantum Dots Optimized for Targeted Bioimaging. *Small* 5, 1302–1310.
- Lovrić, J., Bazzi, H.S., Cuie, Y., Fortin, G.R.A., Winnik, F.M., Maysinger, D., 2005. Differences in subcellular distribution and toxicity of green and red emitting CdTe quantum dots. *J. Mol. Med.* 83, 377–385.
- Michalet, X., Pinaud, F.F., Bentolila, L.A., Tsay, J.M., Doose, S., Li, J.J., Sundaresan, G., Wu, A.M., Gambhir, S.S., Weiss, S., 2005. Quantum Dots for live cells, in vivo imaging, and diagnostics. *Science* 307, 538–544.
- Michalet, X., Weiss, S., Jäger, M., 2006. Single-molecule fluorescence studies of protein folding and conformational dynamics. *Chem. Rev.* 106, 1785–1813.
- Nabiev, I., Mitchell, S., Davies, A., Williams, Y., Kelleher, D., Moore, R., Gun'ko, Y.K., Byrne, S., Rakovich, Y.P., Donegan, J.F., Sukhanova, A., Conroy, J., Cottell, D., Gaponik, N., Rogach, A., Volkov, Y., 2007. Nonfunctionalized nanocrystals can exploit a cell's active transport machinery delivering them to specific nuclear and cytoplasmic compartments. *Nano Lett.* 7 (11), 3452–3461.
- Pollack, W., Reckel, R.P., 1977. A reappraisal of the forces involved in hemagglutination. *Int. Arch. Allergy Appl. Immunol.* 54, 29–42.
- Rogach, A.L., Franzl, T., Klar, T.A., Feldmann, J., Gaponik, N., Lesnyak, V., Shavel, A., Eychmüller, A., Rakovich, Y.P., Donegan, J.F., 2007. Aqueous synthesis of thiol-capped CdTe nanocrystals: state-of-the-art. *J. Phys. Chem. C* 111, 14628–14637.
- Samia, A.C.S., Dayal, S., Burda, C., 2006. Quantum Dot-based energy transfer: perspectives and potential for applications in photodynamic therapy. *Photochem. Photobiol.* 82, 617–625.
- Smith, R.A., Giorgio, T.D., 2009. Quantitative measurement of multifunctional Quantum Dot binding to cellular targets using flow cytometry. *Cytometry A* 75A, 465–474.
- Sperling, R.A., Parak, W.J., 2010. Surface modification, functionalization and bio-conjugation of colloidal inorganic nanoparticles. *Philos. Trans. R. Soc. A* 368, 1333–1383.
- Straface, E., Matarrese, P., Gambardella, L., Forte, S., Carlone, S., Libianchi, E., Schmid, G., Malorni, W., 2000. N-Acetylcysteine counteracts erythrocyte alterations occurring in chronic obstructive pulmonary disease. *Biochem. Biophys. Res. Commun.* 279, 552–556.
- Tian, J., Liu, R., Zhao, Y., Peng, Y., Hong, X., Xu, Q., Zhao, S., 2010. Synthesis of CdTe/CdS/ZnS Quantum Dots and their application in imaging of hepatocellular carcinoma cells and immunoassay for alpha fetoprotein. *Nanotechnology* 21, 1–8.
- Tsien, R.Y., Ernst, L., Waggner, A., 2006. Fluorophores for confocal microscopy: photophysics and photochemistry. In: Pawley, J.B. (Ed.), *Handbook of Biological Confocal Microscopy*, third ed. Springer Science + Business Media, New York, pp. 338–352.
- Williams, Y., Sukhanova, A., Nowostawska, M., Davies, A.M., Mitchell, S., Oleinikov, V., Gun'ko, Y., Nabiev, I., Kelleher, D., Volkov, Y., 2009. Probing cell-type-specific intracellular nanoscale barriers using size-tuned Quantum Dots. *Small* 5 (22), 2581–2588.
- Yana, M., Zhanga, Y., Xua, K., Fub, T., Qinb, H., Zhenga, X., 2011. An in vitro study of vascular endothelial toxicity of CdTe Quantum Dots. *Toxicology* 282, 94–103.
- Yezhelyev, M.V., Gao, X., Xing, Y., Al-Hajj, A., Nie, S., O'Regan, R.M., 2006. Emerging use of nanoparticles in diagnosis and treatment of breast cancer. *Lancet Oncol.* 7 (8), 657–667.
- Yu, W.W., Qu, L., Guo, W., Peng, X., 2003. Experimental determination of the extinction coefficient of CdTe, CdSe, and CdS nanocrystals. *Chem. Mater.* 15, 2854–2860.

Apêndice C: Studies on intracellular delivery of carboxyl-coated CdTe quantum dots mediated by fusogenic liposomes

Revista: Journal of Materials Chemistry B

Classificação Qualis (Farmácia): A1

Autores: Rafael B. Lira, Maria A. B. L. Seabra, Anna L. L. Matos, Jéssica V. Vasconcelos, Darlene P. Bezerra, Eneida de Paula, Beate S. Santos and Adriana Fontes

Ano: 2013

Studies on intracellular delivery of carboxyl-coated CdTe quantum dots mediated by fusogenic liposomes†

Cite this: *J. Mater. Chem. B*, 2013, **1**, 4297Rafael B. Lira,^a Maria A. B. L. Seabra,^b Anna L. L. Matos,^a Jéssica V. Vasconcelos,^a Darlene P. Bezerra,^a Eneida de Paula,^c Beate S. Santos^b and Adriana Fontes^{*a}

The use of Quantum Dots (QDs) as fluorescent probes for understanding biological functions has emerged as an advantageous alternative over application of conventional fluorescent dyes. Intracellular delivery of QDs is currently a specific field of research. When QDs are tracking a specific target in live cells, they are mostly applied for extracellular membrane labeling. In order to study intracellular molecules and structures it is necessary to deliver free QDs into the cell cytosol. In this work, we adapted the freeze and thaw method to encapsulate water dispersed carboxyl-coated CdTe QDs into liposomes of different compositions, including cationic liposomes with fusogenic properties. We showed that labeled liposomes were able to fuse with live human stem cells and red blood cells in an endocytic-independent way. We followed the interactions of liposomes containing QDs with the cells. The results were minutely discussed and showed that QDs were delivered, but they were not freely diffused in the cytosol of those cells. We believe that this approach has the potential to be applied as a general route for encapsulation and delivery of any membrane-impermeant material into living cells.

Received 19th February 2013

Accepted 26th June 2013

DOI: 10.1039/c3tb20245c

www.rsc.org/MaterialsB

Introduction

The use of Quantum Dots (QDs) as fluorescent probes for understanding biological functions has emerged as an advantageous alternative over application of conventional fluorescent dyes.^{1,2} QDs have been used for cellular labeling and biomedical research due to their wide absorption and narrow emission spectra, bright fluorescence, high photostability, chemically active surface and size-tunable emission.^{1–6} These optical properties have allowed long term analysis of biological events and labeling of multiple targets simultaneously for reconstruction of multicolor images.⁷ However, especially for living cells, due to their size and physico-chemical properties, QDs have been mostly applied to label and target structures localized in the extracellular membrane.⁸ Therefore, it is still challenging to study intracellular molecules and organelles using QDs. These nanometer sized crystals cannot passively cross the lipid bilayer of plasma membranes and diffuse freely into the cytosol. QDs are endocytosed and confined in vesicular endosomes, limiting their application in experiments of intracellular labeling. Thus, the development of methods to overcome the

plasma membrane and/or escape from endo/lysosomal trapping after endocytosis is required for these fluorophores.

Some methods have been applied to deliver membrane-impermeant compounds to the cell interior. They can be classified as chemical, biological or physical approaches. Chemical strategies rely basically on the use of nanocarriers chemically designed to deliver materials into cells.^{9,10} Biological methods are almost exclusively mediated by viral vectors^{10–12} whereas physical approaches are based mainly on cell membrane manipulations (*i.e.* electroporation and microinjection).^{13,14} Some of these strategies have been tested to deliver QDs into cells and combine their own advantages and disadvantages. For instance, in the case of physical approaches, while electroporation is able to overcome the plasma membrane of many cells at a time by producing transient pores, it causes damage to the biological system and delivers QDs as agglomerates.^{15,16} By microinjection, the material can be introduced into any desired cellular compartment in any amount, but this is a laborious cell-by-cell technique and it also requires specialized equipment.^{16–18}

On the other hand, some chemical strategies for delivery of QDs rely on the use of osmotic lyses such as the “proton-sponge” effects for lysosome leakage¹⁹ or combine the use of photosensitizers to release the endocytosed cargos after light-triggered endosome disruption.²⁰ Nevertheless, these chemical approaches have intrinsically the potential to induce adverse effects after releasing the lysosomal content.

In principle, QDs coated with cell penetrating peptides (CPPs) or other transporting molecules can also be used, but

^aDepartamento de Biofísica e Radiobiologia, Universidade Federal de Pernambuco, Av. Prof. Moraes Rego S/N, 50670-901, Pernambuco, Recife, Brazil. E-mail: adriana.fontes@pesquisador.cnpq.br

^bDepartamento Farmacêuticas, Universidade Federal de Pernambuco, Recife, Brazil

^cDepartamento de Bioquímica, Instituto de Biologia, Universidade Estadual de Campinas, Campinas, Brazil

† Electronic supplementary information (ESI) available. See DOI: 10.1039/c3tb20245c

with them it is more difficult to target intracellular structures specifically since at least two different chemical molecules have to be conjugated to the QD for delivery and labeling purposes (which are the CPPs and the targeting molecules).²¹ Moreover, it is not clear whether the uptake of CPPs or their conjugates is endocytosis-dependent^{22,23} and they may carry the QD particles to different locations inside cells compared to non-conjugated CPPs.²⁴

Another common and important approach relies on lipofection, which uses electrostatic interactions between the external membrane of cationic liposomes and negatively charged materials (*e.g.* oligonucleotides) to promote charge-mediated adsorption to cells, endocytic uptake and release of endocytosed cargo after lysosomal destabilization.^{25,26} However, this approach is limited to the use of anionic cargos and depends on sequential processing steps that vary according to the cell types. The cytosolic release of the transported material is also subject to many variables, including endocytic competence and the net charge of the cargo-carrier system.^{25,27,28}

In this way, the design of a platform for the delivery of free nanoparticles into living cells, which does not depend on the cell uptake ability or the cargo charges, would open up many possibilities for new applications in biomedical and life sciences. In this work, we adapted the freeze and thaw method to encapsulate water synthesized carboxyl-coated CdTe QDs in liposomes of different compositions. Recently, Csizár *et al.*²⁹ reported direct fusion between non-functionalized cationic liposomes and the plasma membrane of different cell lineages. These liposomes with fusogenic properties are a valuable tool to investigate membrane fusion mechanisms and could also be used to design nanocarriers for intracellular delivery of membrane-impermeant compounds without the need for further chemical functionalization. Therefore, after confirming the encapsulation of liposomes with a more simple composition, we also included QDs in these liposomes with fusogenic properties and tested their ability to deliver these nanocrystals into living human-derived umbilical stem cells as well as into red blood cells (RBCs). The final fate of these nanoparticles is investigated and minutely discussed based on the physical-chemical properties of the cargo and the carrier, the QDs and liposomes, respectively. We believe that the method described here has the potential to be applied as a general route for encapsulation and intracellular delivery of any kind of membrane-impermeant material, including QDs and other classes of nanoparticles, and further, this work also gives some insights into the possible charge-mediated interactions between anionic QDs and cationic lipid bilayers.

Experimental methods

Quantum dot synthesis and characterization

Water dispersed MPA CdTe QDs were synthesized according to a previously reported method by some of us.³⁰ QDs were characterized by electronic UV-Vis absorption and emission spectroscopy (using respectively Ocean Optics HR4000 and ISS K2 equipment).

Liposome encapsulation of quantum dots

The following lipids were used in this study: egg phosphatidylcholine (EggPC), 1,2-dioleoyl-*sn*-glycero-3-phosphoethanolamine (DOPE), 1,2-dioleoyl-3-trimethylammonium-propane (DOTAP) and 1,2-dipalmitoyl-*sn*-glycero-3-phosphoethanolamine-*N*-(lissamine rhodamine B sulfonyl) (DPPE-Rh). Three different liposomes were prepared: with EggPC (from now on referred to as PC), with PC:DOTAP and with DOPE:DOTAP:DPPE-Rh (the latter being the fusogenic formulation²⁹). The liposome preparation is described in detail in the ESI†

For encapsulation, QDs were purified to remove residues from the synthesis, the pH suspension was adjusted to approximately 7.5 using a 0.1% (v/v) MPA solution and then added to previously prepared plain vesicle-liposome suspension (3 : 10 QDs : liposomes v/v). QDs' encapsulation in liposomes was carried out after applying 6 to 10 freeze and thaw cycles using liquid nitrogen and a water bath (40 °C) plus vortexing sequentially. Alternatively, the lipid film was hydrated in the presence of the nanoparticles.

Plain and loaded liposomes containing QDs were analyzed by conventional fluorescence microscopy (Leica DMI4000B) and transmission electron microscopy (Hitachi H-300 electron microscope – the preparation of liposomes for this analysis is described in the ESI†). The systems were also analyzed by dynamic light scattering and zeta potential measurements (ZetaSizer Nano ZS90, Malvern). For the acquisition of micrographs by conventional fluorescence microscopy, green QD emission was excited and collected using band pass filters at 480/40 nm and 527/30 nm, respectively. Red liposome emission was detected using excitation and emission band pass filters at 560/40 nm and 645/75 nm, respectively. The images were acquired with a 40× (NA: 0.75) oil-immersion objective.

Cell incubation with fusogenic liposomes

Confluent stem cell samples, obtained after the third or fourth passages, were used for the experiment. First, an amount of 50 µL of 2 mM fusogenic plain liposomes was added to the cellular medium and incubated for 1 h with or without bovine serum medium for trial tests of liposome-membrane fusion at 37 °C and 4 °C. In these experiments, the cells were fixed for observation. Stem cells were washed twice with PBS buffer (137 mM NaCl, 10 mM phosphate, and 2.7 mM KCl) and fixed with 4% paraformaldehyde. Afterwards, the samples were washed twice with PBS.

For fusogenic liposome-mediated QDs' delivery, stem cells were incubated with 50 µL of 2 mM fusogenic loaded-QD liposomes and microscopic observations were performed in real time with living cells, before and during incubation at room temperature and analyzed without fixation. These liposomes were also incubated with red blood cells (RBCs). For the incubation procedure, 50 µL of a 1% (v/v) RBC fraction in saline was incubated with 20 µL of 2 mM loaded-QD liposomes and immediately observed on a microscope by around 20 minutes. As cellular labeling was never observed after incubation with free MPA QDs, even when the QD concentration was 10 fold

higher than that used for liposome encapsulation (see ESI – Fig. S1†), we did not use purified liposomes for cell incubation.

Stem cells and RBCs were analyzed by conventional fluorescence microscopy (as described in Section 2.2). Stem cells were also observed by confocal fluorescence microscopy (multispectral Leica SPII-AOBS) under 488 nm excitation and the detection was centered at 530 and 630 nm for green and red signals, respectively.

Quantum dot–GUV interactions

We also studied the interaction of QDs with cationic Giant Unilamellar Vesicles (GUVs) using a confocal microscope (details of GUV preparation is provided in the ESI†). A 405 nm laser was used to excite QDs through a 60× oil-immersion objective and the fluorescence spectra were collected in the region of 500–550 nm (Olympus FV100 multispectral confocal microscope).

Results

Water synthesized QDs are nanoparticles with sizes ranging from 2–20 nm depending on their surface coating.^{1–6} They are membrane-impermeant especially due to their size and physical–chemical properties (*e.g.* charge and surface coating). Therefore, to deliver QDs (or other materials displaying similar features), one has to surpass the biological plasma membrane barrier. Among the various methods reported, we choose to work with the recently developed liposomes with fusogenic properties to release the encapsulated nanoparticles after liposome fusion with cells.

Quantum dot synthesis and characterization

For the experiments, nanocrystals refluxed for 7 h at 90 °C were used, which generate green emitting QDs.³⁰ The resulting nanoparticles displayed a bright green emission band with a maximum centered at 540 nm and Full-Width at Half Maximum (FWHM) = 51 nm (Fig. 1 – excitation at 365 nm). By the analysis of the first absorption maximum at 476 nm, using Dagtepe's curve³¹ adapted from Rogach's sizing curve,³² the average QD size (d) was estimated to be $d = 2.5$ nm. The QD size obtained by

using absorption spectra is in good agreement with TEM and X-Ray diffraction analysis previously reported by us.^{30,33} The original concentration was estimated to be 40 μ M for these green QDs, using Peng's and collaborators equations.³⁴

Liposome encapsulation of quantum dots

In order to encapsulate QDs in liposomes, we tested and adapted the freeze and thaw method, known to efficiently encapsulate water soluble compounds.^{35,36} The simplest liposomal system used was composed of PC only. Fig. 2(A1 and A2) shows frames of PC liposomes encapsulating fluorescent green QDs. The average encapsulation efficiency for PC liposomes was determined to be 35%. To our knowledge, it is a reasonable encapsulation efficiency for hydrophilic samples.³⁷

In order to generalize the process of QD encapsulation, we also tested the freeze and thaw method for a more complex system, PC : DOTAP (8 : 2 molar ratio), containing a cationic lipid. For this, we usually purified QD suspensions in order to eliminate contaminants from synthesis. This step helps to prevent some tendency of nanoparticles in precipitating highly positive lipid vesicles. Similar to those made with PC, cationic liposomes have also shown a bright green fluorescence after the freeze and thaw cycles (Fig. 2B). Interestingly, the more fluorescent the liposomes are, the darker they appear under phase contrast for all the compositions tested (fluorescent liposomes are optically denser because they are filled with particles – see ESI – Fig. S2†), a further indication of the presence of nanoparticles inside the vesicles. It is worth noting that these images show larger vesicles, whereas smaller ones were also present in the samples (Fig. S2†). However, it was harder to resolve them by optical microscopy due their small dimensions and their Brownian motion.

In contrast to some reports in the literature,^{38–40} simple lipid film hydration in the presence of nanoparticles was not sufficient for us to observe an efficient encapsulation of QDs into liposomes, even though several different experimental conditions were tested (lipid and QD concentration, temperature, vortexing speed, and liposomal composition). It is also worth mentioning that simple QD incubation with plain liposomes did not result in fluorescent vesicles, although some very faint

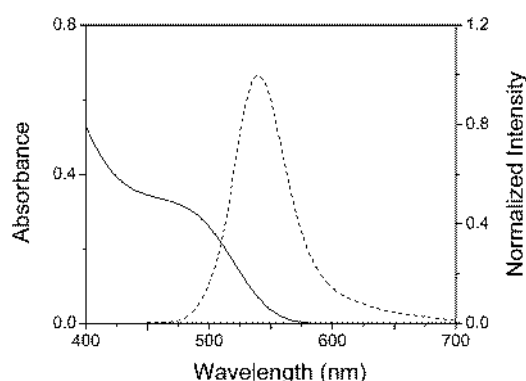


Fig. 1 CdTe QDs' optical characterization. Normalized absorption (solid line) and emission (dot line) spectra.

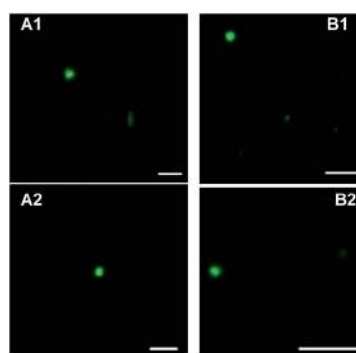


Fig. 2 Fluorescence microscopy images of CdTe QD loaded liposomes. (A) Encapsulation of green QDs in PC liposomes. (B) Encapsulation of QDs in cationic DOTAP-containing liposomes (20% DOTAP). Bars: 10 μ m.

fluorescence could be observed. In other words, the high intensity fluorescence, as seen in Fig. 2, is a result of encapsulation promoted by application of freeze and thaw cycles.

QDs are made of electron dense atoms which allow the identification of nanoparticles by transmission electron microscopy. This property, for example, has been used to localize the traffic and final fate of these nanomaterials into cells.^{41,42} We also probed QD encapsulation by transmission electron microscopy (TEM) of liposomes composed of either PC or PC:DOTAP lipids. Fig. S3 (ESI†) shows empty and QD-containing PC and PC:DOTAP (8 : 2) liposomes. Together with the fluorescence data, TEM images confirm the encapsulation of QDs in liposomes of different composition using the freeze and thaw method.

In order to predict the interactions of these loaded liposomes with cells, an important factor needs to be addressed: the surface charge of these QD-loaded liposomes. Surface charges play a key role in cellular adsorption⁴³ that may eventually lead to internalization of the material, which is highly promoted by positive charges.⁴⁴ Therefore, the different kinds of liposomes (loaded and unloaded), including the fusogenic ones, were characterized by their total surface charges. Fig. 3 shows representative zeta potential (ζ) values for the reported liposome–QD systems. Liposomes comprised of only PC lipids are negative under the experimental conditions (pH around 7.5) and the ζ potential is further decreased in the presence of MPA-coated QDs (since they present negative carboxyl groups on their surface at the reported pH). In contrast and as expected, liposomes containing cationic DOTAP lipids are always positive regardless the use of PC, PE or fluorescent lipids. However, DOTAP-containing liposomes presented a positive zeta potential reduction in the presence of QDs for all lipid compositions tested. Based on the above-mentioned results, one can expect favorable interactions between the cationic liposomes and cells, either containing or not containing QDs due to the net positive charges of the resulting system. Furthermore, the zeta potentials of loaded and unloaded liposomes were also higher than 20 mV (in modulus) indicating that all liposomal systems tested here were stable.⁴⁵

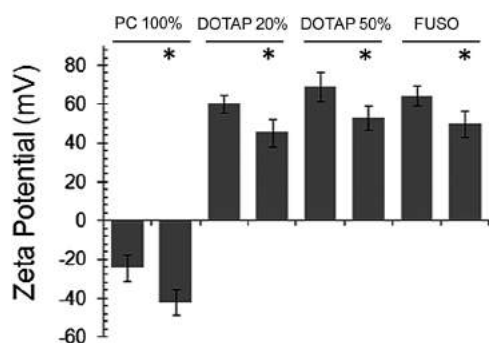


Fig. 3 Zeta potential of different liposomal systems. Asterisks indicate the encapsulated QDs, while their absence indicates empty vesicles. A decay in zeta potentials was observed in the presence of the MPA-coated QDs for all the liposomal systems.

The dynamic light scattering (DLS) analysis indicated average hydrodynamic sizes for the PC unloaded, PC loaded, fusogenic unloaded and fusogenic loaded systems of 150 nm, 100 nm, 160 nm and 250 nm, respectively. As the liposomes were analyzed and used after the freeze and thaw method (without further sonication or extrusion), the average PDI (polydispersity index) for the systems was approximately 0.4. Since there was a reasonable polydispersity presented in the liposomes' preparation, some larger vesicles were also observed and registered by microscopy analysis, when compared to DLS. With respect to the TEM images, although it was possible to see some smaller liposomes compatible with DLS analysis in Fig. S3D of the ESI†, we believe that the consecutive centrifugation steps of the TEM protocol help to select the larger ones to be imaged. Moreover, although very small vesicles could also be seen by optical microscopy, it was also easier to acquire good images from larger ones because of the Brownian motion and the resolution.

Fusogenic liposome encapsulation of quantum dots

In the previous sections we described an efficient method to encapsulate QDs in liposomes and showed that those liposomes containing DOTAP could be able to interact with cells due to the resulting positive surface charges. In the present section, we discuss the interactions of the fusogenic liposomes with human-derived umbilical stem cells as well as with RBCs and the perspectives to deliver membrane-impermeant materials into cells.

(a) Testing the properties of fusogenic liposomes. Lipid-based platforms offer an additional advantage (compared to other carrier systems) for delivery due to their high biocompatibility. They are also able to carry hydrophilic and lipophilic substances and modulate their interactions with the plasma membrane by choosing specific phospholipids for their composition. We choose to work with the recently developed formulations reported by Csiszár *et al.* because they were able to fuse with a large variety of cells.²⁹ Since the fusogenic activity of these systems is dependent on the use of fluorescent lipids, fusion can be followed by the presence of fluorescence in cells. Fig. 4A shows that the whole stem cell population was labeled after fusion with these liposomes and Fig. 4B shows that detailed plasma membrane projections of the cells can be clearly distinguished (arrows). These results are a strong indication of liposome–cell membrane fusion rather than internalization of the vesicles since the cells are homogeneously labeled, in contrast to what would be observed in the case of endocytosis, which would yield only intracellular spotted-like fluorescence.

We could also capture the interaction of fluorescent vesicles with the plasma membrane followed by fusion. Staining of the plasma membrane (Fig. 4C), as well as membrane projection (filopodial-like) structures, can be seen by confocal fluorescence microscopy after the arrival of vesicles onto the membrane (arrowhead in Fig. 4D). However fluorescence from intracellular structures is also observed (Fig. 4C, cells 1 and 2). The latter finding may indicate either (i) there is also some

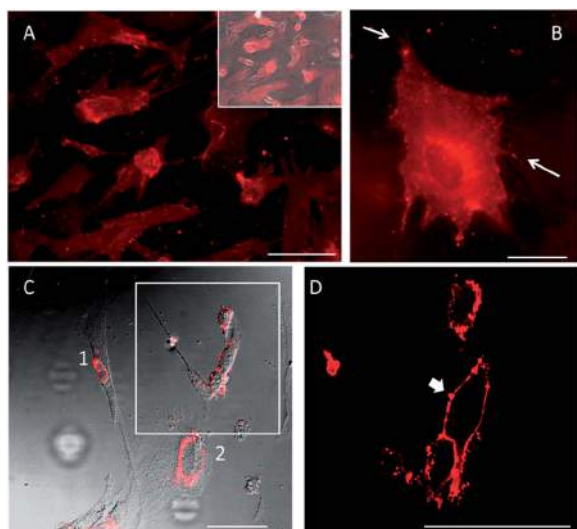


Fig. 4 Fusion of liposomes with stem cells observed by fluorescence microscopy. (A) All cells are labeled by fusogenic liposomes. (B) Fluorescence of membrane projections may be observed (arrows). (C) Different patterns of cellular labeling during/after fusion. Cells 1 and 2 display intracellular fluorescence rather than on the surface. (D) Zoom of the region marked in C showing the arrival of the vesicle followed by membrane fusion. Bars: (A): 100 μm ; (B): 25 μm ; (C–D): 75 μm .

endocytosis of the vesicles (besides liposome–membrane fusion) or (ii) there is an inward trafficking of the fluorescent plasma membrane (as will be discussed later).

In order to further characterize the mechanisms of interaction, we performed some modifications in the experimental conditions. Incubation at low temperature (4 $^{\circ}\text{C}$), known to transiently interrupt an active-dependent process such as endocytosis, yields fluorescence labeling similar to that at 37 $^{\circ}\text{C}$, in which the cellular contour (plasma membrane) is stained (Fig. 5A). Moreover, we observed that liposomal fusion is dependent on the relative amount of fluorescent lipids. A ten-fold reduction in the concentration of DPPE-Rh significantly affects the ability of these liposomes to fuse with cells as only few cells are labeled per field (Fig. 5B). Fig. 5C shows the fluorescence image of the labeled cell shown in 5B to demonstrate the same labeling features (cellular contour and detailed membrane projections – arrows). It demonstrates an active role of the fluorescent lipid to trigger fusion rather than being a simple marker. The process is also affected by the presence of bovine serum. For instance, when bovine serum was present in the medium no labeling was observed (Fig. 5D). These results highlight the fusion as the main (if not the only) process in the interaction of these liposomes with cells and the experimental conditions in which it occurs.

(b) Intracellular delivery of QDs encapsulated in fusogenic liposomes. Once we have demonstrated the efficiency of the freeze and thaw method for QD encapsulation in liposomes and established the conditions of liposome–cell fusion, fusogenic liposomes containing QDs were incubated with live stem cells for the observation of QDs' release into cells. Under ideal conditions, the liposome–QD system will fuse with the plasma cell membrane releasing free encapsulated particles inside the

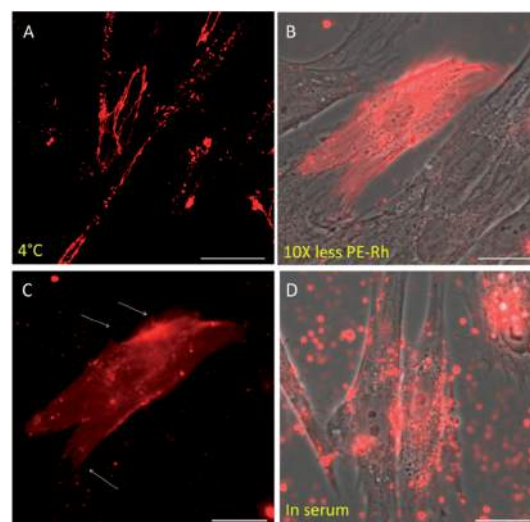


Fig. 5 Conditions under which fusion does (or does not) occur. (A) Confocal image shows that fusion still occurs during incubation at low temperature. (B) We observe the fluorescence of a single cell in the sample when a ten-fold reduction in the amount of fluorescent lipids is used. (C) Fluorescence image of the labeled cell shown in (B) displaying the same features after fusion. Arrows show membrane details. (D) We observe the lack of membrane labeling after incubation in the presence of serum proteins. Bars: (A) 75 μm ; (B–D): 25 μm .

cytosol, which would be seen as a green diffuse pattern in the cell interior. Fig. 6 shows typical real time images of the intracellular delivery of QDs by fusogenic liposomes. After a few minutes of incubation, some cells visualized by differential interference contrast (DIC) microscopy (Fig. 6A) presented red fluorescence (corresponding to the Rhodamine-labeled liposomes) followed by a green fluorescence (corresponding to QDs) – Fig. 6B and C, respectively. Interestingly, merged images always show co-localized red/green fluorescence (Fig. 6D and E). It is an indication that liposomes and QDs are in close proximity and that the QDs are probably not released from the (former liposome) membranes, that is, into cells. If very closer interactions occur, it is possible that some green fluorescence from QDs might be transferred to red-labeled membranes, leading to a weaker QD fluorescence intensity. Therefore, under the experimental conditions reported here, fusogenic liposomes containing carboxyl-coated QDs were unable to release freely diffusing QDs into the cell cytosol.

We further investigated the delivery of QDs by fusogenic liposomes using RBCs (good cellular models because they do not perform endocytosis). Upon incubation of fusogenic liposomes containing QDs, the cells almost immediately displayed red fluorescence (fusion) followed by a green signal from the QDs (Fig. 7A). As in the case of stem cells, the same pattern was observed for RBCs: both signals are co-localized and no QDs were found inside the RBCs (no intracellular release). These results for a simplified cellular model support the hypothesis of interaction between the charged species in the membrane fusion process.

MPA QDs did not exit the liposomes due to their incapacity to passively cross lipid bilayers, as well documented for most

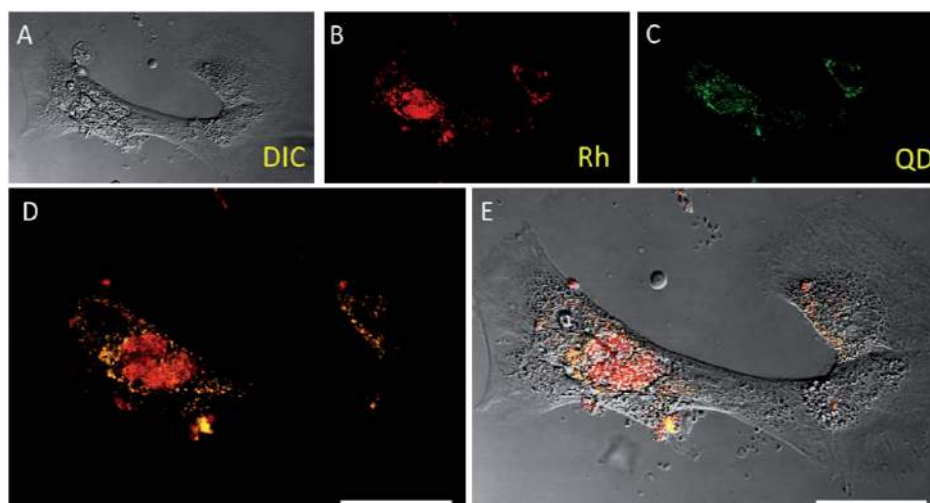


Fig. 6 Intracellular delivery of QDs mediated by fusogenic liposomes. (A–C) DIC, red liposome signal and green QD signal after incubation with stem cells. (D) Fluorescence overlay showing co-localized emission. (E) Merged fluorescence and DIC images. Bars: 50 μm .

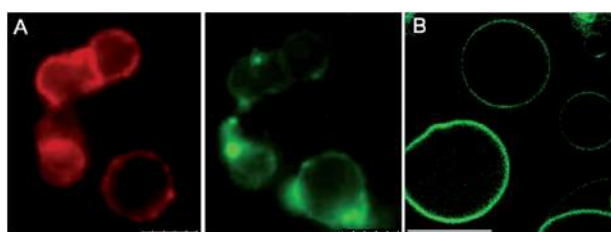


Fig. 7 (A) Frames of co-localized signals of liposomes (red) and QDs (green) on the RBC surface after membrane fusion. (B) QD adsorption onto the surface of PC:DOTAP GUVs (5% of DOTAP lipids) for simulating fusogenic liposomes and further understanding the co-localized signal and interactions of negatively charged QDs and cationic lipids. Bars in (A): 3 μm and in (B): 25 μm .

water-soluble and charged QDs.⁴⁶ This was further confirmed by the fact that we observed that bare MPA QDs (even when the QD concentration was 10 fold higher than that used for liposome encapsulation) were not able to label either RBCs or stem cells. Once encapsulated, QDs must stay trapped in the liposomal core without being released or leaked. QDs should be released only after fusion with cells and the fusion was a process that occurred quickly.

In order to further understand the interactions of anionic QDs with cationic lipids, GUVs were used. As we could not produce GUVs with the actual fusogenic composition, we worked with PC doped with 5% of the cationic DOTAP lipids to yield positive membrane simulating fusogenic vesicles. In this sense, electrostatic interactions (binding) between negative QDs and positive GUV membranes have been observed, as shown in Fig. 7B. This procedure was performed to further explain the co-localized fluorescence in cells observed using a microscope. This experiment was different from those shown in Fig. 2, where we showed QD encapsulation after freeze and thaw cycles. As can be seen in Fig. 7B, the membranes are homogeneously labeled by the nanoparticles, with no detectable signal (passage through) into the lumen of the vesicles. There were some

pattern variations from vesicle to vesicle concerning the labeling intensity, although the general profile was almost identical. This result shows the favorable binding of the negatively charged QDs and cationic lipid bilayers, easily observable using micrometer-scaled GUVs.

Discussion

With the objective of releasing non-permeant QD nanoparticles into cells, we encapsulated them in liposomes with fusogenic properties. The observation of co-localized QDs and lipid signals after fusion with cells indicates that both of them are present in cell membranes after fusion and are spatially close. Once the fusion occurs, QDs should have free access to the cell cytosol. However, we believe that the co-localized fluorescence is a result of a connection between the carboxyl-coated QDs and cationic lipids (even after fusion), probably due to charge attractions that make them capable of interacting electrostatically (evidence also supported by binding of nanoparticles to cationic GUV membranes). Such attachment can also explain the changes in the zeta potential observed after QD encapsulation procedures. This hypothesis is supported by the work described by Zhang *et al.*, where the authors demonstrated that adsorption between charged QDs and zwitterionic membranes can be favored by charges, which in turn can be controlled by the environmental pH and by the membrane and QD compositions.⁴⁷ The authors have shown the existence of an “adsorption window” that can govern the binding (or not) of QDs to lipids when these species display opposite charges. In this way, interactions between the negative carboxyl-coated QDs and cationic membranes (liposomes or cells) may well explain the co-localized pattern observed in Fig. 6 and 7.

Based on the above-mentioned scenario, we propose a possible and simplified mechanism of QD delivery to cells mediated by these fusogenic liposomes as illustrated in Fig. 8. Fig. 8A represents the interaction and fusion of liposomes with the plasma cell membrane. Under ideal conditions, membrane

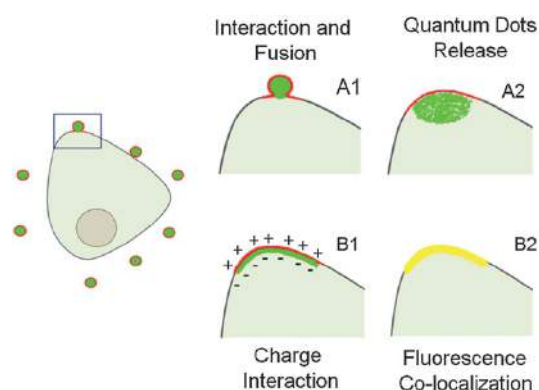


Fig. 8 Illustration of the liposome-mediated QD delivery into cells. Under ideal conditions, after incubation, red fluorescent liposomes interact and fuse with the cell membrane (A1), releasing encapsulated QDs into the cytosol (A2). However, after fusion, charge mediated interactions of MPA-QDs and cationic lipids (B1) impair QD release into the cell, yielding a yellow co-localized signal (B2).

fusion (Fig. 8A1) would lead to cell labeling and release of free QDs inside the cytosol (Fig. 8A2). However, based on the pattern observed by microscopy and on the considerations described above, MPA-coated QDs and cationic lipids are in close contact due to charge-mediated interactions (Fig. 8B1), yielding a co-localized yellow signal (Fig. 8B2).

Some attempts on the use of liposomes to deliver QDs to cells have been described in the literature. Bothun *et al.* have shown a clear difference between the final fate of neutral zwitterionic and cationic liposomes in cells: while the former fail to enter into cells and agglomerate on the cell surface, the latter are taken up and localized in perinuclear areas.⁴⁸ Hydrophobic and hydrophilic QDs co-encapsulated in liposomes were also taken up by cells *via* endocytosis,⁴⁸ however all of them failed to release free nanoparticles into the cytosol and end up trapped in endo/lysosomes instead; or they are trafficked as agglomerates of nanoparticles.⁴⁹ Sigot *et al.* reported a sophisticated system, in which dual-color QDs were encapsulated or attached to biotinylated liposomes containing either fusogenic or pH-sensitive lipids, and the traffic was monitored by fluorescence co-localization images.⁵⁰ However, they have shown that neither of the liposome–QD systems was able to fuse with the cell membrane (plasma and/or endosomal) and release the encapsulated QDs after endocytosis.

In another study, Gopalakrishnan *et al.* have shown that hydrophobic QDs embedded in the bilayer of cationic liposomes containing small amounts of pegylated lipids exhibited fusogenic properties, however, the QDs remained in the plasma membrane after fusion rather than being delivered to the cell interior.⁵¹ In contrast to that work, we used hydrophilic QDs with the aim of releasing the nanoparticles into cells. By analyzing our results we believe that the localization in the membrane is due to adsorption forces rather than being embedded in it. Moreover, some authors have demonstrated that amphiphilic uncharged QDs can translocate the membrane of GUVs and RBCs.^{52,53} It is important to observe that any further QD conjugation would modify their size, surface charge and physico-chemical properties, and may consequently impact their membrane translocation behavior.

These above cited studies and also our studies highlight the importance of understanding the interactions between nanoparticles and cell membranes since they will ultimately dictate the pathway(s) of intracellular delivery. Therefore, it is clear that much effort is worth and has to be applied for the purpose of intracellular delivery, especially when using liposomes as the carrier. The development of such a system will help not only to deliver nanoparticles (and any other membrane-impermeant compound), but also benefits this field bringing a deeper understanding of the controlling parameters involved in these purposes.

We conclude by pointing out some aspects of our reported system:

(i) These vesicles can modify the (negative) membrane of the cell incorporating positive lipids. This is, however, a transient state, where the incorporated material is rapidly trafficked to the recycling pathway in which the rate and fate are highly dependent on the lipid composition.⁵⁴ This must be the reason for the spotted-like fluorescence from cells 1 and 2 in Fig. 4C, again pointing out the process as fusion rather than internalization;

(ii) The pathway is endocytosis-independent (although we cannot ensure a fusion-only process);

(iii) The delivery of QDs into the cells, as reported here, can be a combination of QDs encapsulated and adsorbed in and/or on liposomes, with emphasis on the former since only very faint fluorescence signals were observed for simple QDs incubated with liposomes while very bright images were observed for liposomes encapsulating QDs.

(iv) In contrast to lipo/polyplex systems, which bind only to negative materials, virtually any cargo can be transported after encapsulation in fusogenic liposomes as long as we take into account possible charge-mediated interactions.

(v) Intrinsic limitation on the use of multicolored fluorescent cargo is due to the mandatory presence of a fluorescent lipid-analogue in the liposomal composition. In other words, there might be an overlay in the emission of the lipid-analogue (liposomes) and that from fluorescent cargo. Nevertheless, since the formulation requires only the presence of an electro-negative radical in the molecule, such fluorescence can be tuned over the whole spectral range by the correct choice of the probe. Moreover, the narrow emission of QDs may further facilitate their detection. Furthermore, the presence of a fluorescent probe in the liposomes allows the observation of the trafficking pathway itself as in the present study.

(vi) The use of the freeze and thaw method can be harmful to sensitive materials, such as proteins. The sequential freezing can cause changes in the material properties. Other methods for encapsulating membrane-impermeant materials can also be used. However they should yield similar results.

Conclusions

The area of intracellular delivery is a fast emerging field where much effort needs to be taken to reach the complete goal, starting from the design and construction of the cargo-carrier complex up to the intracellular delivery of the material after

interaction with and processing by cells. A deep understanding on the factors affecting all of these parameters is paramount to the development of more efficient and safer delivery systems. In this work, we showed that freeze and thaw is an efficient method for encapsulating QDs in liposomes for intracellular delivery purposes; nevertheless, charge-mediated interactions seems to play an important role in the delivery of these carboxyl-coated QDs to live cells mediated by cationic fusogenic liposomes.

Acknowledgements

The authors are grateful to CAPES, CNPq and FACEPE. This work is also linked to the National Institute of Photonics (INCT-INFO). We would like to thank the Laboratory of Non-Conventional Polymers (UFPE) for the analysis in the Zeta Nano ZS 90 equipment, Renato Grillo from Campinas State University for his helpful advice in the TEM sample preparation and observation, Aggeu Magalhães Research Center (CPqAM) for the confocal images, Professor Kátia R. Perez for helping with the determination of encapsulation efficiency and Professor Karin Riske for kindly providing phospholipids for this research. We would like to dedicate this work in memory of Prof. Oleg Vladimirovich Krasilnikov.

References

- U. R. Genger, M. Grabolle, S. C. Jaricot, R. Nitschke and T. Nann, *Nat. Methods*, 2008, **5**, 763–775.
- X. Michalet, F. F. Pinaud, L. A. Bentolila, J. M. Tsay, S. Doose, J. J. Li, G. Sundaresan, A. M. Wu, S. S. Gambhir and S. Weiss, *Science*, 2005, **307**, 538–544.
- P. A. Alivisatos, J. R. M. Bruchez, M. Morone, P. Gin and S. Weiss, *Science*, 1998, **281**, 2013–2016.
- I. L. Medintz, H. T. Uyeda, E. R. Goldman and H. Mattoussi, *Nat. Mater.*, 2005, **4**, 435–446.
- X. Michalet, L. A. Bentolila and S. Weiss, *Molecular Imaging: Physics and Bio-Applications of Quantum Dots in Advances in Medical Physics*, ed A. B. Wolbarst and W. R. Hendee, Medical Physics Publishing, Madison, 2008.
- A. Fontes, R. B. Lira, M. A. B. L. Seabra, T. G. Silva, A. G. C. Neto, B. S. Santos, in *Biomedical Research in Biomedical Engineering – Technical Applications in Medicine*, INTECH, Croatia, 2012, p. 269.
- D. E. Ferrara, D. Weiss, P. H. Carnell, R. P. Vito, D. Vega, X. Gao, S. Nie and W. R. Taylor, *Am. J. Physiol.: Regul., Integr. Comp. Physiol.*, 2006, **290**, 114–123.
- S. S. Rajan and T. Q. Vu, *Nano Lett.*, 2006, **6**(9), 2049–2059.
- V. P. Torchilin, *Annu. Rev. Biomed. Eng.*, 2006, **8**, 343–375.
- C. E. Thomas, A. Ehrhardt and M. A. Kay, *Nat. Rev. Genet.*, 2003, **4**, 3346–3358.
- D. Karra and R. Dahm, *J. Neurosci.*, 2010, **18**(30), 6171–6177.
- P. Washbourne and A. K. McAllister, *Curr. Opin. Neurobiol.*, 2002, **12**, 566–573.
- D. Miklavcic and M. Puc, *Electroporation in Wiley Encyclopedia of Biomedical Engineering*, John Wiley & Sons, New York, 2006, pp. 1455–1465.
- T. Y. Tsong, *Biophys. J.*, 1991, **60**, 297–306.
- F. Chen and D. Gerion, *Nano Lett.*, 2004, **4**(10), 1827–1832.
- A. M. Derfus, W. C. W. Chan and S. N. Bhatia, *Adv. Mater.*, 2004, **16**(12), 961–966.
- B. Dubertret, P. Skourides, D. J. Norris, V. Noireaux, A. Brivanlou and A. H. Libchaber, *Science*, 2002, **298**, 1759–1762.
- K. Boeneman, J. B. Delehanty, K. Susumu, M. H. Stewart and I. L. Medintz, *J. Am. Chem. Soc.*, 2010, **132**, 5975–5977.
- M. V. Yezhelyev, L. Qi, R. M. O'Regan, S. Nie and X. Gao, *J. Am. Chem. Soc.*, 2002, **130**, 9006–9012.
- S. Febvay, D. M. Marini, A. M. Belcher and D. E. Clapham, *Nano Lett.*, 2010, **10**, 2211–2219.
- A. M. Derfus, A. A. Chen, D.-H. Min, E. Ruoslahti and S. N. Bhatia, *Bioconjugate Chem.*, 2007, **18**(5), 1391–1396.
- R. Sawant and V. Torchilin, *Mol. Bio. Syst.*, 2006, **6**, 628–640.
- J. B. Delehanty, I. L. Medintz, T. Pons, F. M. Brunel, P. E. Dawson and H. Mattoussi, *Bioconjugate Chem.*, 2006, **17**, 920–927.
- B. Chen, Q. Liu, Y. Zhang, L. Xu and X. Fang, *Langmuir*, 2008, **24**, 11866–11871.
- L. Wasungu and D. Hoekstra, *J. Controlled Release*, 2006, **116**, 255–264.
- V. P. Torchilin, *Annu. Rev. Biomed. Eng.*, 2006, **8**, 343–375.
- M. R. Almofti, H. Harashima, Y. Shinohara, A. Almofti, Y. Baba and H. Kiwada, *Arch. Biochem. Biophys.*, 2003, **410**, 246–253.
- A. Noguchi, T. Furuno, C. Kawaura and M. Nakanishi, *FEBS Lett.*, 1998, **433**, 169–173.
- A. Csizsár, N. Hersch, S. Dieluweit, R. Biehl, R. Merkel and B. Hoffmann, *Bioconjugate Chem.*, 2010, **21**, 537–543.
- R. B. Lira, M. B. Cavalcanti, M. A. B. L. Seabra, D. C. N. Silva, A. J. Amaral, B. S. Santos and A. Fontes, *Micron*, 2012, **5**(43), 621–626.
- P. Dagtepe, V. Chikan, J. Jasinski and V. J. J. Leppert, *J. Phys. Chem. C*, 2007, **111**, 14977–14983.
- A. L. Rogach, T. Franzl, T. A. Klar, J. Feldmann, N. Gaponik, V. Lesnyak, A. Shavel, A. Eychmüller, Y. P. Rakovich and J. F. Donegan, *J. Phys. Chem. C*, 2007, **111**, 14628–14637.
- A. Fontes, B. S. Santos, C. R. Chaves and R. C. B. Q. Figueiredo, II-VI Quantum dots as fluorescent probes for studying trypanosomatides, in A. Al-Ahmadi, ed *Quantum Dots - A Variety of New Applications*, Intech, Rijeka, 1st edn, 2011, pp. 241–260.
- W. W. Yu, L. Qu, W. Guo and X. Peng, *Chem. Mater.*, 2003, **15**, 2854–2860.
- F. Szoka Jr. and D. Papahadjopoulos, *Annu. Rev. Biophys. Bioeng.*, 1980, **9**, 467–508.
- P. Walde and S. Ichikawa, *Biomol. Eng.*, 2001, **18**, 143–177.
- T. Nii and F. Ishii, *Int. J. Pharm.*, 2005, **28**, 198–205.
- W. T. Al-Jamal, K. T. Al-Jamal, P. H. Bomans, P. M. Frederik and K. Kostarelos, *Small*, 2008, **4**(9), 1406–1415.
- C. Yang, N. Ding, Y. Xu, X. Qu, J. Zhang, C. Zhao, L. Hong, Y. Lu and G. Xiang, *J. Drug Targeting*, 2009, **17**(7), 502–511.
- M. Chu, S. Zhuo, J. Xu, Q. Sheng, S. Hou and R. Wang, *J. Nanopart. Res.*, 2010, **12**, 187–197.

- 41 B. N. G. Giepmans, T. J. Deerinck, B. L. Smarr, Y. Z. Jones and M. H. Ellisman, *Nat. Methods*, 2005, **2**, 743–749.
- 42 C. R. Chaves, A. Fontes, P. M. A. Farias, B. S. Santos, F. D. de Menezes, R. C. Ferreira, C. L. Cesar, A. Galembeck and R. C. B. Q. Figueiredo, *Appl. Surf. Sci.*, 2008, **3**(255), 728–730.
- 43 Y. Zhang, M. Yang, N. G. Portney, D. Cui, G. Budak, E. Ozbay, M. Ozkan and C. S. Ozkan, *Biomed. Microdevices*, 2008, **10**, 321–328.
- 44 A. Verma and F. Stellacci, *Small*, 2010, **6**, 12–21.
- 45 F. Quemeneur, M. Rinaudo, G. Maret and B. P  pin-Donat, *Soft Matter*, 2010, **6**, 4471–4481.
- 46 J. B. Delehanty, H. Mattoussi and I. L. Medintz, *Anal. Bioanal. Chem.*, 2009, **393**(4), 1091–1105.
- 47 X. Zhang and S. Yang, *Langmuir*, 2011, **27**(6), 2528–2535.
- 48 G. D. Bothun, A. E. Rabideau and M. A. Stoner, *J. Phys. Chem. Lett.*, 2009, **113**, 7725–7728.
- 49 V. Dudu, M. Ramcharan, M. L. Gilchrist, E. C. Holland and M. Vazquez, *J. Nanosci. Nanotechnol.*, 2008, **8**, 2293–2300.
- 50 V. Sigot, D. J. Arndt-Jovin and T. M. Jovin, *Bioconjugate Chem.*, 2010, **21**, 1465–1472.
- 51 G. Gopalakrishnan, C. Danelon, P. Izewska, M. Prummer, P.-Y. Bolinger, I. Geissb  hler, D. Demurtas, J. Dubochet and H. Vogel, *Angew. Chem., Int. Ed.*, 2006, **45**, 5478–5483.
- 52 T. Wang, J. Bai, X. Jiang and G. U. Nienhaus, *ACS Nano*, 2012, **2**(6), 1251–1259.
- 53 A. Dubavik, E. Sezgin, V. Lesnyak, N. Gaponik, P. Schwille and A. Eychm  ller, *ACS Nano*, 2012, **3**(6), 2150–2156.
- 54 C. Kleusch, N. Hersch, B. Hoffmann, R. Merkel and A. Csisz  r, *Molecules*, 2012, **17**(1), 1055–1073.

Apêndice D: *IN VIVO* AND *IN VITRO* STUDIES OF THIOL - CAPPED CdTe QUANTUM DOTS AS A TOOL FOR BRAIN TUMOR DIAGNOSTICS

Revista: Journal of Biomedical nanotechnology (a ser submetido)

Classificação Qualis (Farmácia): A1

Autores: Seabra, Maria A.B.L., Dubois, L. G., Santos Júnior, E.F., Issac, A.R., Fontes, A., Hochhaus, G., Andrade-da Costa, B.L.S., Moura Neto, V., and Santos, B.S.

Ano: 2014

IN VIVO AND IN VITRO STUDIES OF THIOL - CAPPED CdTe QUANTUM DOTS AS A TOOL FOR BRAIN TUMOR DIAGNOSTICS

Seabra, Maria A.B.L.,¹ Dubois, L. G.,² Santos Júnior, E.F.,³ Issac, A.R.,³ Fontes, A.⁴, Hochhaus, G.,⁵ Andrade-da Costa, B.L.S.,³ Moura Neto, V.,² and Santos, B.S.^{1*}

¹Departamento de Farmácia, Universidade Federal de Pernambuco, Av. Prof. Moraes Rego, 1235 - Cidade Universitária, Recife - PE – Brasil CEP: 50670-901

²Instituto de Ciências Biomédicas, Departamento de Anatomia, Universidade Federal do Rio de Janeiro, bloco F Cidade Universitária - Rio de Janeiro, RJ – Brasil CEP: 21941-590

³Departamento de Fisiologia e Farmacologia, Universidade Federal de Pernambuco, Av. Prof. Moraes Rego, 1235 - Cidade Universitária, Recife - PE - CEP: 50670-901

⁴Departamento de Engenharia Biomédica, Universidade Federal de Pernambuco, Av. Prof. Moraes Rego, 1235 - Cidade Universitária, Recife - PE - CEP: 50670-901

⁵Pharmaceutics Department, University of Florida, J. Hillis Miller Health Center, Room P3-20, 1600 SW Archer Rd. – Gainesville – FL – USA 32610-0494

* Corresponding author. Email: beate_santos@yahoo.com.br

ABSTRACT

Glioblastoma (grade IV) is the most aggressive and infiltrating tumor of the central nervous system (CNS), showing a variety of mutations as well as high degree of vascularity, cell polymorphism and nuclear atypia. Unfortunately early diagnostic of brain tumors is hard, as imaging tools are not efficient for proper diagnosis of these types of tumors, leading to treatment failures. Here we describe a new *in vivo* targeting and imaging method for U87 glioblastoma tumor type xenotransplanted into male swiss mice brain using aqueous colloidal CdTe quantum dots (CdTe QDs) conjugated to anti-glial fibrillar acidic protein (GFAP). We have synthesized and optimized anti-GFAP conjugated red-emitting CdTe QDs to label also U87 tumor cell line *in vitro* and tested their ability to be incorporated in healthy cerebral cortex astrocyte primary cultures. The toxicity of isolated green (530 nm) or red (644 nm) emitting CdTeQDs synthesized for 2 or 10 h was evaluated using MTT assay applied to U87 cells. The tumor growth was visualized inside the brain by the hematoxylin and eosin staining and showed the successful delivery of the U87 cells into the brain parenchyma. CdTe QDs conjugated to anti-GFAP were injected into the tumor region and their uptake by the U87 cell line was visualized by fluorescence microscopy, showing a very specific double-labeling of vimentin-immunoreactive glioblastoma. Compared to U87 tumor cells that easily taken up anti-GFAP conjugated red-emitting CdTe QDs, healthy astrocytes kept, in primary cultures, offered more resistance to their incorporation and were weakly labeled. The results reported here provide new perspectives for using CdTe QDs in glioblastoma detection, suggesting their potential application in imaging-guided surgery.

Keywords

Quantum Dots, U87 cell line, Glioblastoma, Xenograft model, Fluorescence microscopy

INTRODUCTION

Prognosis and diagnosis of brain tumor are not straightforward processes due to different brain tumor characteristics, similarities among many non-neoplastic diseases and the tumor, the limited information on tumor characterization by conventional structural imaging and the accessibility to high cost diagnostic equipments (OMURO *et al.*, 2006). Once detected, the main approach for treatment of these tumors are neurosurgical techniques, radio- and/or chemotherapy. These treatments have a high risk of recurrence, a very common problem with these types of tumors, especially with astrocytomas, which have the highest recurrence rate after surgery with increased malignancy (OMURO *et al.*, 2006). This is also one of the main problems encountered with the low grade gliomas (LGG), that can give rise to tumors grade III and IV (anaplastic astrocytomas and glioblastomas, respectively). These tumor types are more infiltrating, proliferative with high mitotic activity, nuclear atypia and present many genetic mutations as well cellular polymorphism (AEDER; HUSSAINI, 2006).

Lately, with the nanotechnology advances and more understanding of the brain function and its pathologies, there is an increased need for reproducible and noninvasive imaging biomarkers. In the last two decades, quantum dots (QDs), nanometer-sized semiconductor crystals, have been extensively studied and used as fluorescent probes due to their advantages over conventional fluorescent dyes. They show a broad absorption band with a large and flexible cross-section allowing multiphoton microscopy, size tunable emission and high resistance to photobleaching. In addition, QDs provide an active surface for chemical conjugation with proteins, antibodies and short peptides which became them suitable to be applied for labeling fixed and lived cells and tissues (FONTES *et al.*, 2012; LOVRIĆ; CHO; *et al.*, 2005; SANTOS; FONTES, 2008; VALIZADEH *et al.*, 2012)

In order to take advantage of the QDs' active surface and to have them specifically delivered to the biological environment some methods are used to conjugate these nanoparticles. These methods are dependent on what the QDs have attached to their surface as coating material. Usually carboxylic acids, thiol groups or amine groups are the ones exposed at the surface and ready to react (HERMANSON, 2008; SONG; CHAN, 2011). Although several studies have been conducted in the bioimaging area demonstrating successful applications of QDs in cancer imaging (CINTEZA, 2010; MEDINTZ *et al.*, 2005; WANG; CHEN, 2011), there are only few

reports in the literature for in vivo targeting and imaging using QDs, especially in proliferative conditions in the central nervous system. Cai and collaborators demonstrated for the first time the use of arginine-glycine-aspartic acid (RGD) peptide-labeled quantum dots, delivered intravenously in adult rats for targeting and imaging of glioblastoma vasculature and ex vivo tumor tissue staining (CAI *et al.*, 2006).

Glioblastoma multiform (GBM), a grade IV astrocytic tumor (WHO classification 2000) (ROBSON, 2001) is a very aggressive and invasive CNS tumor with high incidence of recurrence and low efficacy of patient's treatment, mainly due to changes in its genetic profile as well as a late diagnostic (AEDER; HUSSAINI, 2006; LIMA *et al.*, 2012). There are few genetic mutations leading to a variety of changes in cell cycle regulation affecting the growth factors signaling cascades. The best way to diagnose a brain tumor is by using molecular genetic markers and histological diagnosis such as cell of origin, tumor differentiation, and tumor grading using WHO classification. Non-invasive techniques such as magnetic resonance imaging (MRI), among others should be in place to help this process. Usually the surgeon performs a stereotactic needle biopsy in order to get a sample and establish the diagnosis. (SMITH; IRONSIDE, 2007).

Besides the GBM's histopathological characteristics, immunohistochemistry plays a very important role in the diagnosis of this type of glioma. Antibodies against the glial filament protein called glial fibrillar acidic protein (GFAP) are the most useful since this protein is expressed in mostly tumors originated from astrocytes (PATHAK *et al.*, 2006; SMITH; IRONSIDE, 2007). GFAP is the astrocytic main intermediate filament and a member of the cytoskeletal protein family with molecular weight 50 KDa. In CNS injuries, trauma, genetic mutations and pathologies such as brain tumor, the signaling pathway leading to astrogliosis is turned on and a rapid synthesis of GFAP occurs, which can be observed through the high expression of this protein or by the immunostaining with the GFAP antibody (anti-GFAP). The increase in its expression gives this protein a unique value when studying these diseases, injuries and development of this system. (ENG *et al.*, 2000).

Fluorescence guidance has been investigated and used by neurosurgery as a potential tool in maximizing the extent of high-grade glioma resection (LI *et al.*, 2013), especially considering that the recurrence of brain tumors usually occurs close to the primary site of initial resection. In

this aspect, techniques based on the use of QDs have shown promise as potential future tools especially when these nanoparticles are conjugated to antibodies which recognize specifically tumorigenic cells (ARNDT-JOVIN *et al.*, 2009; KANTELHARDT *et al.*, 2010), permitting the intraoperative identification of individual or small clusters of residual tumor cells.

Therefore, considering that QD-labeled antibodies can provide a quick and reliable method for imaging-guided surgery, the main purpose of this study was to develop a method for labeling U87 glioblastoma *in vivo* in swiss mice using a human tumor xenograft model. We have synthesized and optimized anti-GFAP conjugated red-emitting aqueous colloidal CdTe QDs. In addition, we tested also the ability of these QDs to be incorporated in healthy cerebral cortex astrocyte primary cultures as well as in U87 cell line *in vitro*. The toxicity of isolated green (530 nm) or red (644 nm) emitting CdTe QDs was evaluated using MTT assay applied to U87 cells.

MATERIALS AND METHODS

Reagents

All reagents for QDs synthesis and conjugation were purchased from Sigma Aldrich otherwise stated. Cadmium Perchlorate hydrate (cat # 401374), Tellurium powder (cat # 264865), Sodium Borohydride (cat # 480886) and Mercaptosuccinic Acid (cat # M6182). Nitrogen gas was purchased from Air Liquide (at 78.3 %). Ketamine Hydrochloride (Syntec), Xylazine Hydrochloride (Syntec), Diazepam injection USP (Bayer) were bought from a local pharmacy. MTT [3-(4,5-dimethylthiazol-2-yl)-2,5-diphenyltetrazolium bromide] was purchased from Life technologies (cat # M-6494). Monoclonal Anti-Glial Fibrillary Acidic Protein (GFAP) (cat # G3893) was purchased from Sigma Aldrich and Black 96-well Optiplat F HB microplates (cat # 6005320) were purchased from PerkinElmer. Phosphate-Buffered Saline (PBS) (Invitrogen). Dulbecco's Modified Eagle Medium Nutrient mixture F-12 powder (D-MEM/F-12) (cat # 12400-016) from Gibco.

Quantum Dots Synthesis

Aqueous colloidal dispersion of CdTe QDs were synthesized in water according to a previously reported method developed with some modifications. (LIRA *et al.*, 2013). Briefly, QDs were prepared by adding an aqueous solution of Te^{2-} (prepared using by reducing metallic tellurium with NaBH_4 , under nitrogen atmosphere) in a 0.01 M $\text{Cd}(\text{ClO}_4)_2$ solution at $\text{pH} > 10$ in the presence of MSA (mercaptosuccinic acid) as the stabilizing agent. The molar ratio of Cd:Te:MSA used was either 5:1:6 or 2:1:6, and the reaction occurred under nitrogen atmosphere at 90 °C and constant stirring for 2 or 10 h resulting in green and red emitting QDs, respectively.

Covalent conjugation of QDs with GFAP

MSA-coated CdTe QDs were chemically conjugated to anti-GFAP using coupling reagents EDC or EDAC (1-ethyl-3-(3-dimethylaminopropyl)carbodiimide hydrochloride) and sulfo-NHS (N-hydroxysulfosuccinimide) (HERMANSON, 2008). Briefly, a suspension of QD at $8.95 \times 10^{-7} \text{ mol L}^{-1}$ at pH 5.6 was mixed with an aliquot of 1 mL of EDC (0.4 mg mL^{-1}) and aliquot of 1 mL of Sulfo-NHS (1.1 mg mL^{-1}) in ultrapure water. 2 μL of anti-GFAP at $53.6 \mu\text{g}$

mL⁻¹ was added into the system and incubated at room temperature for 2 h under gentle stirring. The system QD-MSA-anti-GFAP and the controls (QD-MSA alone, anti-GFAP alone and QD-MSA + EDC + Sulfo-NHS all in water) were incubated in microplate well (200 µL/well) for 2 h at 37 °C. After 2 h, the wells were washed 3x with PBS and the microplate was brought to the microplate reader.

Measuring the Relative Fluorescence

In the microplate reader, the fluorescence signal of conjugated QDs and controls were analyzed using the following combination of emission filters for the green emitted QDs and for the red emitted QDs respectively: F535 (535 nm/12.5 nm) and F595 (595 nm/30 nm). The acquisition time was 1 s and the lamp CW was set at 20.000 W. Microplate-based fluorescence measurements were analyzed using WALLAC 1420 microplate reader software Victor2 (PerkinElmer).

QDs Optical and Structural Characterization

Absorption spectra of isolated and conjugated QDs were collected using a Spectrophotometer Evolution 600 V-VIS Thermo Scientific in the range of 200 to 800 nm. Emission spectra of isolated and conjugated QDs (excited at 365 nm) were recorded using a Fluorimeter ISS K2 (xenon lamp of 300 W as excitation source). Isolated QDs were also structurally characterized by X-ray diffraction Analysis (Siemens Nixford D5000). The size of the CdTe QDs was determined using Dagtepe's empirical relation which applies the wavelength of the first absorption maximum ((DAGTEPE *et al.*, 2007)):

$$r = 1.38435 \frac{0.00066\lambda}{1 - 0.00121\lambda} \quad \text{Equation 1}$$

Where the λ is the first maximum absorption and r is the particle radius.

Quantum dots' toxicity against U87 cell line: MTT Assay

U87 cells were plated into a 24 well plate with DMEM F-12 medium and the MTT assay was performed according to Maysinger et al. (CHOI *et al.*, 2007). In summary, U87 at 1×10^5 cells/well were plated into a 24 well plate for 24 h. Then, each medium was aspirated and 500 μ l of new medium were added to 6 wells (control) and 450 μ l of new medium plus 50 μ l of QDs at 8.95×10^{-7} M were added to the other wells. All experiments were done with non washed and washed QDs in triplicates. Washed QDs refer to the QDs which were passed through a membrane (Pierce Concentrator 20 K MWCO, Thermo Scientific) in order to remove excessive amount of Cadmium, before doing the MTT assay. Plates were incubated at 37°C and 5% CO₂ for 1 h or 24 h. MTT stock solution (5 mg/mL) were added to each well and incubated at 37°C and 5% CO₂ for 2-5 h (under inspection until color change). Media was removed gently and DMSO was added to each well and pipetted up and down to dissolve crystals. The plates were incubated for 5-30 min at 37°C and read at $\lambda = 550$ nm using a benchmark microplate reader Dynex MRX Revelation Plate Reader, Chantilly, VA, USA.

Cell labeling with Anti-GFAP conjugated CdTe-MSA

Astrocyte Primary Culture

Astrocyte primary cultures were prepared from newborn (3-days old) Swiss mice cerebral cortices, as described previously by (LOUREIRO *et al.*, 2010). Briefly, mice were decapitated, brain structures were removed and maintained in PBS-Glucose 0.6 % solution. The meninges were carefully stripped off. Cells were mechanically dissociated and plated in (DMEM)/F12 containing 10% fetal bovine serum (FBS; pH 7.4) supplemented with glucose (33 mM), glutamine (2 mmol L⁻¹), and sodium bicarbonate (3 mmol L⁻¹). They were kept into a culture flask for 10 days at 37°C, 5% CO₂ and 85% humidity and media was changed every two days. Then the cells were plated using the same medium into a 24-well plate (Corning Inc., New York, NY) at 1×10^4 cells/well, previously coated with polylysine (1.5 μ g/ml, Sigma). 24 h later, media was removed and DMEM F12 without FBS and phenol red was added. To each well besides the control, 50 μ L of QDs isolated (at 8.95×10^{-7} mol L⁻¹) and 50 μ L of anti-GFAP conjugated QDs (at 1.21×10^{-6} mol L⁻¹) were added and incubated at 37°C, 5% CO₂ and 85%

humidity for 30 min. All procedure was performed in triplicates. After incubation, cells were washed three times with saline (0.9 % (m/v) NaCl) and fluorescence images were taken using DMI 4000 B fluorescence microscope (Leica Microsystems, Wetzlar, Germany; 20 × objective). All filters were excitation filter: bandpass 560/40 and suppression filter: bandpass 645/75 and excitation filter: bandpass 480/40 suppression filter: bandpass 527/30 for the red and green emitting QDs respectively. For any superposed images the filters used were excitation filter: bandpass 360/40 suppression filter : longpass 470.

Culture of Human Glioblastomas U87 Cell line

The method used was previously described by (FARIA *et al.*, 2006). In summary, U87 cells were grown in DMEM-F12supplemented with 10% FBS at 5% CO₂ at 37°C and after 48 h they were trypsinized, plated into 24-well plate at 1 x 10⁶ cells/well and incubated overnight at 5% CO₂ at 37°C. Media were removed after 24 h and DMEM F12 without FBS and phenol red was added. Then, the experiment was carried out as described above for astrocyte primary cultures.

In Vivo Experiments – Tumor Implantation

The human U87 glioblastoma cell line was grown in DMEM-F12 supplemented with 10 % FBS in 5% CO₂ at 37°C. Cells for intracerebral injection were trypsinized with PBS/EDTA at 0.02% for 5 min from sub confluent cultures, and then centrifuged. PBS/EDTA was removed and the cell line was resuspended in serum-free DMEM-F12 medium at 1 x 10⁵ cells.

Animal and Tumor Cell Injection. This study was approved by the Ethics Committee of the Center for Health Sciences (Centro de Ciências da Saúde - CCS) at the Federal University of Rio de Janeiro (Universidade Federal do Rio de Janeiro - UFRJ) (Protocol No. DAHEICB 015) and by the Brazilian Ministry of Health Ethics Committee (CONEP No. 2340). Male Swiss mice weighting 30-35 g (~2 months old) were obtained from the Biomedical Sciences Institute (UFRJ, Brazil), and housed under constant temperature, humidity and with access to food and water *ad libitum*. For intracranial inoculations, animals were anesthetized with intraperitoneal injection (i.p.) of Diazepam (100 mg/kg) and a mixture of ketamine (100 mg/kg) and xylazine (10 mg/kg) and placed in a stereotaxic instrument (Insight, Ribeirão Preto, Brazil). A small burr hole was made into the skull and 5 µL of cell suspension was injected manually at 0.5 µL/min injection rate to minimize the pressure at the injection site, controlled by Hamilton syringe. Coordinators

for intracranial inoculation were -1.0 mm anteroposterior, + 2.5 mm mediolateral and -3.0 mm dorsoventral from bregma, around the animal's caudate- putamen nuclei, according to x stereotaxic atlas coordinates (Paxinos and Watson, 1986).

Treatment with CdTe QDs. The procedure to inject the CdTe QDs was the same as the one described above. Animals containing U87 tumor were divided in 3 groups with 3 animals each . After 72 days of tumor cell injection, 5 uL of saline (control group A), Quantum Dots (washed group B) and anti-GFAP conjugated Quantum Dots (group C) were injected into the brain at the same stereotaxic coordinates as the tumor cells injection. After this treatment for 15 min, each animal was anesthetized with intraperitoneal injection (i.p.) of ketamine (100 mg/kg) and xylazine (10 mg/kg) and perfused transcardially with saline (0.9 % NaCl) followed by 4% paraformaldehyde in 0,1 M phosphate buffer (PB, pH 7,4). After perfusion, the brains were dissected starting from the prefrontal cortex back to the inferior limit of the brainstem (the olfactory bulb and cochleas were excluded). They were then postfixed for 2 h in the same fixative, rinsed in PB and weighted (wet weight). Subsequently, the brains were cryoprotected in sequential solutions of 10%, 20% and 30% sucrose in PB. Brains were serially cut on a cryostat (Leica) into 20 µm-thick sections across the coronal plane. All sections were collected serially in PB and arranged in six series. Each series contained 8 brain sections.

Hematoxilin and Eosin Staining

One of the series was used for hematoxilin and eosin staining. Brain slices were mounted over a gelatinized slide and placed into an incubator at 37°C. The slides were sequentially immersed in xylene twice for 5 min, mixed in a solution of xylene and 100% ethanol (1:1 ratio) for 5 min, 100% ethanol twice for 5 min and rinsed in tap water for 5 more min. Then, they were placed in Harris hematoxylin solution for 3 min, rinsed in tap water for 5 min and then immersed in an alcoholic solution of eosin for 3 min. After this step, slides were dehydrated in 100% ethanol and cleared in xylene 100% and then mounted with coverslips using Entelan (Merck).

Immunohistochemistry (IHC) with anti-Vimentin

Brain slices from animal's brain A2 (control) and C3 (QD-MSA-anti-GFAP) were placed over a slide and washed in phosphate buffer (PB) at 0.1 M. A solution of 3% BSA + 1% triton in PB was added for 1 h, and then the slices were rinsed 3 times (10 min each) with PB at 0.1 M. A

solution containing the primary antibody X-Vimentin (mouse anti-vimentin, Diagnostic Biosystems) at 1:300 in PB 0.1 M + 0.3 % triton was added overnight at 4°C. Slices were rinsed 3 times as mentioned above, followed by incubation in the biotinylated X-mouse secondary antibody (DyLight 488 Anti-Mouse IgG, Rockland) at 1:5000 in PB at 0.1 M + 0.3% triton for 3 h at room temperature. After 3 washes in PB, brain sections were mounted in gelatinized slides with glycerol 60% . They were stored into -20 °C until further analysis.

RESULTS AND DISCUSSION

Quantum Dots' Characterization

Structural analysis

The X-ray diffraction profile for CdTe-MSA QDs (data not shown) presents 3 peaks at $2\theta = 23.96^\circ$, 40.26° and 46.64° . The highest intensity peak is located at $2\theta = 23.96^\circ$, consistent with the (111) diffraction peak of cubic zinc blend CdTe structures according to the Joint Committee on Powder Diffraction Standards – International Center for Diffraction Data (JCPDS – ICDD) crystallographic database entry 00-015-0770. The other two peaks represent the (220) and (311) crystal planes. These results also corroborate with data already published by Zeng and collaborators where they found values of $2\theta = 23.8^\circ$, 39.3° e 46.5° for CdTe QDs. (ZENG *et al.*, 2008). Applying Scherrer's equation we find that the crystallites present sizes between $d = 3 - 4$ nm. These results agree well with the TEM analysis of the nanocrystals (data not shown).

Spectroscopic analysis

In the absorption spectra of QDs suspensions, the first observable peak (at the highest wavelength) indicates the lowest excited energy state and the particle size derived from the first maximum may be estimated according to Dagtepe's empirical equation, (DAGTEPE *et al.*, 2007). The absorption spectra for the green and red emitting CdTe QDs are shown in Figure 1. In both spectra there is large absorption cross section which is a very important property for biological applications of the QDs since it allows a simultaneous excitation of different emitting QDs using a single light source. Considering the CdTe bulk bandgap energy ($E_g = 1.5$ eV; $\lambda = 825$ nm), a great shift to the left in the absorption spectrum indicates particles in a strong quantum confinement. The first absorption maxima observed are $\lambda = 542$ nm and $\lambda = 647$ nm for the green and red emitting CdTe-MSA QDs, respectively.

Concentrations of the QDs suspensions were calculated according the Yu's adaptation of the Lambert-Beer's Law $A = \epsilon C L$ where A is the absorbance at the first absorption peak; ϵ is the extinction coefficient of the CdTe QDs; C is the concentration and L is the path which is equal to 1 cm (YU *et al.*, 2003). The concentrations of the QDs used here were estimated and are described in Table 1.

Figure 1: Absorption and normalized emission spectra of the green (a) and red (b) emitting CdTe-MSA QDs. Excitation at $\lambda = 365$ nm.

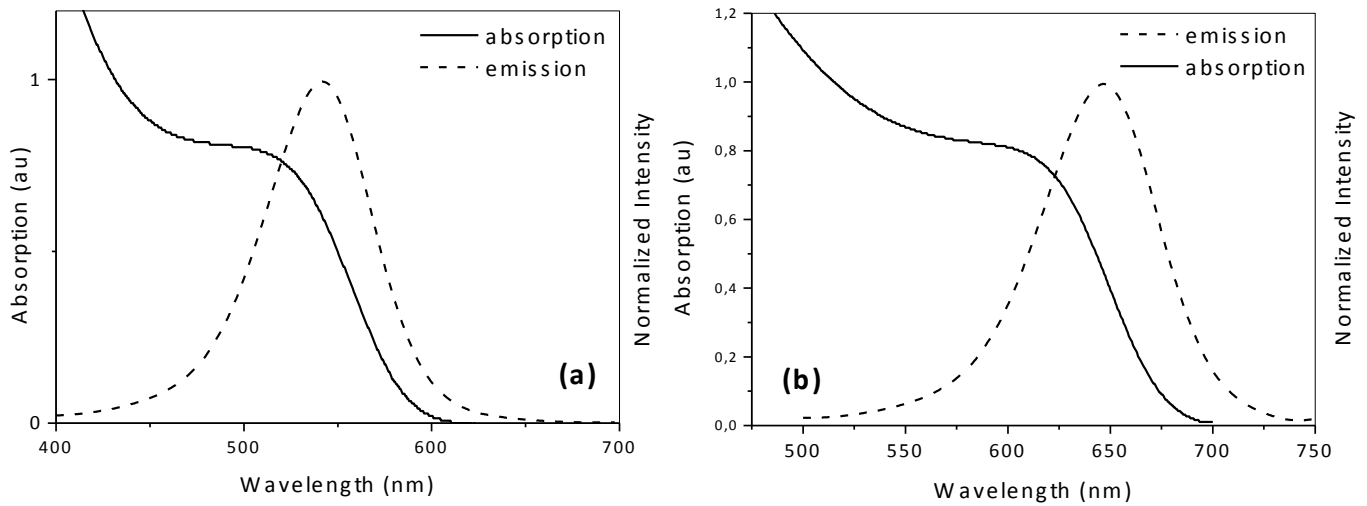


Table 1: Structural and spectroscopic data estimated by applying Dagtepe et al. and Yu et al. empirical approximations for size and concentrations of isolated and conjugated CdTe QDs used here.

Parameters	CdTe-MSA*	CdTe-MAS**	CdTe-MSA-GFAP
Peak position (nm)	518	610	570
Diameter (nm)	2.8	3.8	3.3
Concentration (mol L⁻¹)	1.22×10^{-6}	8.95×10^{-7}	1.21×10^{-6}

* and ** represent slightly different preparation conditions

When comparing the red emitting QDs with the red emitting QDs conjugated with anti-GFAP, there is only a slight blue shift of the first absorption maximum from 610 nm to 570 nm, nevertheless maintaining the original band profile. The absorption spectra of the anti-GFAP conjugated CdTe particles show no changes in the absorption spectra, suggesting no size alteration after the bioconjugation procedure.

The emission signal intensities and bandwidth, calculated as the full width at half maximum (FWHM) indicate the primary relaxation mechanisms which may be ascribed to the

band profile. Exciton recombination, radiative and non-radiative relaxation in energy traps resulting from defects in the nanoparticle's surface, are related to their fluorescence band profile. According to the emission spectra, the green and red emitting CdTe-MSA (Figures 1(a) and (b)) show band maxima at $\lambda = 542$ nm (FWHM = 72 nm) and $\lambda = 646$ nm (FWHM = 67 nm) respectively, and the conjugated CdTe-MSA-anti-GFAP was at $\lambda = 632$ nm (FWHM = 58 nm).

Relative Fluorescence Intensity – QDs-MSA-Anti-GFAP

Mercaptosuccinic acid-coated green and red emitting CdTe QDs were covalently attached to the anti-GFAP through adaptation of the known EDC and Sulfo-NHS procedures as described in the method section. During the reaction between the water soluble EDC and the carboxyl group on the CdTe QDs surface, an active ester intermediate is formed and Sulfo-NHS is added into the reaction since the NHS has been known to stabilize the EDC intermediate. Once there is the sulfo-NHS ester intermediate formation, it reacts with one of the antibody's amine residue resulting in a stable amide bond between the QDs and the antibody (CHAN *et al.*, 2002; HERMANSON, 2008). CdTe QDs' bioconjugation was evaluated using the fluorescence plate reader and the relative fluorescence intensity (RFI) for both red and green emitting QDs was obtained by the Equation 2 (CARVALHO *et al.*, 2014).

$$RelativeFLI (\%) = \frac{conjugateFL - controlFL}{controlFL} \times 100\% \quad (2)$$

where *conjugateFL* is the fluorescence intensity of the conjugated QD and *controlFL* is the average control fluorescence. Results are shown in Table 2.

Table 2: Fluorescence intensity measurements obtained in triplicate. Detection of free and conjugated QDs systems by covalent binding.

Systems	Fluorescence Intensity (a.u.)	Relative Fluorescence
	2h / 24h	Intensity (%)
Control 1 (anti-GFAP)	883 / 741	
Control 2 (QD-MSA _{red})	791 / 952	
Control 3 (QD-MSA _{red} + EDC+ Sulfo-NHS)	787 / 887	
Average Control	820 / 860	
QD-MSA_{red}-anti-GFAP	3380 / 5082	1138 / 1677
Control 1 (anti-GFAP)	742 / 1114	
Control 2 (QD-MSA _{green})	827 / 827	
Control 3 (QD-MSA _{green} + EDC+ Sulfo-NHS)	834 / 916	
Average Control	801 / 952	
QD-MSA_{green}-anti-GFAP	3410 / 2046	752 / 545

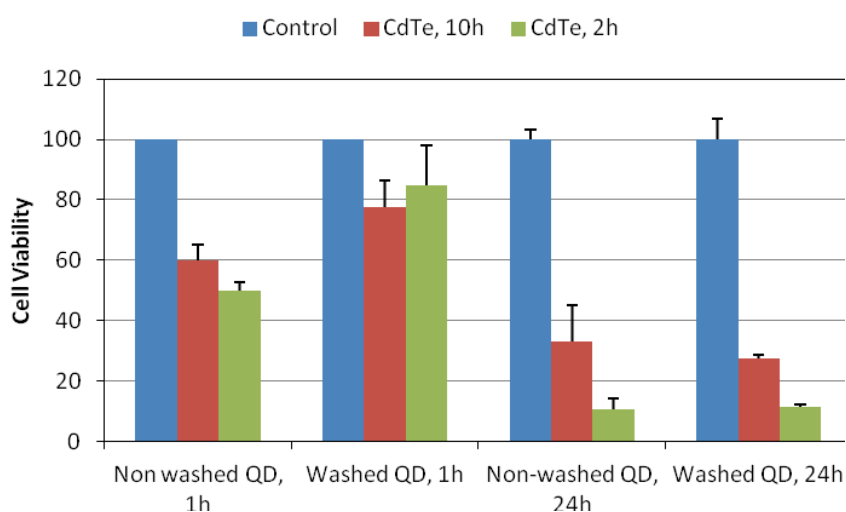
The emission spectrum for the red emitting QD-MSA-anti-GFAP showed a blue shift of the maximum emission peak from 646 nm to 632 nm (excitation at $\lambda=365$ nm) confirming the bioconjugation (CARVALHO *et al.*, 2014). The red emitting QDs when conjugated covalently with the antibody against GFAP has RFI% = 1138/1677 (2h/24h) showing a more effective conjugation than for the green emitting QDs which had RFI% = 752/545 (2h/24h) under the same conditions.

Toxicity Assay – MTT

Cytotoxicity measured by the use of MTT reagent is a very useful assay to assess cell viability as a function of redox potential. Active cells convert the water-soluble MTT to an insoluble purple formazan, which is solubilized in DMSO and its concentration determined by optical density (MOSMANN, 1983).

Results from the MTT assay are shown in Figure 2. Non washed green or red emitting QDs reduced cell viability 1 h after incubation, compared to control condition ($p < 0.036$; T test) or washed QDs ($p < 0.011$; T test), where excessive amount of cadmium was removed. After 24 h of QDs incubation, cell viability was about 90 and 70% lower using green and red-emitting QDs, respectively, when compared to control condition. In this case, no difference in the effects of washed and non-washed QDs was detected.

Figure 2. U87 Cell viability test using MTT reagent with isolated QDs synthesized in water at different ratios and time of reaction. Concentration of 1×10^5 cells/well and incubation time of 1 h and 24 h respectively



Since these nanocrystals have cadmium as a heavy metal core for their application in biomedical research as therapeutic and diagnostic tools, it is necessary to understand QDs' physicochemical properties and toxicity (PELLEY *et al.*, 2009; ROBERTS *et al.*, 2013). QDs cytotoxicity has been investigated by several researchers around the world and, taken their results together, it is clear that their toxicity depends on many factors derived from their properties as well as the environment (AL-HAJAJ *et al.*, 2011; CLIFT *et al.*, 2011; NURUNNABI *et al.*, 2013; ROBERTS *et al.*, 2013; WIECINSKI *et al.*, 2013). Properties such as QDs size, charge, concentration and shell coating material (capping and functional groups) play important roles and directly affect their toxicity levels. Additionally, the environment considers QDs exposition to proteolysis, changes in pH and other factors still to be found in this

area. Unfortunately most of the studies on QDs available do not consider routes of exposure, stability, half-lives and behavior in environment media (RZIGALINSKI; STROBL, 2009).

In the viability assays carried out in the present study it was detected that green emitting QDs were more toxic to U87 cell line in vitro than red emitting QDs, even when they were incubated for 1h. It is noteworthy that this toxicity was strongly reduced and almost reached control values when the QDs were washed to remove excessive amount of cadmium and other products involved in their synthesis. Such results are in agreement with those reported by Maysinger et al. (LOVRIĆ; BAZZI; *et al.*, 2005). These authors found that QD-induced cell toxicity was increased with small green emitting QDs in comparison to large equally charged red emitting QDs. A very important point to make is that QDs toxicity is also related to their distribution inside the cell. Maysinger et al. (2005) also observed that red emitting QDs were distributed throughout the cytoplasm of N9 (murine microglial) cells but did not enter the nucleus, while the green emitting QDs were localized mainly in the nuclear compartment. Similar results were also found here (and presented in Figure 4) showing that the red emitting QDs are distributed into the cytoplasm of the U87 cells.

Shiohara and collaborators (SHIOHARA *et al.*, 2004) observed CdSe/ZnS QDs capped with mercaptoundecanoic acid (MUA) to be cytotoxic to HeLa cells and primary human hepatocytes at concentrations of 100 µg/mL using MTT assay. This toxicity was attributed to the MUA, since it was shown before that this acid alone caused severe cytotoxicity in murine T-cell lymphoma (EL-4) cells at 100 µg/mL (HOSHINO *et al.*, 2011).

In our study, both QDs were coated with mercaptosuccinic acid (MSA) as a stabilizer and were different in size, due to the synthesis conditions, which affects cell uptake and the route for their internalization. The washed QDs showed around 20% less toxicity as compared with the non-washed ones when the incubation time was 1 h, but the difference vanishes after 24 h incubation, at which point no significant difference in toxicity or size remains, in agreement with the results obtained by Maysinger et al in PC12 (rat pheochromocytoma) and N9 cell lines. Another important point to mention is that due to pH variation in the medium caused by the MSA, which is an acid, the QDs shell could be degraded, exposing the QDs core containing cadmium and activating oxidative stress inside the cells.

It would be reasonable to expect small QDs to enter cells easier than large ones, a phenomenon that should be observable as long as the difference is large enough. Unfortunately, this is not the case here where green emitting CdTe and red emitting CdTe had 2.8 and 3.8 nm hydrodynamic radii, respectively. QDs concentration is also very important to the toxicity, but unfortunately there is no correlation to the studies published in this area because the QD dose/exposure concentrations vary in their units as well as the number of QDs/cells. (HARDMAN, 2006).

Mechanisms involved in cell death induced by QDs are not well known, since many factors are involved in the nanoparticles uptake. QD core degradation releasing Cd²⁺ into the environment, is probably involved, leading to loss of function by intracellular components or free radical formation followed by oxidative stress on the cell. Recently, researchers have been investigating the use of antioxidant molecules with the QDs incubation or coating QDs with molecules such as N-acetylcysteine (NAC) and Cysteamine in order to decrease their toxicities, and it has been shown that CdTe QD-induced toxicity was directly involved in Fas upregulation and lipid peroxidation, confirming that not only the QD's core plays a role in these nanoparticles toxicity, but also the coating. (CHOI *et al.*, 2007).

Despite all the potential mechanisms of QDs toxicity above mentioned, future studies should be carried out in order to investigate the time course of the CdTe QDs's toxicity used in the present study, considering that their using in tumor neuroimaging should be done in very short time of exposure.

Taken the MTT and conjugation results together, the red emitting QDs presented less toxicity than the green one and also showed a more efficient conjugation, being the one to be chosen for the *in vitro* and *in vivo* studies.

Incorporation of GFAP-conjugated and non conjugated CdTe-QDs in astrocyte primary cultures

Images in Figure 3 show contrast phase and fluorescent microscopy of astrocyte primary cultures incubated with non-conjugated and conjugated CdTe QDs.

Isolated emitting CdTe QDs' fluorescence is lightly dispersed along the culture and presents a non-specific labeling. On the other hand, red-emitting conjugated CdTe QDs were able to be incorporated in several astrocytes, but especially when they demonstrated signals of membrane disruption or were detached from the bottom of wells. Most of astrocytes attached to wells did not incorporate these QDs and it seems their membrane is intact. Compared to healthy astrocytes, U87 cells kept in culture demonstrated higher fluorescence signal and a specific labeling as shown in Figure 3 (b).

Figure 3: Fluorescence microscopy Images showing the healthy astrocytes primary cultures. (a) phase contrast image; (b) same image showing the labeling with conjugated CdTe-anti-GFAP QDs; (c) phase contrast image and (d) same image showing the fluorescence pattern of isolated CdTe QDs.

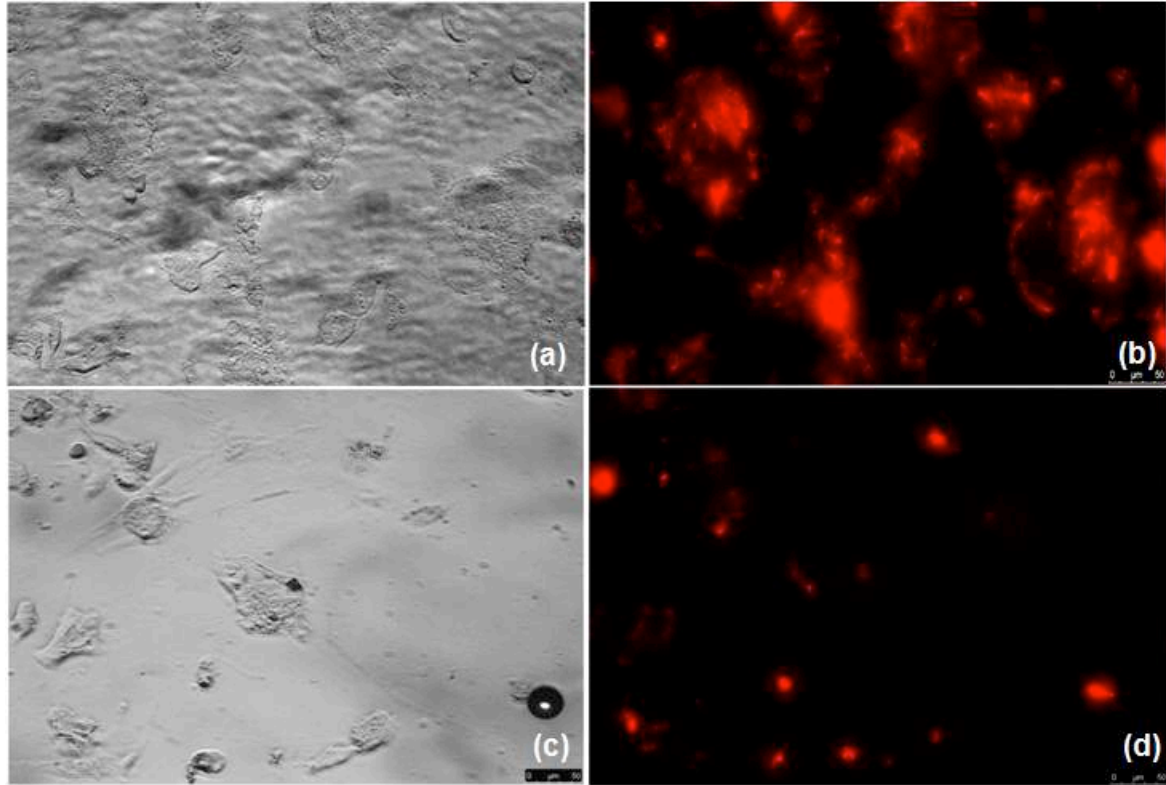
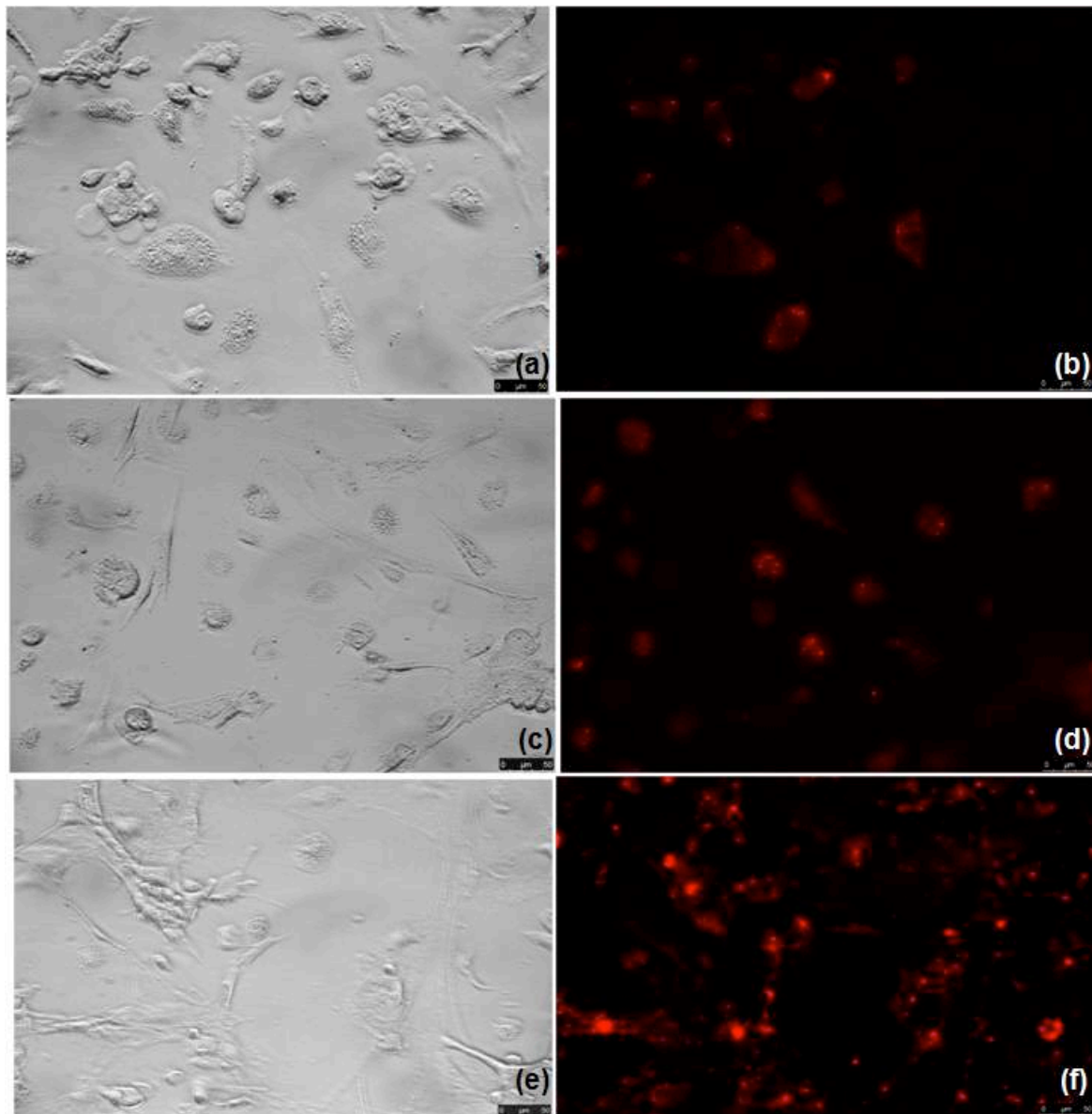


Figure 4: Fluorescence microscopy Images showing the human tumor U87 cell line cultures. Images (a, c, and e) show phase contrast image and (b, d, f) are the respective fluorescence images showing the specific labeling with CdTe-MSA-anti-GFAP QDs.

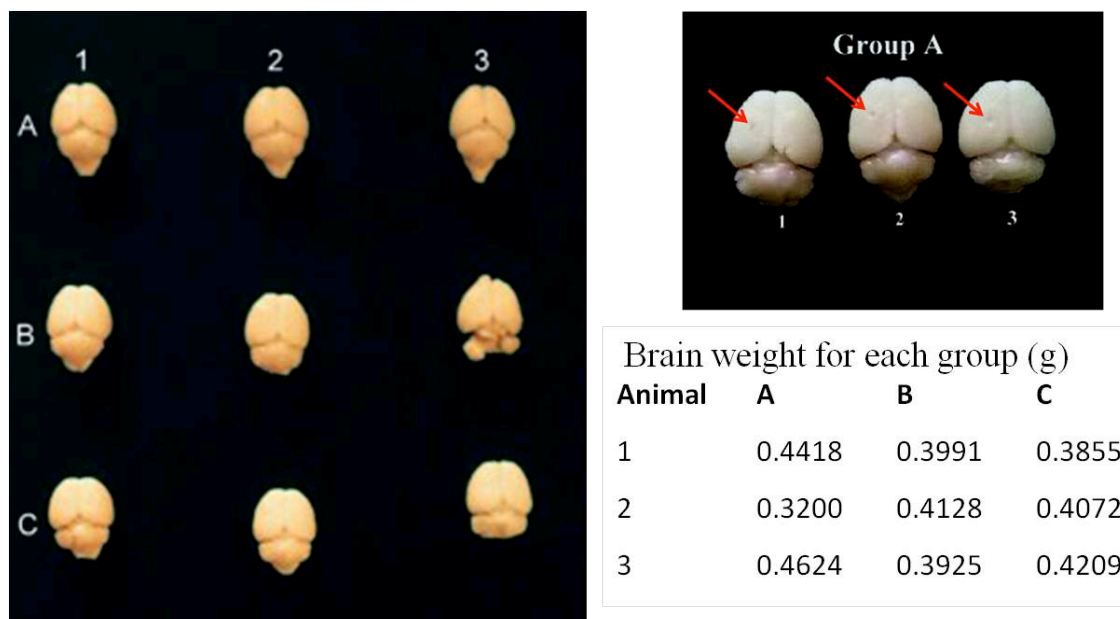


These images are showing the U87 tumor cells being labeled with conjugated CdTe QDs with anti-GFAP in culture. The cells suffering show a very strong labeling, on the other hand the healthy cells show no labeling. This is probably due to the disrupted membrane when the cells are going through apoptosis.

The U87 Xenotransplant model

As described in methods, adult mice were submitted to U87 xenotransplant in the right cortical hemisphere. Figure 8 shows low magnification images of 9 mice fixed brains after 72 days post inoculation of 1×10^6 U87 cells, followed by injection of 5 μ l of QDs and 3 control brains where no treatment was performed. Brain weights and images of all groups are shown in Figure 5 and the average weight is 0.4081 g, 0.4015 g and 0.4045 g for A, B and C groups respectively, demonstrating a uniform weight distribution among the groups. No macroscopic changes were observed in shape or color and no swelling was observed in the surface of cerebral cortex. The similarity in the injection region among the groups can be visualized in higher magnification (Figure 5, Group A).

Figure 5: Mice brain images for all the groups studied. In the inset (Group A) the injection site is shown with an arrow (at higher magnification). The brain weight is also described for all the animals.



The brain micro-injection system was developed for extra-cellular fluid clearance studies by Cserr et al (CSERR; OSTRACH, 1974) and improved by Yahamada and collaborators to deliver accurately U87 glioma cells by intracranial injection technique into the *caudate putamen* nuclei in mice (YAMADA *et al.*, 2004). Tumor growth can be influenced by factors, such as number of cells injected, cell availability after injection, tissue disruption of the injection site, tumor growth in the parenchyma, in the ventricles or subcutaneous and the injection flow rate.

By controlling these factors and adjusting them precisely, the authors were able to deliver any type of cells and amount into a specific area of the mouse brain.

In our studies, the method used was modified from Yamada to adjust our needs which is the nanoparticles' intracranial delivery. The U87 human glioblastoma cells were injected into the mice's brain manually and after 72 days of the tumor formation, the QDs were added as described in the method section.

H&E staining (Figures 6 – 8, B images) indicates the cells were injected into the *caudate putamen* successfully. The volume of cells injected was 5 μ L of containing the U87 cells in serum-free media, to avoid any inflammatory response and possible induced angiogenesis in the brain, and the injection flow rate was 0.5 μ L/min and cells concentration was 1×10^5 cells. It was observed a reflux along the Hamilton needle during its removal when cells were injected in the brain of animal B2 due to the high volume injected, which in this case increased the pressure in the injection site. It was not observed any animal death neither an exophytic (extracranial) tumor growth.

Hematoxylin & Eosin (H&E) Staining

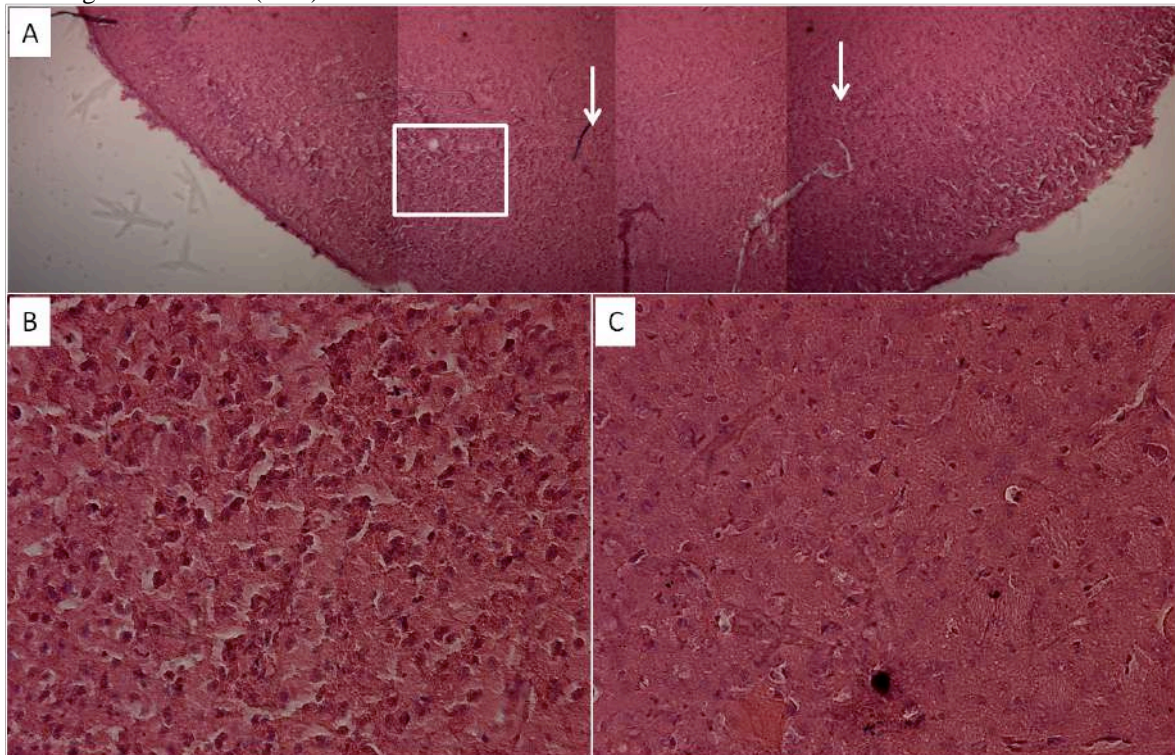
Hematoxylin and Eosin staining was first introduced by Böhmer and Fishers in 1865 & 1875 respectively, and still is one of the most used stain in medical diagnosis to study the tissues and biopsies histology. In this case, hematoxylin colored the nuclei in dark blue to purple and the eosinophilic structures on cytoplasm is colored by eosin in pink (GILL, 2012).

Figures 6 - 8 show the H&E stained brain sections for animals A2 (control), B3 (CdTe-MSA) and C2 (CdTe-MSA-anti-GFAP). In all cases, part A shows the cells injection pathway into the mice's brain following the coordinates to deliver tumor cells U87 into the *caudate putamen* region as explained in the methods section. The injection pathway is shown as a straight line stained by H&E depicted in Figure 6 – 8 (A) for all groups and did not show any traumatic brain damage due to the needle insertion with no edema and inflammation in the injection site. In the end of this injection pathway the tumor formation is observed by the disrupted membrane and cellular modifications in all cases. Part B of the images shows the tumor formation. Part C

shows the contralateral side of the injection pathway. In all treated animals, the contralateral hemisphere showed normal tissue architecture with no cell disorganization.

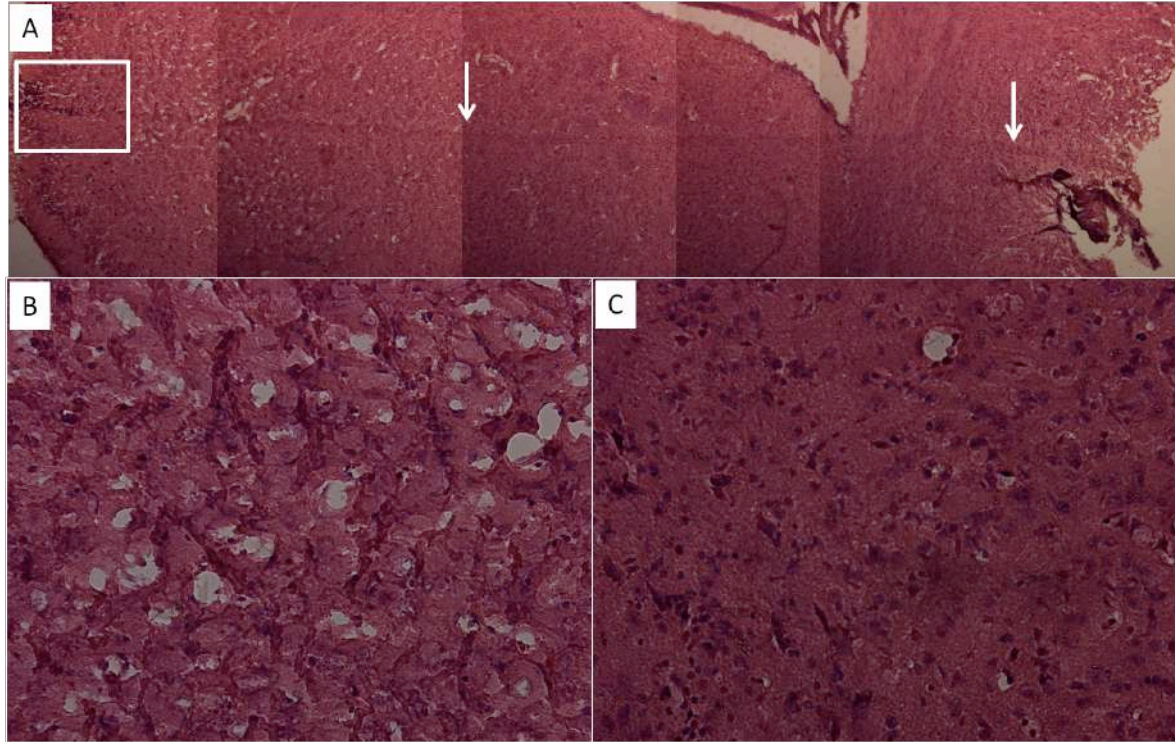
The injection pathway showed on the H&E stained on figure A for all groups did not show any traumatic brain damage due to the needle insertion with no edema and inflammation on the injection site. The tumor formation is well observed on all the B images of Figure 6 -8.

Figure 6. H&E stained brain section of animal A2 (control). A shows the injection pathway indicated by the arrows (x5). In image B the tumor formation is observed and Image C is the contralateral side showing normal cells. (x 20)



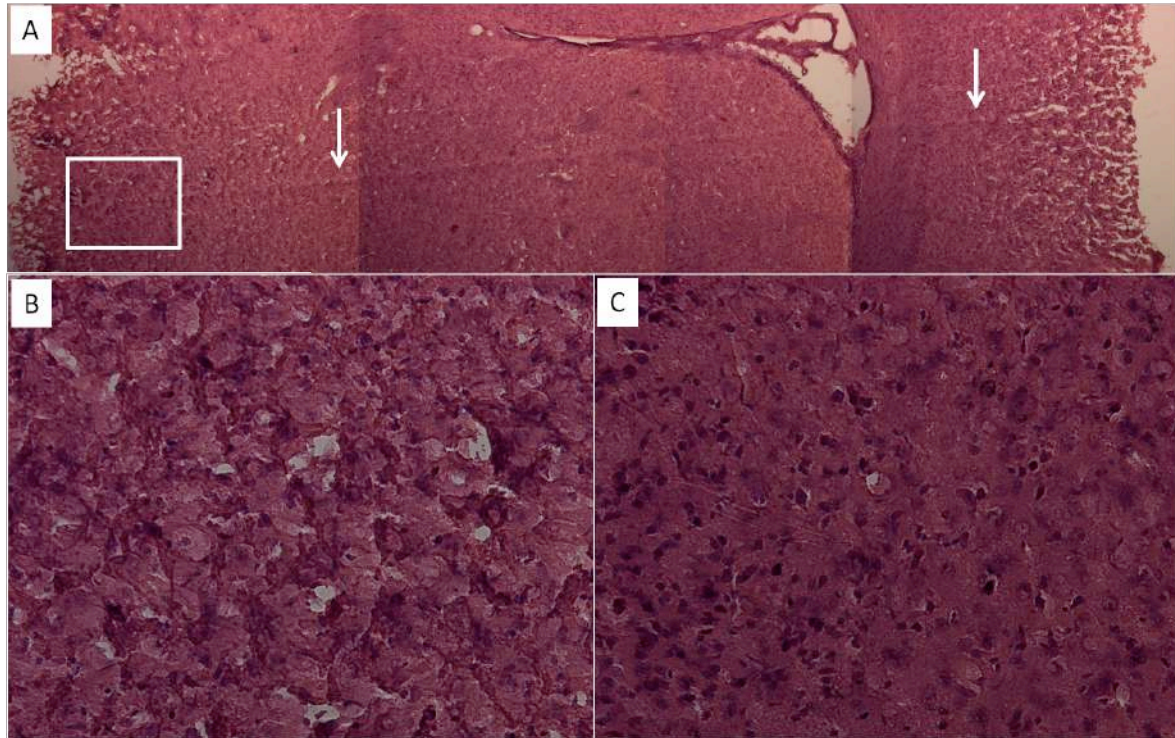
The formation of glioblastoma is represented on image B. The histological examination show a large irregular mass, with poorly supported abnormal vasculature, cells in proliferation with larger nuclei and cell pleomorphism. The contralateral side shows normal cells with define small nuclei, and no membrane disruption and no pleomorphism, indicated the tumor stayed at the site of injection.

Figure7: H&E stained brain section of animal B3 labeled with CdTe-MSA. Image A shows the injection pathway indicated by the arrows (x5). In image B the tumor formation is observed and Image C is the contralateral side showing normal cells.



The tumor in animal B3 was labeled with isolated CdTe QDs. Image B shows a very pleomorphic cell population with an abnormal vasculature and multinucleated cells. Since this animal was exposed to the QDs' treatment, it is showing cystic regions with slightly differences from the control group showed in figure 6B which was treated with saline only. This is probably due to QDs' toxicity effects. On the contralateral side (figure 7C), normal and small cells with a very well defined nuclei.

Figure 8: H&E stained brain section of animal C2 labeled with CdTe-MSA-anti-GFAP. A shows the injection pathway indicated by the arrows (x5). In image B the tumor formation is observed and Image C is the contralateral side showing normal cells.



The tumor in animal C2 was labeled with conjugated CdTe QDs and it is showed in image B. As can be observed, the tumor shows a very pleomorphic cell population with an abnormal vasculature and multinucleated cells. Since this animal was exposed to the QDs' treatment as well as animal B3 (figure 7), it is showing cystic regions with slightly differences from the control group showed in figure 6B which was treated with saline only. On the contralateral side (figure 7C), normal and small cells with a very well defined nuclei are shown and it confirms that the tumor grew only in the site of injection.

All the H&E shows how precise and efficient was the method to deliver tumor cells into the Swiss mice's brain, with no tumor formation in any other place.

Taking advantage of the QDs fluorescent properties, *in vivo* studies to evaluate and confirm tumor formation were also followed by fluorescence microscopy. The images

represented by figures 9 and 10 shows the red fluorescence from the labeling with conjugated QDs. Figure 9 shows the pathway of the injection site with no damage caused by the syringe needle. The cells were delivery precisely into the brain as it is observed by the fluorescence on images c and d. The injection pathway was clean showing a precise technique to deliver cell into the brain corroborating with the H&E staining. On Figure 9 e and f shows a higher magnification of the tumor formation site.

Figure 10 also shows fluorescence microscopy images. Images a and b shows the brain section for the control animal A1. Image b is showing autofluorescence and c and d are images of the brain section of the animal C3 with was labeled with conjugated QDs. Image d shows a very specific labeling over the entire tumor and probably the tumor invade another hemisphere via the corpus callosum and this invasion is well defined and called “butterfly” glioma (SMITH; IRONSDALE, 2007).

Fluorescence microscopy is a very powerful technique which takes advantage of particles with fluorescence properties.

Figure 9: Microscopy image of C3 pathway of the injection site. (a, b and e) represents the phase contrast image while (c, d and f) shows the respective immunofluorescent fluorescent images using CdTe-MSA-anti-GFAP QDs.

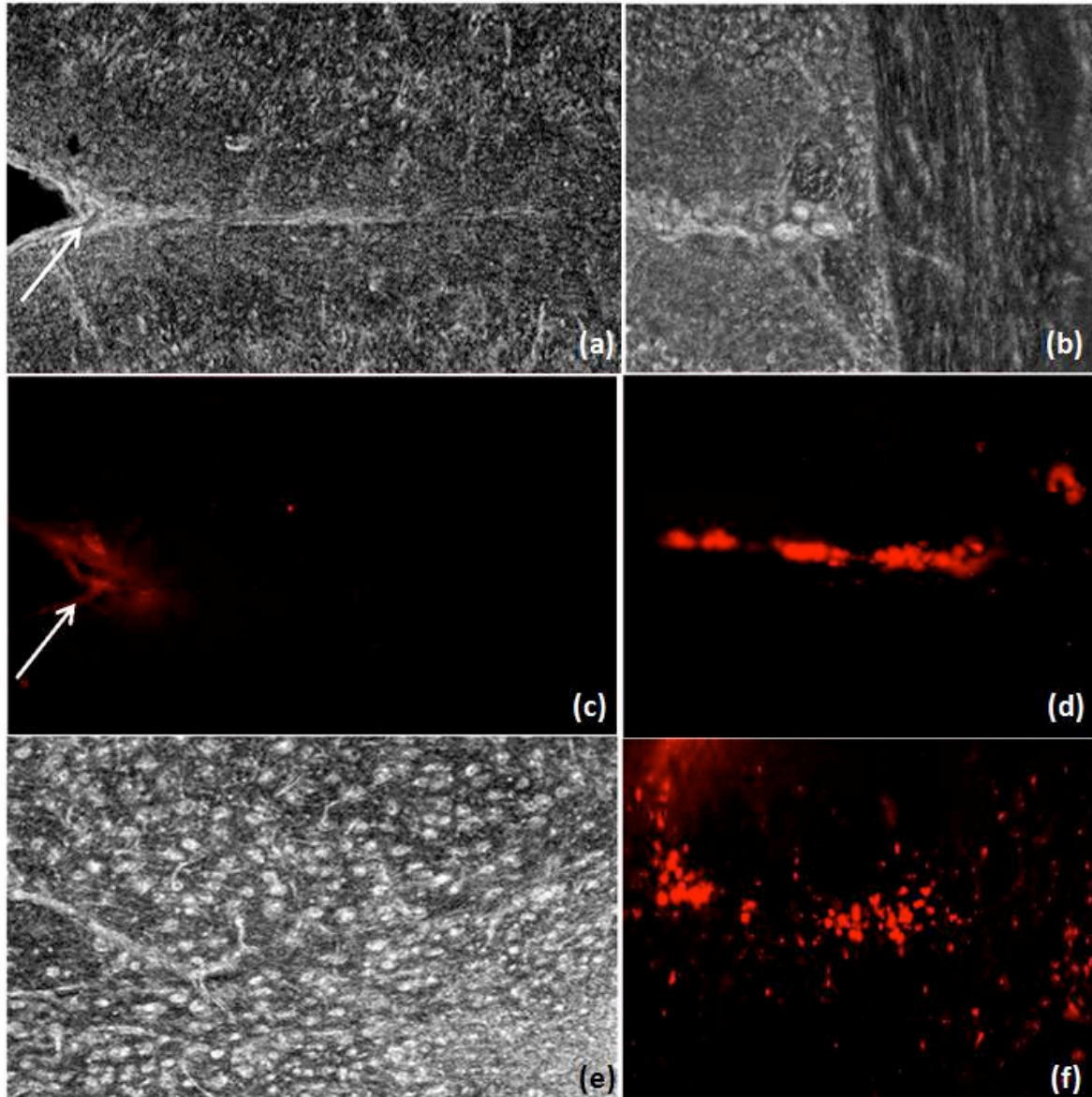
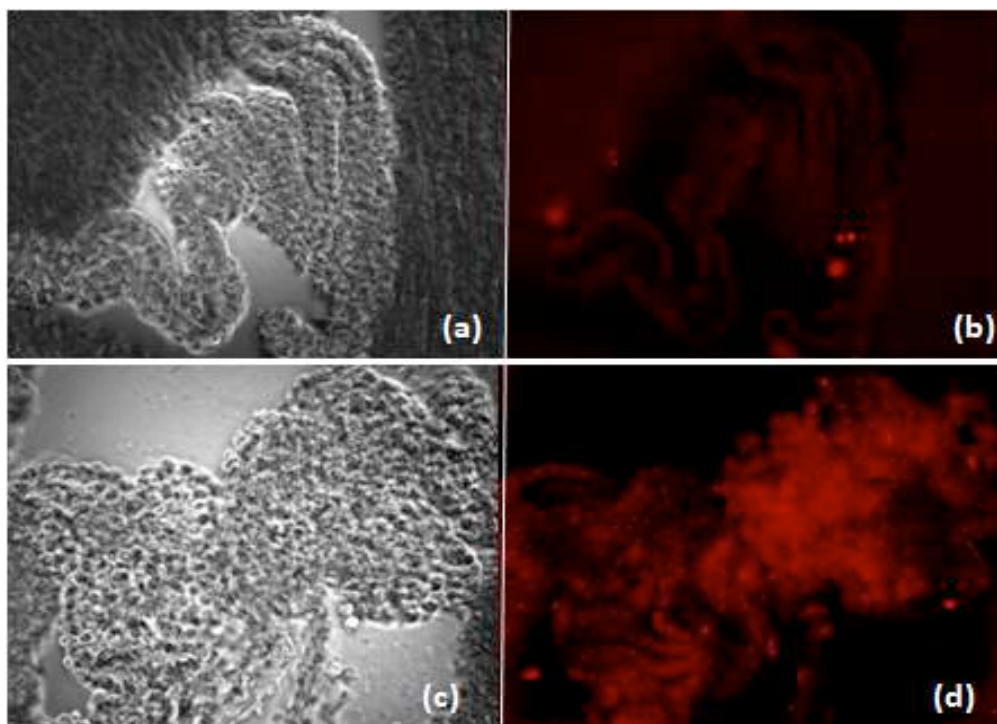


Figure 10: Image of the brain section of control animal A1 (a-b) phase contrast and fluorescence image. (c-d) Image of the brain section of animal C3 labeled with CdTe-MSA-anti-GFAP QDs.



The following figures 11 and 12 show the labeling of the tumor region on brain sections of the animal C2 with conjugated CdTe QDs. GFAP already on the surface of the QDs was doubly immunostained with vimentin using the secondary antibody Dylight 488 as described in the methods section. Can be seen in Figure 11 and 12, by the fluorescence microscopy, there are three cell types which were distinguished immunocytochemically: First one are the astrocytes co-expressing glial fibrillary acidic protein (GFAP) and vimentin (Figure 11 and 12 D), the second one type are the astrocytes expressing only GFAP (Figure 11C and 12 B) and the third type are the astrocyte-like cells expressing only vimentin. The colocalization between vimentin and GFAP means the cells are in a proliferative reactivity during injury which can easily show the tumor formation, corroborating with all the H&E staining and fluorescence microscopy results (JANECZKO, 1993).

Figure 2. Low magnification of U87 tumor in phase contrast and fluorescence showing animal C2 brain section labeled with conjugated CdTe QDs: (a) = phase contrast image; (b) = Dylight (488) - anti-Vimentin immunostaining; (c) = CdTe-MSA-anti-GFAP (632 nm) labeling; (d) = overlap between (b) and (c).

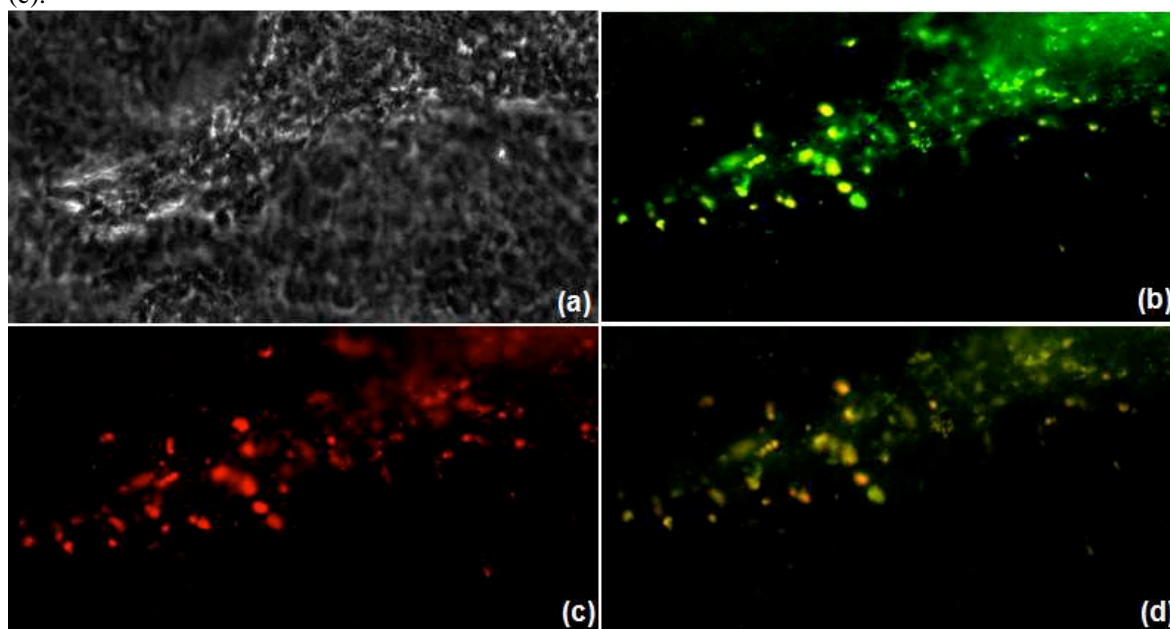
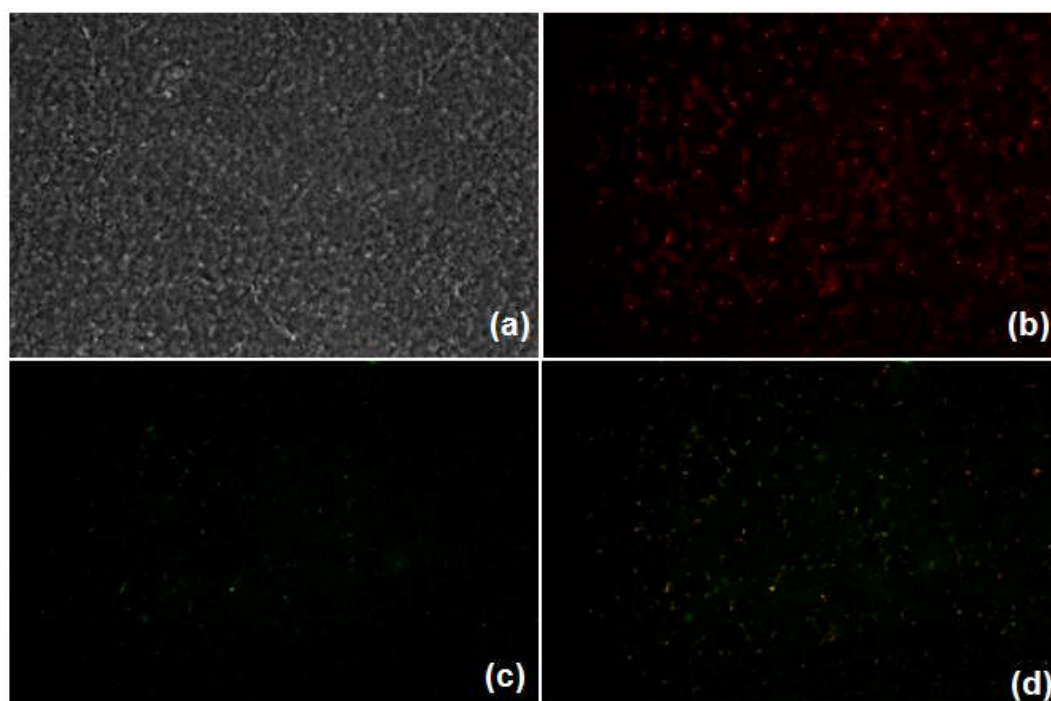


Figure 12: High magnification of U87 tumor in phase contrast and fluorescence showing animal C2 brain section labeled with conjugated CdTe QDs: (a) = phase contrast image; (b) = Dylight (488) - anti-Vimentin immunostaining; (c) = CdTe - GFAP (632 nm) labeling; (d) = overlap between (b) and (c).



CONCLUSION

The thiol-capped CdTe QDs synthesis and their conjugation with the antibody was characterized and proved to function well. The conjugation using coupling reagents work as well. The xenograft tumor model developed here worked for modeling the central nervous system cancer to be diagnosed using nanoparticles fluorescence, and the method showed to be precise and efficient to deliver the tumor U87 cell line into any region of the brain in mice.

One of the main factors to take in account when developing fluorescent probes for *in vivo* imaging is the QDs' toxicity, which in our case did not happen until after 1 h, and may be caused by the MSA coating on the green and red emitting CdTe QDs. The MTT results with the washed QDs, which would have decreased the free cadmium concentration in the medium, showed lower toxicity in the short timeframe when compared with the non-washed. However, the difference disappeared after 24 h, probably due to the shell being degraded and the core, which contains cadmium, exposed. It is important to point out that once the QDs are being degraded, the oxidative stress cascades and lipid peroxidation in the membrane can be turned on, confirming previous results from other groups mentioned before.

The labeling of the tumor cells *in vitro* and the tumor *in vivo* with CdTe-MSA-anti-GFAP was specific to the tumor region and effective as observed by fluorescence microscopy and corroborated with the results from the doubly labeling and colocalization of both GFAP and vimentin. These results together show a very important tool for the diagnosis of a tumor *in vivo* and during the intraoperative surgery, by guiding the neurosurgeon to remove all the tumor labeled cells and avoid tumor resection.

ACKNOWLEDGMENTS

The authors are grateful to Fundação de Amparo à Ciência e Tecnologia do Estado de Pernambuco (FACEPE), Coordenação de Aperfeiçoamento de Pessoal de Nível Superior (CAPES), Conselho Nacional de Desenvolvimento Científico e Tecnológico (CNPq), Federal University of Rio de Janeiro and Pharmaceutics Department in the College of Pharmacy at University of Florida - Gainesville USA. This work is also linked to the National Institute of Science and Technology in Photonics (INFo). The authors are grateful to Prof. Regina Bressan from the Aggeu Magalhães Research Center, Recife, Brazil.

REFERENCES

- AEDER, S. E.; HUSSAINI, I. M. Transformation of Normal Astrocytes Into a Tumor Phenotype. In: DAMIR JANIGRO (Ed.). **The Cell Cycle in the Central Nervous System**. [S.l.]: Humana Press, 2006. p. 433–447.
- AL-HAJAJ, N. A.; MOQUIN, A.; NEIBERT, K. D.; *et al.* Short ligands affect modes of QD uptake and elimination in human cells. **ACS nano**, v. 5, n. 6, p. 4909–18, 28 jun 2011.
- ARNDT-JOVIN, D. J.; KANTELHARDT, S. R.; CAARLS, W.; *et al.* Tumor-targeted quantum dots can help surgeons find tumor boundaries. **IEEE transactions on nanobioscience**, v. 8, n. 1, p. 65–71, mar 2009.
- CAI, W.; SHIN, D.-W.; CHEN, K.; *et al.* Peptide-labeled near-infrared quantum dots for imaging tumor vasculature in living subjects. **Nano letters**, v. 6, n. 4, p. 669–76, abr 2006.
- CARVALHO, K. H. G.; BRASI, A. G.; FILHO, P. E. C.; *et al.* Fluorescence Plate Reader for Quantum Dot-Protein Bioconjugation Analysis. **Journal of Nanoscience and Nanotechnology**, v. 14, n. 5, p. 3320–3327, 1 maio 2014.
- CHAN, W. C. .; MAXWELL, D. J.; GAO, X.; *et al.* Luminescent quantum dots for multiplexed biological detection and imaging. **Current Opinion in Biotechnology**, v. 13, n. 1, p. 40–46, fev 2002.
- CHOI, A. O.; CHO, S. J.; DESBARATS, J.; LOVRIĆ, J.; MAYSINGER, D. Quantum dot-induced cell death involves Fas upregulation and lipid peroxidation in human neuroblastoma cells. **Journal of nanobiotechnology**, v. 5, p. 1, jan 2007.
- CINTEZA, L. O. Quantum dots in biomedical applications: advances and challenges. **Journal of Nanophotonics**, v. 4, n. 1, p. 042503, 1 set 2010.
- CLIFT, M. J. D.; BLANK, F.; GEHR, P.; ROTHEN-RUTISHAUSER, B. Nanotoxicology: A Brief Overview and Discussion of the Current Toxicological Testing In Vitro and Suggestions for Future Research. **General, Applied and Systems Toxicology**. [S.l.]: John Wiley & Sons, 2011. p. 1–26.
- CSERR, H. F.; OSTRACH, L. H. Bulk flow of interstitial fluid after intracranial injection of Blue Dextran 2000. **Experimental Neurology**, v. 45, n. 1, p. 50–60, out 1974.
- DAGTEPE, P.; CHIKAN, V.; JASINSKI, J.; LEPPERT, V. J. Quantized Growth of CdTe Quantum Dots; Observation of Magic-Sized CdTe Quantum Dots. **Journal of Physical Chemistry C**, v. 111, n. 41, p. 14977–14983, 18 out 2007.

ENG, L. F.; GHIRNIKAR, R. S.; LEE, Y. L. Glial fibrillary acidic protein: GFAP-thirty-one years (1969-2000). **Neurochemical research**, v. 25, n. 9-10, p. 1439–51, out 2000.

FARIA, J.; ROMÃO, L.; MARTINS, S.; *et al.* Interactive properties of human glioblastoma cells with brain neurons in culture and neuronal modulation of glial laminin organization. **Differentiation; research in biological diversity**, v. 74, n. 9-10, p. 562–72, dez 2006.

FONTES, A.; LIRA, R. B. DE; SEABRA, M. A. B. L.; *et al.* Quantum Dots in Biomedical Research. In: RADOVAN HUDAK, M. P. AND J. M. (Ed.). **Biomedical Engineering-Technical Applications in Medicine**. Rijeka, Croatia: InTech, 2012. v. 232p. 269–290.

GILL, G. W. H&E Staining: Oversight and Insights. Connecticut: ASCP, 2012. p. 104–114.

HARDMAN, R. A Toxicologic Review of Quantum Dots: Toxicity Depends on Physicochemical and Environmental Factors. **Environmental Health Perspectives**, v. 114, n. 2, p. 165–172, 20 fev 2006.

HERMANSON, G. T. **Bioconjugate Techniques**. 2nd. ed. Rockford: Elsevier Inc., 2008. p. 215–222

HOSHINO, A.; HANADA, S.; YAMAMOTO, K. Toxicity of nanocrystal quantum dots: the relevance of surface modifications. **Archives of toxicology**, v. 85, n. 7, p. 707–20, jul 2011.

JANECZKO, K. Co-expression of GFAP and vimentin in astrocytes proliferating in response to injury in the mouse cerebral hemisphere. A combined autoradiographic and double immunocytochemical study. **International journal of developmental neuroscience : the official journal of the International Society for Developmental Neuroscience**, v. 11, n. 2, p. 139–47, abr 1993.

KANTELHARDT, S. R.; CAARLS, W.; VRIES, A. H. B. DE; *et al.* Specific visualization of glioma cells in living low-grade tumor tissue. **PloS one**, v. 5, n. 6, p. e11323, jan 2010.

LI, Y.; REY-DIOS, R.; ROBERTS, D. W.; VALDÉS, P. A.; COHEN-GADOL, A. A. Intraoperative Fluorescence-Guided Resection of High-Grade Gliomas: A Comparison of the Present Techniques and Evolution of Future Strategies. **World neurosurgery**, 9 jul 2013.

LIMA, F. R. S.; KAHN, S. A.; SOLETTI, R. C.; *et al.* Glioblastoma: therapeutic challenges, what lies ahead. **Biochimica et biophysica acta**, v. 1826, n. 2, p. 338–49, dez 2012.

LIRA, R. B.; SEABRA, M. A. B. L.; MATOS, A. L. L.; *et al.* Studies on intracellular delivery of carboxyl-coated CdTe quantum dots mediated by fusogenic liposomes. **Journal of Materials Chemistry B**, v. 1, n. 34, p. 4297, 2013.

LOUREIRO, S. O.; ROMÃO, L.; ALVES, T.; *et al.* Homocysteine induces cytoskeletal remodeling and production of reactive oxygen species in cultured cortical astrocytes. **Brain research**, v. 1355, p. 151–64, 8 out 2010.

LOVRIĆ, J.; BAZZI, H. S.; CUIE, Y.; *et al.* Differences in subcellular distribution and toxicity of green and red emitting CdTe quantum dots. **Journal of molecular medicine (Berlin, Germany)**, v. 83, n. 5, p. 377–85, maio 2005.

LOVRIĆ, J.; CHO, S. J.; WINNIK, F. M.; MAYSINGER, D. Unmodified cadmium telluride quantum dots induce reactive oxygen species formation leading to multiple organelle damage and cell death. **Chemistry & biology**, v. 12, n. 11, p. 1227–34, nov 2005.

MEDINTZ, I. L.; UYEDA, H. T.; GOLDMAN, E. R.; MATTOUSSI, H. Quantum dot bioconjugates for imaging, labelling and sensing. **Nature materials**, v. 4, n. 6, p. 435–46, jun 2005.

MOSMANN, T. Rapid colorimetric assay for cellular growth and survival: Application to proliferation and cytotoxicity assays. **Journal of Immunological Methods**, v. 65, n. 1-2, p. 55–63, dez 1983.

NURUNNABI, M.; KHATUN, Z.; HUH, K. M.; *et al.* In vivo biodistribution and toxicology of carboxylated graphene quantum dots. **ACS nano**, v. 7, n. 8, p. 6858–67, 27 ago 2013.

OMURO, A. M.; LEITE, C. C.; MOKHTARI, K.; DELATTRE, J.-Y. Pitfalls in the diagnosis of brain tumours. **Lancet neurology**, v. 5, n. 11, p. 937–48, nov 2006.

PATHAK, S.; CAO, E.; DAVIDSON, M. C.; JIN, S.; SILVA, G. A. Quantum dot applications to neuroscience: new tools for probing neurons and glia. **The Journal of neuroscience : the official journal of the Society for Neuroscience**, v. 26, n. 7, p. 1893–5, 15 fev 2006.

PELLEY, J. L.; DAAR, A. S.; SANER, M. A. State of academic knowledge on toxicity and biological fate of quantum dots. **Toxicological sciences : an official journal of the Society of Toxicology**, v. 112, n. 2, p. 276–96, dez 2009.

ROBERTS, J. R.; ANTONINI, J. M.; PORTER, D. W.; *et al.* Lung toxicity and biodistribution of Cd/Se-ZnS quantum dots with different surface functional groups after pulmonary exposure in rats. **Particle and fibre toxicology**, v. 10, p. 5, jan 2013.

ROBSON, D. K. Pathology & Genetics. Tumours of the Nervous System. World Health Organisation Classification of Tumours. P. Kleihues and k. Cavenee (eds). IARC Press,

Lyon, 2000. No. of pages: 314. ISBN: 92 832 2409 4. **The Journal of Pathology**, v. 193, n. 2, p. 276–276, fev 2001.

RZIGALINSKI, B. A.; STROBL, J. S. Cadmium-containing nanoparticles: perspectives on pharmacology and toxicology of quantum dots. **Toxicology and applied pharmacology**, v. 238, n. 3, p. 280–8, 1 ago 2009.

SANTOS, B. S.; FONTES, A. CHAPTER 26 Semiconductor Quantum Dots for Biological Applications. p. 773–798, 2008.

SHIOHARA, A.; HOSHINO, A.; HANAKI, K.; SUZUKI, K.; YAMAMOTO, K. On the Cytotoxicity Caused by Quantum Dots. **Microbiol. Immunol**, v. 48, n. 9, p. 669–675, 2004.

SMITH, C.; IRONSIDE, J. W. Diagnosis and pathogenesis of gliomas. **Current Diagnostic Pathology**, v. 13, n. 3, p. 180–192, jun 2007.

SONG, F.; CHAN, W. C. W. Principles of conjugating quantum dots to proteins via carbodiimide chemistry. **Nanotechnology**, v. 22, n. 49, p. 494006, 9 dez 2011.

VALIZADEH, A.; MIKAEILI, H.; SAMIEI, M.; *et al.* Quantum dots: synthesis, bioapplications, and toxicity. **Nanoscale research letters**, v. 7, n. 1, p. 480, jan 2012.

WANG, Y.; CHEN, L. Quantum dots, lighting up the research and development of nanomedicine. **Nanomedicine : nanotechnology, biology, and medicine**, v. 7, n. 4, p. 385–402, ago 2011.

WIECINSKI, P. N.; METZ, K. M.; KING HEIDEN, T. C.; *et al.* Toxicity of oxidatively degraded quantum dots to developing zebrafish (*Danio rerio*). **Environmental science & technology**, v. 47, n. 16, p. 9132–9, 20 ago 2013.

YAMADA, S.; KHANKALDYAN, V.; BU, X.; *et al.* A METHOD TO ACCURATELY INJECT TUMOR CELLS INTO THE CAUDATE/PUTAMEN NUCLEI OF THE MOUSE BRAIN. **Tokai J Exp Clin Med**, v. 29, n. 4, p. 167 – 173, 2004.

YU, W. W.; QU, L.; GUO, W.; PENG, X. Experimental Determination of the Extinction Coefficient of CdTe, CdSe, and CdS Nanocrystals. **Chemistry of Materials**, v. 15, n. 14, p. 2854–2860, jul 2003.

ZENG, Q.; KONG, X.; SUN, Y.; *et al.* Synthesis and Optical Properties of Type II CdTe/CdS Core/Shell Quantum Dots in Aqueous Solution via Successive Ion Layer Adsorption and Reaction. **Journal of Physical Chemistry C**, v. 112, n. 23, p. 8587–8593, 12 jun 2008.